UNIVERSITY OF MINNESOTA
ST. ANTHONY FALLS LABORATORY
Engineering, Environmental and Geophysical Fluid Dynamics

Project Report No. 490

Groundwater Recharge from a Changing Landscape

by

Timothy Erickson and Heinz G. Stefan

Prepared for

Minnesota Pollution Control Agency
St. Paul, Minnesota

May, 2007
Minneapolis, Minnesota

Abstract

Urban development of rural and natural areas is an important issue and concern for many water resource management organizations and wildlife organizations. Change in groundwater recharge is one of the many effects of urbanization. Groundwater supplies to streams are necessary to sustain cold water organisms such as trout. An investigation of the changes of groundwater recharge associated with urbanization of rural and natural areas was conducted. The Vermillion River watershed, which is both a world class trout stream and on the fringes of the metro area of Minneapolis and St. Paul, Minnesota, was used for a case study. Substantial changes in groundwater recharge could destroy the cold water habitat of trout. In this report we give first an overview of different methods available to estimate recharge. We then present in some detail two models to quantify the changes in recharge that can be expected in a developing area. We finally apply these two models to a tributary watershed of the Vermillion River.

In this report we discuss several techniques that can be used to estimate groundwater recharge:
(1) the recession-curve-displacement method and
(2) the base-flow-separation method that both use only streamflow records (Rutledge 1993, Lee and Chen 2003);
(3) a recharge map developed by the USGS for the state of Minnesota (Lorenz and Delin 2007);
(4) a minimal recharge map developed by the Minnesota Geological Survey using statistical methods (Ruhl et al. 2002);
(5) a first approximation equation developed by Cherkauer and Ansari (2005);
(6) a simple water budget developed by Allen et al. (1996) for use with the FAO-56 Penman-Monteith evapotranspiration equation;
(7) a Green-Ampt model that estimates recharge using the Green-Ampt equation for estimating infiltration depth; and
(8) an analytical equation for estimating recharge developed by Kim (1996).
Not all methods can be used to project the changes to groundwater recharge caused by land use or climate change in an area.

The easiest way to estimate a change in groundwater recharge due to land use change (urban development) in a watershed is to use a water budget. We will present three models to estimate the important water budget components, i.e. infiltration, evapotranspiration, percolation or groundwater recharge, and run-off. The three models are:
(1) the FAO (Food and Agriculture Organization under UNESCO) model using the SCS method for infiltration on a daily timescale,
(2) the FAO model using the Green-Ampt method for estimating infiltration on an hourly timescale, and
(3) the Green-Ampt model on an hourly timescale.

To apply the models and investigate the potential change in groundwater recharge due to urban development, the sub-watershed of a second order tributary of the Vermillion River near Lakeville, Minnesota, was chosen as the study site. The Vermillion River is located in Dakota and Scott Counties just south of the Twin Cities in Minnesota, and is a designated DNR trout stream that flows into the Mississippi River. The specific sub-watershed covers 6.78 km^2 (1675.3 acres) area and was selected because it has both undeveloped (i.e. agricultural and natural) land, and developed (i.e. urban residential and commercial) areas. About 60% of the sub-watershed is undeveloped, and about 40% is developed land. The soils in the sub-watershed are mostly glacial deposits of sandy loams, silty loams, silty clay loams, and loams.

The model estimates for groundwater recharge under 2004 land use conditions ranged from 12% to 24% of 829 mm of annual precipitation. The full urban development of the study site (plus 100 years scenario) would result in a decrease of groundwater recharge to a range of 9% to 14% of precipitation. To make this projection, the impervious areas were raised from 18% for the present scenario to 36% for the fully developed scenario. The case study shows that an increase of 18% for the impervious area will decrease the recharge by ~20% to 40% of its present value. A change of this magnitude will substantially affect the water supply to the aquifer which discharges into the cold water stream.

Table of Contents

1. Introduction

As urban development encroaches on rural and natural areas, groundwater recharge may decrease. The volume of stored and/or available groundwater may decrease because of reduced infiltration. The construction of roads, buildings, and parking lots will typically increase the amount of impervious areas. More surface runoff, less water infiltration into the soil, and less water recharge to aquifers are often the consequence of urban development. This is an important issue not only for ground water withdrawal to meet society's need, but also for cold-water organisms, such as trout, in groundwater-fed streams. If the groundwater recharge rate is decreased, less groundwater will be available to feed coldwater streams, and more, warmer surface run-off will raise stream temperatures. How urbanization affects the cold-water streams of Minnesota needs to be investigated, i.e. the effect of land-use on the flow of groundwater to cold-water streams and reasonable upper limits of urban development and groundwater withdrawal need to be found.

Groundwater recharge is defined for use in this paper as the amount of water that flows beyond the root zone, i.e. the reach of vegetation, and ultimately reaches an aquifer through vertical percolation or seepage annually or seasonally. Groundwater recharge will be referred to as "groundwater recharge" or simply "recharge" for the purposes of this paper. Seasonal recharge is the recharge that occurs after the spring thaw and before the winter freeze, i.e. approximately April through November for Minnesota. The two major sources of groundwater recharge to aquifers are infiltration and percolation from precipitation, and seepage from surface water bodies. The fraction of precipitation that becomes recharge depends on many factors that influence the water's ability to reach the saturated zone (aquifer). A large fraction of precipitation becomes surface runoff that flows overland to streams and lakes. The remaining water infiltrates into the soil and a large portion of this water will be intercepted and discharged back into the atmosphere by plants in a process called evapotranspiration. The amount of water that reaches the aquifer (recharge) depends on various climate parameters including intensity and duration of rainfall events, soil characteristic (such as soil's permeability, moisture content, and thickness) and depth, topography, vegetative land cover, and aquifer depth that can be hard to quantify due to the spatial and temporal variations that exist in natural systems. It can therefore be difficult to model groundwater recharge.

Many different methods have been developed to estimate groundwater recharge. For example, Arnold et al. (2000) developed regional estimates of recharge at the sub-basin scale throughout the upper Mississippi River region using a water balance approach and two different methods that were based on streamflow. Dumouchelle and Schiefer (2002) estimated ground water recharge rates for 103 basins throughout Ohio using streamflow records and basin characteristics. Some studies that have used multiple regression approaches on climat/soil/topography parameters Cherkauer 2004, Cherkauer and Ansari 2005). Arnold and Allen (1996) developed a multi-component model called SWAT estimates, e.g. for three watersheds in Illinois. Lorenz and Delin (2007) developed a recharge map for the state of Minnesota using streamflow records,

precipitation, and soil parameters. Finch (1998) used a simple water budget model to study the effects of land parameters on groundwater recharge.

To improve the permitting process for urban development and groundwater resources it is important to understand the hydrology of groundwater recharge, and the methods used to estimate groundwater recharge. In this paper we will review methods for estimating recharge and describe methods that can be used to forecast changes in groundwater recharge due to urbanization or other land cover changes.

Methods developed to estimate groundwater recharge can be divided into two categories: empirical and physics-based methods. The empirical methods are based on coefficients that were estimated by linear regressions from stream flow records, soil data and/or topographic data. This paper will cover some of the empirical models that use only streamflow records such as the recession-curve-displacement method and the base-flow-separation method (Rutledge 1993, Lee and Chen 2003); a recharge map developed by the USGS for the state of Minnesota (Lorenz and Delin (2007)), a minimal recharge map developed by the Minnesota Geological Survey (Ruhl et al. (2002)) using statistical methods, and a first approximation equation developed by Cherkauer and Ansari (2005) will also be discussed in Section 2. Since empirical methods use existing conditions and data from the past to form relationships, they are not always suitable to forecast the effects of a changing landscape on groundwater recharge.

Physics-based methods are needed to estimate recharge changes resulting from land-use changes. Physics-based models describe the hydrologic processes that occur in the soil column and usually rely on a soil water balance. The physics-based methods estimate recharge by relating infiltration and evapotranspiration of water to recharge (Fig.1.1) using a soil moisture budget. The soil water budget will be discussed in Section 1.3. Land-use has large effect on the amount of water that infiltrates and/or transpires change, and the consequence is a change in groundwater recharge. The physics–based models discussed in this paper are the FAO model developed by Allen et al. (1996) for use with the FAO-56 Penman-Monteith evapotranspiration equation, a Green-Ampt model that estimates recharge using the Green-Ampt equation for estimating infiltration depth, and an analytical equation for estimating recharge developed by Kim (1996). These methods will be discussed in Section 4.

The purpose of this paper is not only to review some of the available methods to estimate groundwater recharge, but also to illustrate their use for predicting the changes caused by urbanization of natural and agricultural lands. The seasonal recharge for a sample site will be estimated in Section 7.

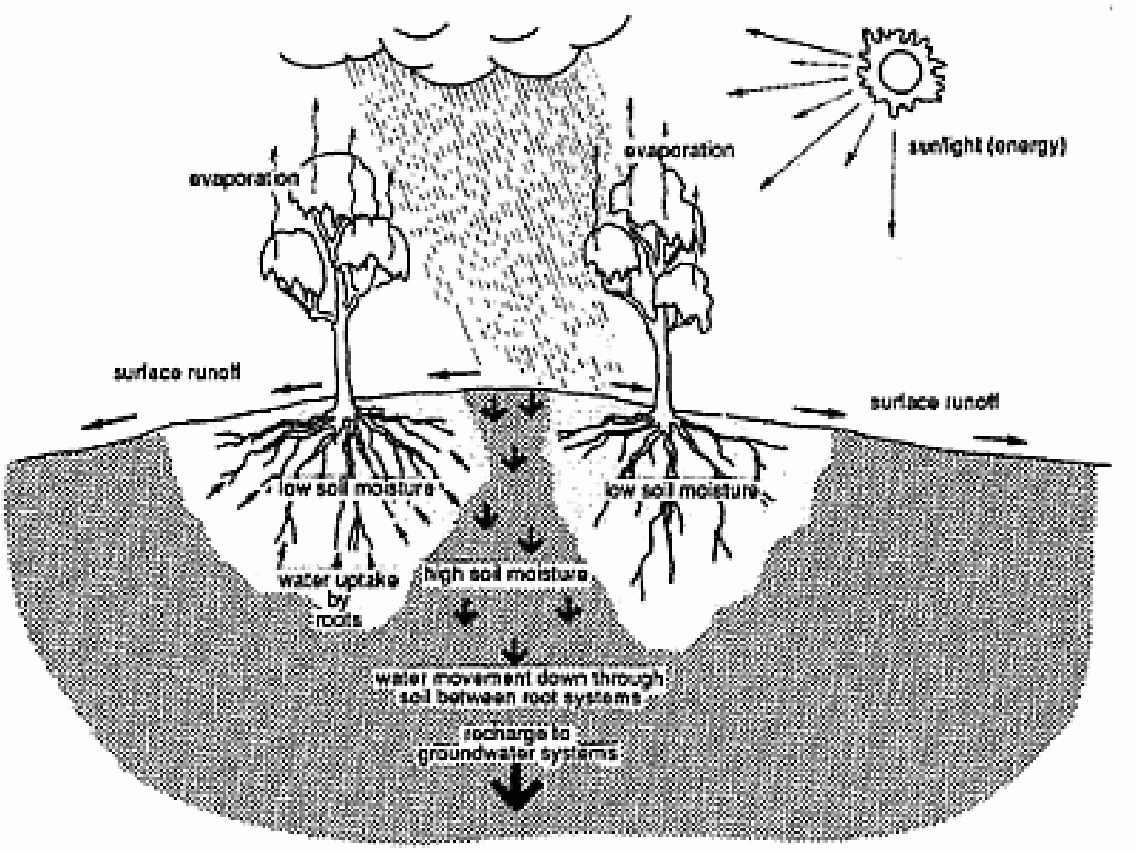

Figure 1.1 Schematic of the physical processes that control groundwater recharge (from Clifton et al. 1999)

1.1 Groundwater budget

A groundwater budget is a quantitative expression of the balance between the total water gains and losses of an aquifer over a period of time. The water entering the aquifer is equated to the water leaving the aquifer, plus or minus the changes in storage in the aquifer. The groundwater budget can be stated as

$$R + GW_{in} - Q_s - Q_w - GW_{out} = \Delta S/t \qquad [1.1]$$

where R = recharge to the aquifer,
GW_{in} = influxes from upgradient portions of the ground water system,
GW_{out} = effluxes to downgradient portions of the ground water system,
Q_s = discharge to or from surface water bodies,
Q_w = abstractions from ground water system through wells,
$\Delta S/t$ = change in ground water storage in the system per unit time.

Each term in (1.1) has units of volume or depth per time, and artificial recharge and leakage through aquifers to deeper aquifers are assumed negligible. At the ground-

watershed scale, i.e. without lateral flows across any ground water divides, (1.1) simplifies to

$$R - Q_s - Q_w = \Delta S/t \qquad [1.2]$$

The budget equation can be rearranged to give the discharge to surface water bodies. If well abstractions are ignored, the budget can be given as

$$Q_s = R \pm \Delta S/t \qquad [1.3]$$

The groundwater in storage can fluctuate over time. If the long-term change in storage $\Delta S/t$ can be assumed to approach zero the recharge R in (1.3) can be taken as equal to the discharge Q_s to a surface water body such as a stream, where it provides the base-flow. Base-flow is the streamflow minus the surface runoff from a rainfall event. Equation (1.3) is the basis for estimating groundwater recharge from streamflow records using hydrograph separation methods such as the base-flow separation method and the recession-curve displacement method to be described in Section 2. Empirical models use linear regression and streamflow records to estimate recharge.

The major sources of groundwater recharge come from two sources; direct precipitation and seepage from surface water bodies such as lakes and wetlands. Water on the land surface enters the soil by infiltration and gravity moves it down by percolation or seepage to the aquifer. Percolation is unsaturated flow through the soil caused by the gravity effects on excess water in a soil, whereas seepage is saturated flow through the pore system under wetlands, lakes, ponds, ditches, streams and rivers. Recharge, R, is defined as the net quantity of water entering the saturated zone (aquifer) and is assumed to be the sum

$$R = Q_p + Q_{See} \pm \Delta S/t \qquad [1.4]$$

where Q_p is percolation (m^3/s), Q_{See} is seepage (m^3/s), and $\Delta S/t$ is short-term change in storage (m^3/s) in the aquifer. If a steady-state condition is assumed (approximated in natural systems over long periods), the $\Delta S/t$ term approaches zero. Percolation is related to precipitation, infiltration, and evapotranspiration; and seepage is related to the soil type and the shape of the surface water body. A brief introduction to percolation and seepage is provided below; a more detailed description of each can be found in Sections 3.0 and 5.0, respectively.

1.2 Percolation/Infiltration

Percolation is defined as unsaturated flow through a porous medium. Percolation recharge is the small fraction of annual precipitation that percolates down through the soil to the saturated zone (aquifer). The amount of percolation that reaches the aquifer depends on the water's infiltration rate on the land surface and the water uptake rate in the root zone; the plants send this water back to the atmosphere. Infiltration is the depth

of water that infiltrates the soil during a rain event. Evapotranspiration is the depth of water used by plants and returned to the atmosphere by evaporation and transpiration. The soil moisture represents the water in the soil and is dependent on the other processes.

Soil moisture can be expressed by a soil water balance. The soil water balance is similar to the groundwater budget but the soil water budget is for a region near the ground surface. The soil water budget tracks the soil's moisture and can be expressed as

$$\Delta s = I(s) - ET(s) - R_p(s) \qquad [1.5]$$

where s = soil moisture.
Δs = change in soil moisture (m),
I = infiltration (m),
ET = evapotranspiration (m)
R_p = percolation (m)

According to (1.5), percolation, infiltration, and evapotranspiration are functions of soil moisture. Percolation and the components of (1.5) are explained further in Section 3.0.

1.3 Seepage

The saturated flow under surface water bodies such as wetlands, lakes, ponds, streams, rivers, and other channels is called seepage. Seepage is important to the groundwater budget because unlike percolation, seepage is a constant flow as long as water remains in the surface water body. Seepage is related to the shape and dimensions of a water body and the permeability of the soil under it. Equations used to estimate the volume of seepage will be presented in Section 4.0.

2. Empirical models of groundwater recharge

Several methods have been developed to estimate groundwater discharge and groundwater recharge using streamflow records. Many of these methods assume that the groundwater discharge to a stream is equal to the groundwater recharge (see equ. 1.3). It is aslo implied that the ground-watershed is equal to the surface watershed, that no flow crosses the boundary divide; and that leakage to deep aquifers is negligible.

To understand these methods, it is useful to examine a runoff hydrograph. The *hydrograph* is a plot of the stream discharge versus time. It shows three phases in response to a rainfall event (Figure 2.1).

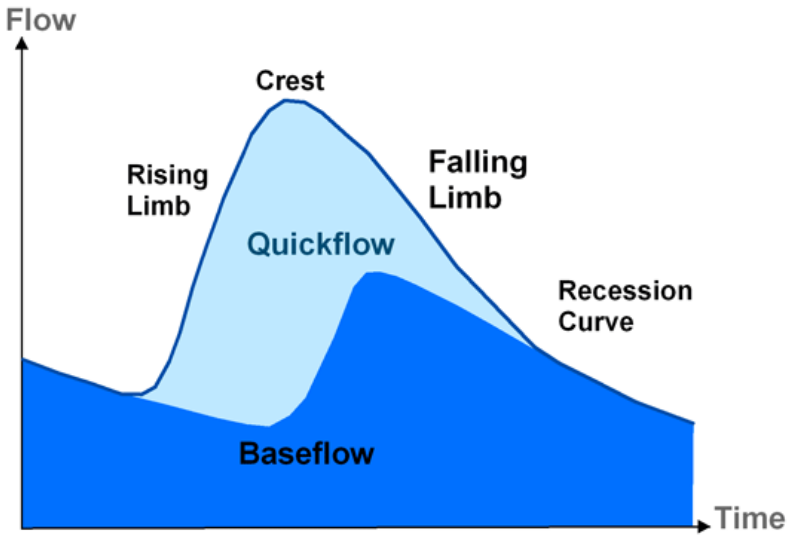

Figure 2.1 Components of a stream hydrograph after a rainfall event (from www.connectedwater.gov.au/processes/baseflow.html)

(1) Prior to a rainfall event, low-flow or *base-flow* occurs in the stream, especially at the end of a dry period.

(2) With rainfall, streamflow increases (rising limb) due to surface runoff (quick flow) and interflow in the soil. The associated rise of the stream level reduces or can even reverse the hydraulic gradient from the surrounding groundwater levels towards the stream. This produces a reduction in the base-flow component at this stage.

(3) The crest of the hydrograph is followed by the falling limb of the flood hydrograph. As stream level declines, and the water table rises in a delayed response to infiltrating rainfall, the hydraulic gradient towards the stream increases. Consequently increased seepage into the stream occurs, and the base-flow component starts to increase. At some point in time along the falling limb, surface runoff (quickflow) ceases and streamflow is again entirely base-flow. Over time, base-flow declines as the natural storage of water in the soil and aquifers is gradually drained during the dry period, until the next significant rainfall event occurs.

Two widely used methods are the recession-curve-displacement method, often referred to as the Rorabaugh method that consists of a set of calculations that will estimate total recharge for each streamflow peak (Rutledge and Daniel 1994), and the base-flow-separation method, which is the estimation of a continuous or daily record of base flow under the streamflow hydrograph (Rutledge and Daniel 1994). Both methods assume that the base-flow of a stream is equal to the groundwater discharge, but this assumption is not always valid. A variety of natural phenomena and human interventions can affect the base-flow. Base-flow can also be released from storage basins, such as reservoirs, lakes, wetlands, or from snow melt. Stream regulation, industrial discharges, and irrigation and

drainage can vastly modify a stream's base flow (Schilling 2003). After large flood events temporary stream bank storage can contribute to base-flow.

These methods are widely used because they only require stream discharge records to estimate groundwater recharge, but they do have a high degree of subjectivity associated with them. Computer programs have been developed to lessen some of the subjectivity associated with manual analysis by multiple workers. Unfortunately groundwater recharge estimates by any models are hard to validate because groundwater recharge cannot be directly measured.

Below is a discussion of several empirical methods to estimate groundwater recharge. Four of them use stream flow records:
(1) the recession-curve-displacement method;
(2) the base-flow-separation method;
(3) a regional groundwater recharge map developed by the USGS for the state of Minnesota by using the regional regression recharge (RRR) model that applies the recession-curve-displacement method (Lorenz and Delin 2007);
(4) a regional map of the five county Metro Area (Minneapolis and St. Paul, MN) developed by the Minnesota Geological Survey (MnGS);
(5) a first approximation equation developed by Cherkauer and Ansari (2005) to estimate recharge as a ratio of recharge to precipitation.

2.1 Recession-curve-displacement method

The recession-curve-displacement method (Rorabough's method) is intended for analysis of flow systems that are driven by area diffuse-recharge where the stream can be considered as the sole sink (discharge boundary) of the groundwater flow system. Groundwater recharge is considered to be approximately concurrent with the peaks in the streamflow (Rutledge and Daniel 1994). This method has the strongest theoretical basis of any of the hydrograph-separation techniques. It is based on the closed-form solution of the one-dimensional groundwater flow equation (Halford and Mayer 2000). The method is only applicable to stream systems and catchments where regulation and diversion of flows can be considered negligible. The recharge estimate is for the watershed or drainage area upstream from a gauging station where the discharge data are collected. This method can be used to express groundwater recharge in units of specific discharge (such as inches or mm per year), if the area of contribution (the ground-watershed) is known and equal to the drainage area of the surface-water system (the watershed).

Daily or continuous streamflow records are the only required data. If continuous streamflow records are available, there may be no lower limit to the size of watershed or drainage area but if daily streamflow records are used, the drainage area must be of sufficient size so that the time base of surface runoff exceeds the time increment of the streamflow records. The upper limit of drainage or recharge area is dependent on the uniformity of the weather system and the accuracy of the time base of surface runoff.

The recession-curve-displacement method can be executed using the steps shown in Figure 2.2 (Rutledge 1993):

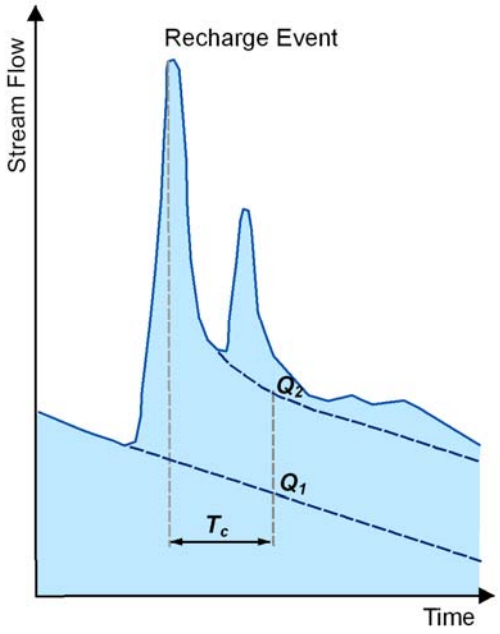

Procedure for the recession curve displacement method (after Rutledge and Daniel 1994):

(1) Estimate the recession index (K) from the stream hydrograph record
(2) Calculate the critical time (T_c), using the relationship $T_c = 0.2144K$
(3) Locate the time on the hydrograph which is T_c days after the peak, where streamflow recessions will be extrapolated to
(4) Extrapolate the pre-event recession curve to derive Q_1
(5) Extrapolate the post-event curve to derive Q_2
(6) Calculate total potential groundwater recharge using these parameters

Figure 2.2 Graphical determination of the recession index (K) and critical time (Rutledge and Daniel 1994).

The recession-curve-displacement method starts by determining the recession index (K). The recession index (K) is the time (days) required for groundwater discharge to decline through one log cycle, i.e. Q_0 to $0.1Q_0$. The recession index (K) is a constant that represents the physical properties of the aquifer. The recession index can be estimated by taking periods of records where the streamflow recession is allowed to go undisturbed (by precipitation, regulation, etc.) long enough so that the trace of the hydrograph becomes a straight line and its slop can be determined (Rutledge and Daniel (1994)). Winter or non-growing season records should be used to eliminate effects of evapotranspiration and limit the effects of precipitation. Otherwise, the recession index can be determined graphically by superimposing numerous recessions and an average recession can be determined from the graph.

Rutledge and Daniel (1993 & 1994) automated the recession-curve-displacement method by developing a computer program called RORA (named after Rorabough). Their goal was to remove some of the subjectivity inherent in the method. When two investigators apply the method manually on the same watershed, they typically obtained different estimates of groundwater recharge. The RORA program removes this subjectivity and standardizes the results. Information about RORA and the programs script can be found on the USGS website at http://water.usgs.gov/ogw/rora/.

2.2 Base-flow-separation method

Base-flow is the long-term discharge in a stream between rainfall events. Base-flow is fed from natural storage, such as groundwater, but can be vastly modified by man-made interference. Streams that sustain flow continuously throughout the year (called perennial streams) have often a high base-flow component.

Many techniques which often involve considerable subjectivity in their application, have been developed to estimate base-flow under the stream flow hydrograph record, and to relate it to groundwater discharge to a stream, e.g. by assuming that ground-water discharge equals streamflow during base-flow. The methods often require two steps: (1) locating the periods of negligible surface runoff and (2) interpolating groundwater discharge between these periods (Rutledge 1993).

Computer techniques have been developed for base-flow separation estimation from streamflow records, and have allowed for increase speed and repeatability of results. A program called PART was developed by Rutledge (1993) using a method first described by Rutledge (1992) and based on antecedent streamflow recession. The method of base-flow-record estimation that is used in PART is a form of streamflow partitioning that is similar to that of other investigators (Rutledge 1993, Rutledge and Daniel 1994) in that (1) daily values of streamflow are used and (2) linear interpolation is used to estimate groundwater discharge during periods of surface runoff (Rutledge 1993). More information and the script for PART can be found on the USGS website at http://water.usgs.gov/ogw/part/.

2.3 Groundwater recharge at the regional scale using the U.S. Geological Survey recharge map

A groundwater recharge map for the state of Minnesota was created by the United States Geological Survey (USGS) using a regional regression model. The regional regression recharge (RRR) model was developed by Lorenz and Delin (2007) to estimate the spatial distribution of groundwater recharge in sub-humid regions. The RRR model uses a regression of basin-wide estimates of recharge from surface water drainage basins, precipitation, growing degree days (GDD), and average basin specific yield (SY). SY is defined as the ratio of the volume of water that drains from a soil due to gravity to the total soil volume (Lorenz and Delin 2007). Decadal average values of recharge, precipitation, and GDD were used in the development of the RRR model. Estimates for recharge were derived by analysis of the stream base-flow using the computer program RORA (Section 2.1) that was based on the Rorobaugh method. The proposed form of the RRR model (Lorenz and Delin 2007) is

$$R_i = \beta_0 + \beta_1 P_i + \beta_2 GDD_i + \beta_3 LC_i + e_i \qquad [2.1]$$

where

R_i = estimated recharge (averaged over some time period) for observation i (cm/yr),

P_i = precipitation for observation i (cm/yr),
GDD_i = growing degree days, in (ºC) above 10ºC for observation i,
LC_i = landscape characteristic for observation i,
e_i = the residual for observation i (assumed to be correlated but identical and normally distributed),
$\beta_0, \beta_1, \beta_2,$ and β_3 = regression coefficients.
i = subscript, referring to a sub-region or watershed.

This linear model is an approximation of a model, which is more complicated and non-linear.

Growing degree days (GDD) is defined as the annual sum of the average temperature minus a base temperature, for example 10 ºC, with negative values counted as zero for each day. According to Lorenz and Delin (2007), precipitation and growing degree days (GDD) were included as climate factors to estimate the net precipitation available for recharge. GDD was selected instead of evapotranspiration (ET) as a measure for estimating precipitation lost from the system and not available for recharge because (1) GDD is the primary factor in estimating ET; (2) annual estimates of ET are not universally available; and (3) there are several methods of estimating ET, which would be complicated to use across a large study area. GDD and precipitation data for the RRR model were obtained from the Minnesota State Climatology Office for 1977 to 2000. The data were converted to annual values on a 10 km grid over the entire state using ARC/INFO software.

Specific yield (SY) was chosen to represent the landscape characteristic in equation (2.1). SY is defined as the ratio of the volume of water that drains from a soil due to gravity to the total soil volume (Lorenz and Delin 2007). An attractive feature of using SY as the spatial explanatory variable is that it can be easily estimated from data in the State Soil Geographic Database (STATSGO), which is available for the entire United States. A reasonable approach is to estimate SY as the difference between the water content of saturated soil (θ_s) and the water content of soil at field capacity (θ_{fc}) (assumed to be the water content at 2330 cm of pressure head). The value of θ_{fc} is assumed to give the water content that is retained in the soil after it is drained by gravity. These values were computed using soil texture, bulk density, amount of organic matter, and other characteristics in the STATSGO database using the Rawls method (Rawls et al. 1982).

Of the 340 continuous record gauging stations in Minnesota, 38 gauging stations (covering 25% of the state) were chosen to develop the model The criteria for inclusion were (Lorenz and Delin 2007):
(1) gauging stations have at least a 10-year period of record;
(2) gauging stations have no missing data within the 10-year periods;
(3) the flow is not significantly affected by regulation and diversion structures, such as a dam;
(4) the basin lies wholly within Minnesota or has soils that are not different from those found in Minnesota;
(5) the basin has a drainage area of less than 5000 km^2;

(6) if a basin is nested within a larger basin, then it must be restricted to less than 15% of the larger basin; and
(7) the basin has soils data that can be used to estimate landscape characteristics.

For the 38 watersheds chosen, recharge was estimated using RORA (Section 2.1). Using the recharge estimates, precipitation data, GDD data and SY_{Rawls} data, the coefficients in equ. (2.7) were estimated. The final regression equation that estimates average groundwater recharge was

$$R = 14.25 + 0.6459P - 0.02231GDD + 67.63SY_{Rawls} \quad [2.2]$$

where

R = groundwater recharge (cm/year),
P = precipitation (cm/year),
GDD = growing degree days (ºC above 10ºC days),
SY_{Rawls} = specific yield computed by Rawls method (-).

Equation (2.2) was developed to estimate recharge on a regional or basin scale. It should not be used on a local scale or for point estimates due to the spatial variability of soil properties. Lorenz and Delin (2007) state that (1) local conditions such as confining units at or near the land surface can greatly reduce the estimated recharge rates to aquifers and (2) local hydraulic properties and topography can affect the estimation of recharge but were not considered in this analysis. The recharge estimates can be used at a scale appropriate fro STATSGO mapping units.

The residual standard error for average recharge was 2.79 cm/year with 129 degrees of freedom and ρ was 0.5422 as determined by the maximum likelihood method. The overall ρ value for the model is < 0.0001 based on the likelihood ratio test between the regression model and the null model, which includes only the intercept term and the correlation structure

Lorenz and Delin (2007) developed a map illustrating spatial distribution of the RRR rates in Minnesota (Figure 2.5) that was generated by applying the coefficients of the regression model (equation 2.2) to the statewide data sets of P, SY, and GDD. In some areas where P and SY values were small, the computed recharge was negative; in these situations, the recharge rate was set to 0. The RRR rates illustrated in Figure 2.5 generally are representative of the average soil conditions in an area.

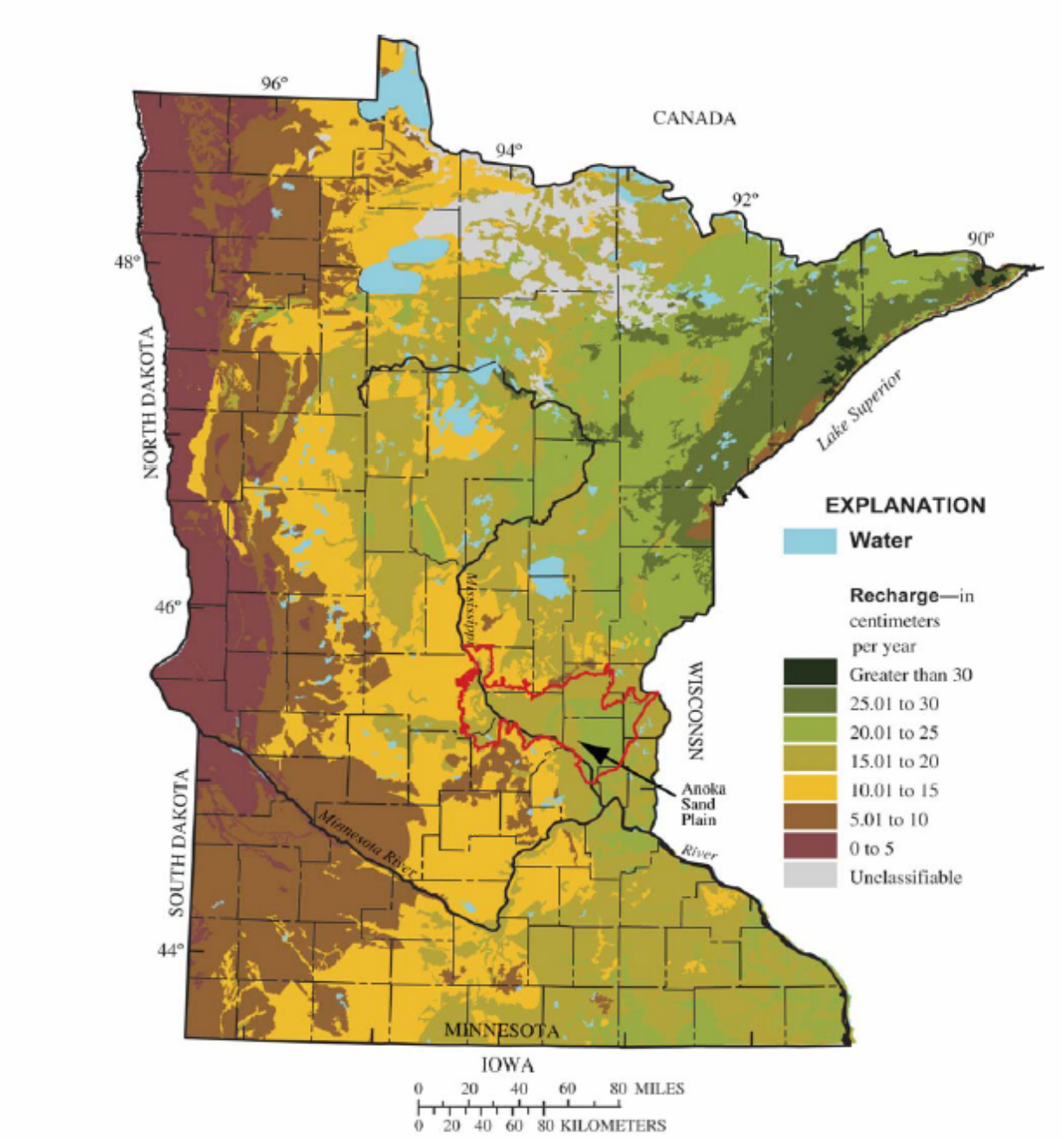

Figure 2.5 Average annual recharge to surficial materials in Minnesota (1971 to 2000). Estimate based on the RRR model (Lorenz and Delin 2007).

Greatest recharge occurs in sand-plain and outwash areas, but recharge in these areas is sensitive to the amount of annual precipitation and potential evapotranspiration. The greatest estimated recharge was about 32 cm per year in areas of high specific yield (greater than 0.19) where the difference between precipitation and potential evapotranspiration is about 25 cm per year. The lowest estimated recharge was near 0 cm per year in areas of low specific yield (less than 0.15) and with less than 52 cm per year

precipitation. Low recharge is projected for the northwestern part of Minnesota where glacial Lake Agassiz sediments are present (Lorenz and Delin 2007).
The USGS recharge map can be a good tool for preliminary estimates and validation of other models. The RRR model and map should be used for larger areas and not for point estimates of recharge.

2.4 Groundwater recharge at the regional scale using the Minnesota Geological Survey recharge map

The Minnesota Geological Survey (MnGS) developed a minimal recharge map for the seven-county metropolitan area of the Twin Cities, Minnesota. The map was developed using the watershed characteristics method. The following summary of the watershed characteristic method was taken from a USGS report on estimating recharge for unconfined and confined aquifers (Ruhl et al. 2002).

The watershed characteristics method is described in detail by Kudelin (1960) and Shmagin (1997). The method was used to estimate minimal recharge in three stages—first for the entire State of Minnesota, next for east-central Minnesota, and finally for the study area based on the results for east-central Minnesota.

The method gives estimates of minimal recharge to hydrogeologic units based on the unity of ground and surface waters (Winter and others, 1998); it does not give estimates for points or surface areas. Long-term streamflow records for the period 1935-81 were statistically analyzed in a multi-dimensional approach (Shmagin and others, 1998, 1999). Streamflow characteristics during this period of observation were considered representative of the entire state-wide streamflow data base. The basis of the method is to acquire comparable minimal monthly base-flow data for watersheds, which entails analyses of streamflow data and associating these data with maps that depict the upperlying hydrogeologic units. The hydrogeologic units are depicted based on multiple-scale ground-water flow systems. The mapped units combined with the analyzed streamflow data become the basis for the estimation of minimal ground-water recharge by hydrogeologic regions and sub-regions.

Streamflow records indicate that monthly streamflow is lowest during February when streamflow typically consists of base flow (ground-water discharge) with little or no surface runoff. Minimal monthly streamflow data for east-central Minnesota (Lindskov, 1977) were compiled for 101 watersheds and analyzed by multivariate statistics (Shmagin and others, 1998, 1999). Based on these analyses, streamflow data for each analyzed watershed were adjusted in relation to the mean monthly streamflow for February during the common period of record (1935-81).

Based on analyses of the hydrogeologic and streamflow data, the February monthly streamflow was assumed to be a measure of the minimal ground-water recharge rate. This rate was considered a conservative estimate of actual recharge because the basis of estimation is February base-flow. Recharge estimates by this method, therefore, are considered minimal ground-water recharge. Although the statistical analyses used to

assign values of minimal ground-water recharge are complex, the mapped values are easily understandable. These mapped values provide a useful representation of relative recharge rates in the study area (Figure 2.6).

Minimal ground-water recharge in the study area, as determined by the watershed characteristics method, generally ranged from 0.1 to less than 2.5 in/yr (0.3 to less than 6.3cm/yr). Figure 2.6 shows the variation of minimal ground-water recharge from less than 0.1 to greater than 2.5 in/yr. Each of the ranges that represent recharge from 0.1 to less than 2.5 in/yr extends over a similarly sized portion of the study area.

In the southeastern part of the study area minimal ground-water recharge was greater than or equal to 2.5 in/yr (Figure 2.6), with a maximum of 5.6 in/yr. In a still smaller portion of the southeastern part of the study area, the rate was less than 0.1 in/yr. This area correlates with sub-crops of the Platteville Limestone and Glenwood Shale (Mossler and Tipping, 2000), which are Ordovician bedrock formations that collectively act as a confining unit.

2.5 First approximation equation for estimating groundwater recharge at the watershed scale.

Cherkauer and Ansari (2005) developed the following empirical relationship to estimate recharge as a fraction of precipitation

$$R/P = 0.0085\{K_v / (S\, D^{0.3})\} - 4.18\{D_w / L_f\} + 0.0025\{N\} + 0.022 \qquad [2.3]$$

where R/P = normalized annual recharge (recharge R per unit precipitation P in m/m)
K_v = effective vertical hydraulic soil conductivity, permeability coefficient = K_s (m/d)
S = average hill slope in a watershed (m/m)
D_w = average depth to the water table (m)
L_f = length of flow to main channel = drainage area/(2 X channel length) (km)
D = portion of developed land in watershed (%) , and
N = portion of natural land cover (%).

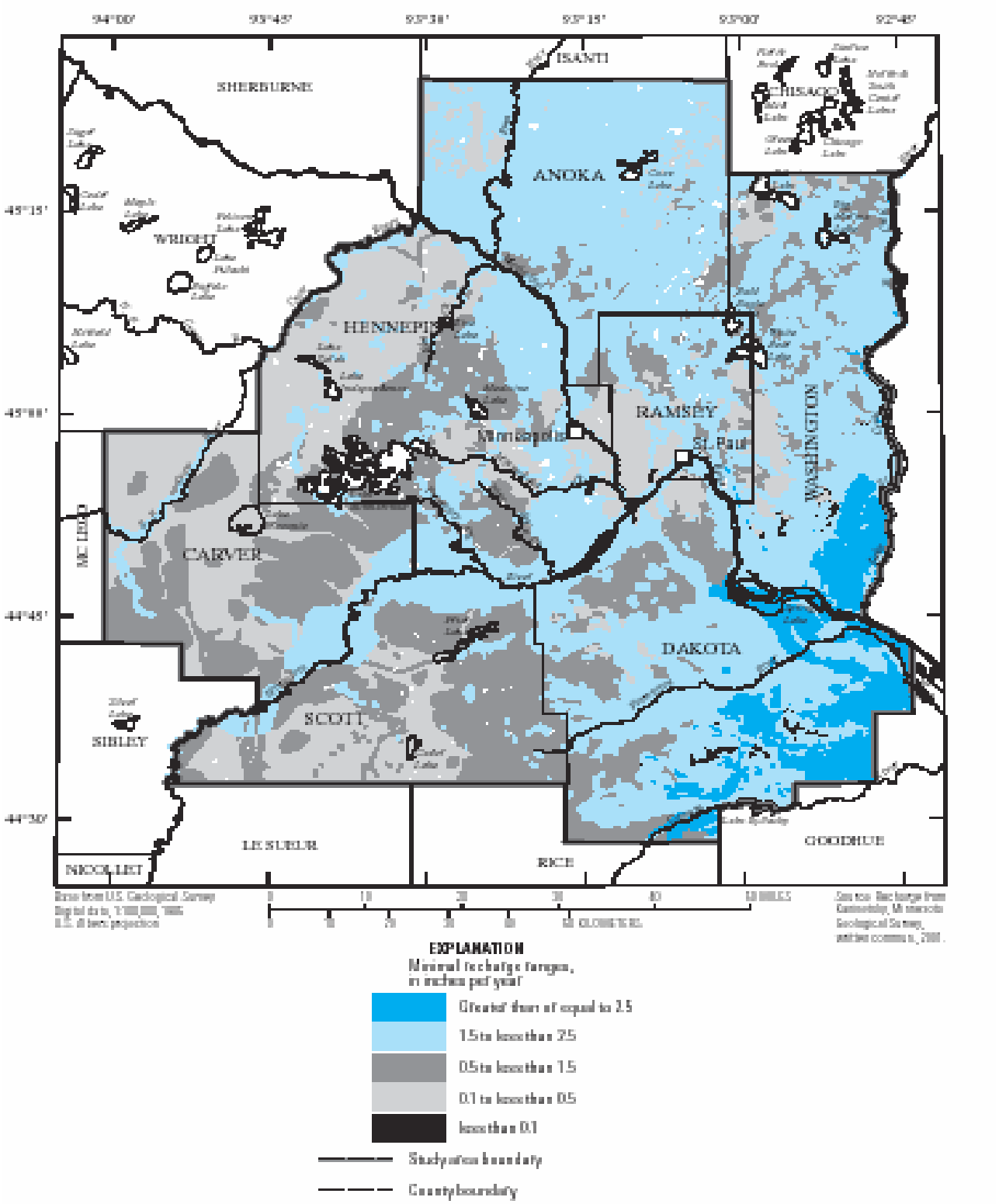

Figure 2.6 Minimal groundwater recharge based on statistical analysis of watershed characteristic in the Twin Cities metropolitan area (Minnesota Geological Survey, Ruhl et al. 2002)

Cherkauer and Ansari (2005) group land cover into five categories:
(1) natural land, N, which includes woodlands, wetlands, parks, and golf courses;
(2) agricultural land;
(3) developed land, D, which include residential, commercial, and industrial areas;
(4) extractive land which includes quarry and aggregate operations; and
(5) open water.

Only two of the land classes, N and D, are included in the empirical equation.

The first term in equation (2.3) is a ratio to represent the vertical flux of water through the soil. The vertical flux occurs when the surface soil is saturated and under a vertical hydraulic gradient of unity. Then

$$q_v = C_1 K_v \qquad [2.4]$$

where q_v is the vertical flux (m/d), and C_1 is a dimensionless proportionality coefficient. The denominator of the first term, i.e. $SD^{0.3}$, represents the surface runoff flux, q_h, which can also be described as a flux that varies directly with surface slope and inversely with ground surface roughness:

$$q_h = (C_2 S) / F_r \qquad [2.5]$$

where q_h is the horizontal flux (discharge per unit area) (m/d), S is ground surface slope (m/m), F_r is surface roughness (m), and C_2 is a proportionality coefficient with dimensions (d^{-1}). The watershed's roughness is affected by the extent of land development, D; land development reduces the watershed's roughness. The inverse of roughness F_r can be estimated as

$$F_r^{-1} = C_3 D^x \qquad [2.6]$$

where the exponent x was determined empirically to be 0.3, by optimizing the correlation of runoff flux with R/P. C_3 is a proportionality coefficient (m^{-1}). Taking a ratio of q_v to q_h and substituting equation (2.6) produces $(C K_v)/(S D^{0.3})$ for the first dimensionless term in equation (2.3). The proportionality coefficient, C, has dimensions of (d/m). The first term indicates that recharge should vary proportionally to soil conductivity and inversely with surface slope and land development as is intuitively reasonable. Normalized recharge, R/P, varies directly with the amount of natural cover, N, and the distance water travels overland to reach the main channel, L_f; it also varies inversely with the depth of the water table, D_w.

Equation (2.3) was formulated using numerous watersheds in Southern Washington County, in south-eastern Wisconsin. The watersheds are mainly traversed by a glacial interlobate moraine consisting of clay, silt and sand with shallow aquifers consisting of both sand and gravel. The land-use is primarily agricultural, residential, or low-density commercial or industrial. According to Cherkauer and Ansari (2005), equation (2.3) should be used within the following limits: $K_v \leq 2.7$ m/day; $N \leq 30\%$; $S \geq 0.03$; $D_w \geq 9.1$ m; and $D \geq 5$ %.

Equation (2.3) gives an easy, first estimate for recharge. It was developed and used for watersheds in south-eastern Wisconsin. The coefficients were estimated using linear regression and streamflow records and may have to be adjusted if the equation is applied to other watersheds. It is nevertheless useful because it accounts for developed area and natural area explicitly. Equation (2.3) estimated annual recharge for the study area to within five percent error.

3.0 Unsaturated flow in the soil column (Percolation)

The unsaturated flow through a porous medium or soil column is called percolation. Percolation is influenced by the soil moisture available in the soil column and the hydraulic conductivity of the soil. The main driving force behind percolation is gravity. Percolation recharge (deep percolation) is the soil moisture that percolates beyond the root zone (root depth) of the vegetative cover. Percolation can be difficult to model because of the spatial and temporal variability in the processes that influence the soil moisture, i.e. infiltration and evapotranspiration. Two common ways of describing percolation are described below.

(1) Percolation is the depth of soil moisture that exceeds the soil's field capacity after a rainfall event. Allen et al. (1998) states deep percolation will occur when the soil moisture content is above the soil's field capacity following a heavy rain or irrigation event. After a rain event, the soil moisture content is assumed to be at field capacity within the same day as the rain event. Therefore, groundwater recharge due to deep percolation can be estimated indirectly as the amount of soil moisture that is above the field capacity of the soil after a heavy rain event.

(2) Percolation is dependent of the soil's saturation and hydraulic conductivity. By assuming that percolation depends on the soil' saturation alone, the instantaneous percolation can be estimated directly. If we assume that the only vertical driving force of percolation is gravity (i.e. no capillary forces), percolation is equal to the hydraulic conductivity, K, of the soil and is given as:

$$q_p = K(s) = K_s s^{(2+3m)/m} \qquad [3.1]$$

where

q_p = percolation (mm/s),
K = unsaturated hydraulic conductivity (mm/s),
K_s = the saturated hydraulic conductivity (mm/s),
s = soil saturation (-),
m = Brooks and Corey's pore size distribution index (-)

In order to model deep percolation successfully, the processes that influence the soil moisture content must be understood. Soil moisture relates to infiltration and

evapotranspiration which can be estimated by a variety of methods. A brief discussion of the most common and widely used methods to estimate infiltration and evapotranspiration follows.

3.1 Soil characteristics and parameter definitions

In order to understand the processes of percolation, infiltration and evapotranspiration, some soil parameters have to be defined.

Porosity (η) of a soil is defined as the percentage of air voids in a soil column and is given as the ratio of the volume of voids (V_v) and total volume (V):

$$\eta = \frac{V_v}{V} \qquad [3.2]$$

Soil Moisture Content (θ) represents the amount of moisture in a soil and is defined by the ratio between the volume of water (V_w) and total volume (V) of a soil column:

$$\theta = \frac{V_w}{V} \qquad [3.3]$$

At saturation (θ_s), the soil moisture content is equal to the soil's porosity (η). Some specific levels of soil moisture content or moisture retention parameters are important to infiltration and evapotranspiration and are defined below:

Field Capacity (θ_{fc}) is defined as the amount of water held in soil after excess water has drained away and the rate of downward movement has materially decreased, which usually takes place within 2 - 3 days after a rain or irrigation in pervious soils of uniform structure and texture. Field capacity can also be defined as the soil moisture content that is held in the soil against gravitational forces or is the point where gravity forces are no longer the dominating force for drainage.

Wilting Point (θ_{wp}) is the lowest amount of soil moisture that can be extracted by plants for evapotranspiration. When the soil moisture drops below the wilting point, plants will start to wilt and become permanently damaged.

Residual Moisture (θ_r) is the soil moisture that can not be drained from the soil, even under strong vacuum pressure, due to strong molecular bonding to the soil particles.

Figure 3.1 shows the relation among the retention parameters and soil texture classes. Some average values for the retention parameters can be found in Table B.2 in Appendix B.

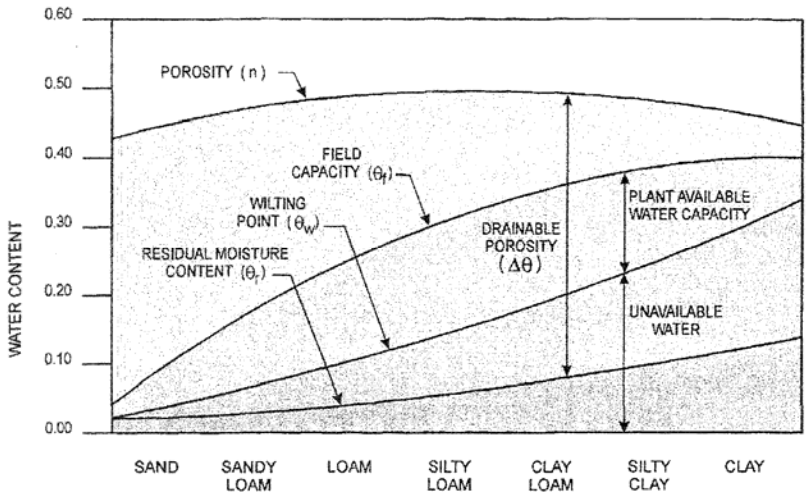

Figure 3.1 Relationship among moisture retention parameters and soil texture classes (Delleur 1998)

Effective Porosity (θ_e) is the maximum moisture content that can be abstracted from the soil column:

$$\theta_e = \eta - \theta_r \qquad [3.4]$$

Degree of Saturation (s) gives the fraction of the total volume of voids that are filled with water or the ratio of soil moisture content (θ) to saturated soil moisture content (θ_s). The degree of saturation will range from 0 to 1 and is given by:

$$s = \frac{V_w}{V_v} = \frac{\theta}{\theta_s} \qquad [3.5]$$

Effective Soil Saturation is the ratio of the available moisture to the maximum possible available moisture content:

$$s_e = \frac{\theta - \theta_r}{\eta - \theta_r} \qquad [3.6]$$

Hydraulic conductivity (K) is an important parameter for infiltration in the soil. Its definition is based on Darcy's law and can be given as "The volume of liquid flowing perpendicular to a unit area of porous medium per unit time under the influence of a hydraulic gradient of unity" (Delleur 1998). A soil's hydraulic conductivity has been expressed by [3.1]

Brooks and Corey's pore size distribution index (m) in [3.1] is defined as an empirical coefficient quantifying the distribution of pore sizes in a soil; it can be estimated using the logarithmic relationship between soil saturation (s) and the soil suction head (Ψ_f). The pore size distribution index can be estimates by draining a soil sample in stages, measuring s and Ψ_f at each stage, and fitting equation (3.8) to the resulting data (Mays 2005). The fitting equation is expressed as

$$s = \frac{\theta - \theta_r}{\theta_s - \theta_r} = \left(\frac{\psi_b}{\psi_f} \right)^m \quad [3.7]$$

where

m = Brooks and Corey's pore size distribution index (-),
s = soil saturation (-),
θ = soil moisture content (-),
θ_r = residual soil moisture content (-),
θ_s = saturated soil moisture content (-),
Ψ_b = air entry suction head (cm),
Ψ_f = wetting front suction head (cm).

The *wetting front suction head* (Ψ_f) is the energy due to the electrostatic forces between the water molecule polar bonds and the soil particle surface that draw the water around the particle surfaces and leaves air in the center of the voids. The *air entry suction head* (Ψ_b) also called bubbling pressure head, is the part of total head produced by the air exiting the soil. Rawls et al (1983) expressed the wetting front suction head in terms of the Brooks and Corey (1964) water retention parameters (Ψ_b and m) as

$$\Psi_f = \frac{2 + 3m}{1 + 3m} \left(\frac{\Psi_b}{2} \right) \quad [3.8]$$

where

Ψ_f = wetting front suction head (cm),
m = Brooks and Corey's pore size distribution index (-),
Ψ_b = air entry suction head (bubbling pressure head) (cm).

Rawls and Brakensiek (1983,1985) estimated soil parameters as a function of United States Department of Agriculture (USDA) textural classification. The parameters are listed in Table B.5 in Appendix B. These values were derived from the geometric mean of infiltration tests preformed on a large number of soil samples. The hydraulic conductivity used in the Green-Ampt infiltration equation is taken as half the saturated hydraulic conductivity (k_s) listed in Table B.5 (Rawls et al. 1982). There is a high variance in the parameters in Table B.5, however they provide good initial estimates of infiltration and percolation parameters and can be further calibrated in the models.

3.2 Infiltration estimation

Infiltration is defined as the process of water penetrating into the soil. The rate of infiltration is influenced by the condition of the soil surface, vegetative cover, and soil properties including porosity, hydraulic conductivity, and moisture content (Mays 2005). Infiltration is usually described as unsaturated flow until the water reaches the water table, where it becomes saturated flow. This point can be seen in Figure 3.2: If R(t) is the precipitation rate of a rainfall event and I(t) is the infiltration rate in a soil column, the point where the two functions intersect is called the time of ponding (t_i). This is also the time where infiltration transforms from unsaturated flow to saturated flow; the shaded are

under both curves is the total infiltration depth; the area above the infiltration curve and below the precipitation curve is the runoff depth or water that flows over the surface to an outlet or stream.

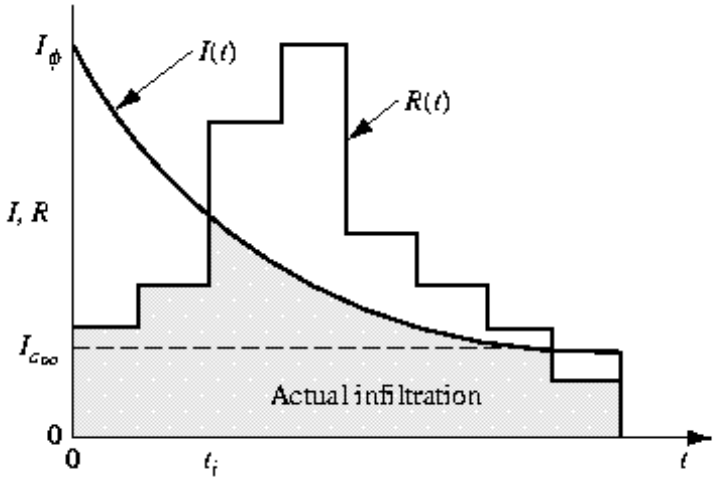

Figure 3.2 Relationship between infiltration (I) and precipitation or rainfall (R) (from http://www.cmdlet.com/demos/mgfc-course/mgfcinf.html)

The continuity equation for one-dimensional unsteady flow in a porous medium has to be satisfied by infiltration and is given as

$$\frac{\partial \theta}{\partial t} + \frac{\partial q_p}{\partial z} = 0 \qquad [3.9]$$

where θ = moisture content (-),
t = time (s),
q_p = percolation flux (m/s),
z = depth (m).

Darcy's law [3.10] relates the Darcy flux (q_p) to the rate of head-loss per unit length of soil. For flow in the vertical direction the head-loss per unit length is the change in total head (h) over a distance (z), where the negative sign in [3.10] indicates that total head decreases in the direction of flow due to friction.

$$q_p = -K \frac{\partial h}{\partial z} \qquad [3.10]$$

where K = hydraulic conductivity (m/s),
h = the sum of piezometric head (z) and suction head (Ψ_f) , i.e. $h = z + \Psi_f$.

Using Darcy's law [3.10] and soil water diffusivity, Equation (3.9) can also be expressed by the diffusion equation

$$\frac{\partial \theta}{\partial t} = -\frac{\partial q}{\partial z} = \frac{\partial}{\partial z}\left(D_s \frac{\partial \theta}{\partial z} + K \right) \qquad [3.11]$$

where D_s = soil water diffusivity (m^2/s), defined as

$$D_s = K \frac{\partial \psi_f}{\partial \theta} \qquad [3.12]$$

Equation (3.11) is a one-dimensional form of Richards' Equation, which governs unsteady unsaturated flow in a porous medium. Several methods have been developed to solve Richards' equation (Green-Ampt 1911, Horton 1940, Phillip 1957, Smith 1972, Parlange 1975, Swartzengruber 1987). They can be divided into two groups: empirical relationships and physics-based relationships. Empirical models use coefficients that are obtained by fitting of infiltration data to the empirical equations. One empirical model reviewed in this paper is the SCS method, developed by the U.S. Department of Agriculture, and widely used to determine surface runoff. The physics-based models use approximate analytical solutions to Richards' equation. Two widely used solutions are the Green-Ampt equation and Phillip's equation. Both equations assume a homogenous soil with initial uniform moisture content (θ_i). Each of the methods considered in this paper is briefly presented below; a more detailed discussion of each method can be found in Appendix A.

SCS method

The U.S. Department of Agriculture Soil Conservation Service (SCS) (1972), now the National Resources Conservation Service (NRCS), developed a rainfall-runoff relationship for watersheds. The SCS method relates infiltration to the total amount of precipitation during a storm event using land-use coefficients, CN numbers, to account for interception, retention and other processes that relate to run-off and infiltration. For the storm as a whole, the depth of excess precipitation or direct runoff P_e is always less than or equal to the depth of total precipitation P; likewise, after runoff begins, the additional depth of water retained in the watershed F_a, is less than or equal to some *potential maximum retention* S_{cn} (Figure 3.3).

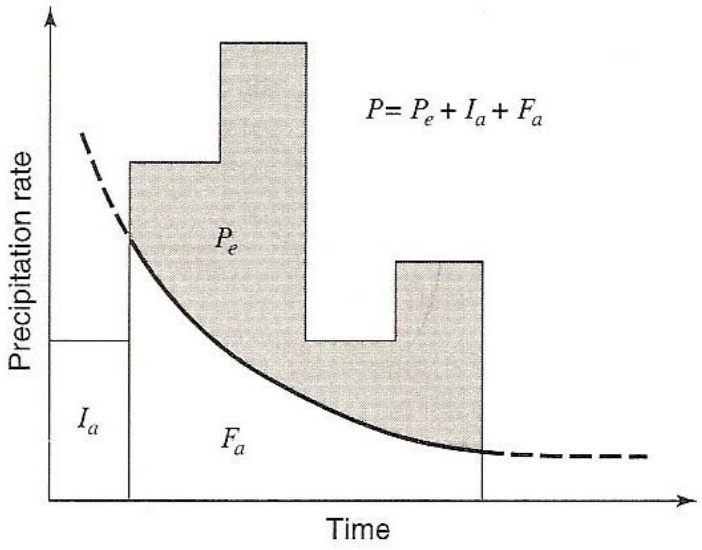

Figure 3.3 Variables in the SCS method of rainfall abstraction: I_a = initial abstractions, P_e = rainfall excess, F_a = continuing abstraction, and P = rainfall (from Mays, 2005).

There is some amount of rainfall I_a (initial abstraction before ponding) for which no runoff will occur; the potential runoff therefore is $P - I_a$. The SCS method assumes that the ratios of the two actual to the two potential quantities are equal, i.e.

$$\frac{F_a}{S_{cn}} = \frac{P_e}{P - I_a} \qquad [3.13]$$

From continuity,

$$P = P_e + I_a + F_a \qquad [3.14]$$

Field studies have shown that in first approximation

$$I_a = 0.2 S_{cn} \qquad [3.15]$$

Combining (3.13), (3.14), and (3.15) and solving for P_e gives

$$P_e = \frac{\left(P - 0.2 S_{cn}\right)^2}{P + 0.8 S_{cn}} \qquad [3.16]$$

Empirical studies by the SCS indicate that the potential maximum retention can be estimated as

$$S_{cn} = \frac{1000}{CN} - 10 \qquad [3.17]$$

where *CN* is a runoff curve number (see Appendix B) that is a function of land use, antecedent soil moisture, and other factors affecting runoff and retention in a watershed. If the above equations can be used to determine runoff for storms as a whole, the total abstractions can be used to determine the precipitation depth of infiltration. We will assume that all abstracted water will infiltrate after the rainfall event, although some of the abstracted water will remain in ponds and evaporate. With this assumption we can obtain a rough estimate of water remaining in the watershed that can infiltrate.

If the total abstractions (A) are substituted into the continuity equation (3.14) the solution is

$$A = P - P_e \qquad [3.18]$$

and substituting (3.16) for P_e gives

$$A = P - \frac{(P - 0.2S_{cn})^2}{P + 0.8S_{cn}} \qquad [3.19]$$

simplifying produces an equation to be used to calculate infiltration

$$A = \frac{0.04S_{cn}(30P - S_{cn})}{P + 0.8S_{cn}} \qquad [3.20]$$

A limit has to be imposed on (3.20). If the precipitation (P) is less than the initial abstractions (I_a), equ.(3.20) will not work but the infiltration can be assumed to be equal to precipitation (P).

The SCS method is widely used for estimating runoff and infiltration because of its simplicity and its ability to describe a variety of land uses. It is crucial to select a curve number that accurately represents the watershed. Curve numbers and the methods used to select a representative CN value are described in Appendix B.

One problem with the SCS method is that it estimates infiltration using the rainfall event as a whole and does not account for the rainfall event's length and intensity. This may lead to an overestimate of infiltration for short, high intensity storms, i.e. the rain may not have the time to infiltrate. Other methods have been developed to account for the intensity and period of a rainfall event. Two methods that estimate infiltration and do account for intensity and duration of rainfall are the Green-Ampt method and Phillip's method.

Green-Ampt method

The Green-Ampt method can be used to estimate infiltration for rainfall events with uniform and non-uniform rain intensity. Green and Ampt (1911) developed an

approximate solution for Richards' equation (3.11) that has been widely used and improved upon. It is easy to use and relies on a few soil properties that can be estimated using Table B.5 in Appendix B. A description of the Green-Ampt method can be found in many textbooks, and is given in Appendix A. *Green and Ampt* (1911) started their analysis with the distribution of soil moisture during the downward movement of water during a rainfall event (Figure 3.4). The soil moisture profile changes as a function of time (Figure 3.5) during the wetting event as the wetting front propagates downward.

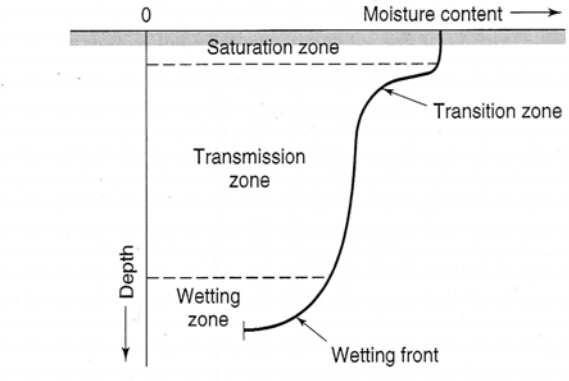

Figure 3.4 Moisture zones during infiltration (Mays 2005 after Chow et al. 1998)

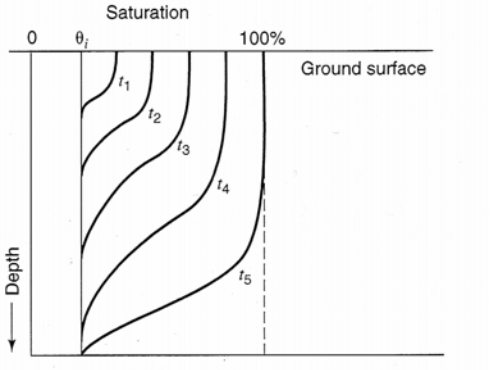

Figure 3.5 Moisture profile as a function of time for water added to the soil surface (Mays 2005)

Green and Ampt (1911) proposed a simplified picture of the wetting front (Figure 3.6). The wetting front is a sharp boundary dividing the soil with moisture content (θ_i) below from a saturated soil with moisture content η above (Mays 2005).

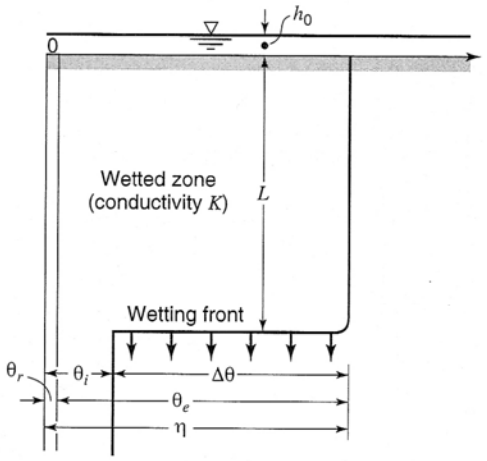

Figure 3.6 Variables in the Green–Ampt infiltration model. The vertical axis is the distance from the soil surface; the horizontal axis is the moisture content of the soil (Mays 2005 after Chow et al. 1998)

The Green-Ampt equation for infiltration rate (f) is

$$f(t) = K\left[\frac{\psi\Delta\theta}{F(t)} + 1\right] \qquad [3.21]$$

and cumulative infiltration F is

$$F(t) = Kt + \psi\Delta\theta \ln\left(1 + \frac{F(t)}{\psi\Delta\theta}\right) \qquad [3.22]$$

where K = hydraulic conductivity of the soil (cm/hr)
Ψ = the wetting front soil suction head (cm)
$\Delta\theta$ = the change of water content available for infiltration = (η-θ_i)
η = soil porosity (-)
θ_i = the initial moisture content (-).

The Green-Ampt method was originally developed assuming a homogenous soil with initial uniform moisture content (θ_i) for (3.21 and 3.22) which are the most widely used Green-Ampt equations, but many researchers have expanded the Green-Ampt method to cover scenarios of non-uniform soil moisture. These expansions are discussed in Appendix A. The Green-Ampt method is widely accepted and used to estimate infiltration.

Phillip's equation

Phillip (1957) presented a closed-form solution for the soil infiltration capacity. Starting from the diffusion-type unsaturated flow equation, Richards' 1-D flow equation, and assuming a homogeneous soil with an initial uniform moisture content (θ_i) and applied moisture content at the surface (θ_s), Phillip (1957) derived a series expansion solution for the cumulative infiltration (F) as a function of time (Delleur 1998) as:

$$F(t) = \sum_{n=1}^{\infty} A_n(\theta) t^{n/2} + K_i t \qquad [3.23]$$

where the coefficients A_n are functions of the volumetric moisture content. These coefficients are the solution of ordinary partial differential equations, and K_i is the permeability corresponding to the initial volumetric moisture content. Phillip (1957) proposed that the first two terms could be used to model infiltration satisfactorily, resulting in

$$f(t) = \frac{1}{2} S_s t^{-1/2} + A \qquad [3.24]$$

where $f(t)$ = infiltration rate (cm/hr),
S_s = sorptivity (cm/hr$^{1/2}$),

t = time from ponding (hr),
A = parameter with dimension of conductivity (cm/hr)

Sorptivity is defined as the characterization of the ability of the soil to absorb water in the absence of gravity (Delleur 1998). Youngs (1964) developed an approximation for S_s:

$$S_s = \left(2(\eta - \theta_i)K\Psi_f\right)^{1/2} \quad [3.25]$$

where S_s = sorptivity (cm/hr$^{1/2}$),
η = total soil porosity (-),
θ_i = initial soil water content (-),
K = effective hydraulic conductivity (cm/hr),
Ψ_f = wetting front suction head (cm)
The time of ponding, t_p (hr), can be estimated as

$$t_p = \frac{S_s^{\,2}\left(i - A/2\right)}{2i(i - A)^2} \quad \text{for } i \geq A \quad [3.26]$$

The cumulative infiltration (F) as a function of infiltration capacity (f) can be given as

$$F = \frac{S_s^{\,2}\left(f - A/2\right)}{2(f - A)^2} \quad \text{for } f \geq A \quad [3.27]$$

Phillip's equation is not as widely used as the Green-Ampt equation. It requires a few more steps to estimate infiltration but produces results comparable to the Green-Ampt equation. Phillip's equation was used by Kim et al. (1996) to develop an analytical solution to estimate groundwater recharge as will be described in Section 4.3.

3.3 Evapotranspiration estimation

Evapotranspiration (ET) is a major component of the hydrologic cycle. ET is important to groundwater recharge as an abstraction because it accounts for the water that plants extract through their roots from the soil water that has infiltrated from the ground surface. ET depends on plant type, climate, and soil characteristics. A standard method for estimating ET (Allen el at. 1998) is to first estimate a reference ET (ET_o) that is multiplied by a crop coefficient (k_c) to obtain the potential ET (ET_c). Crop coefficients depend on plant characteristics and local conditions. The potential ET (ET_c) is multiplied by a stress coefficient (k_s) to represent the water stress on the crop to obtain actual ET (ET_a). Therefore ET_a can be estimated using

$$ET_a = k_c k_s ET_0 \quad [3.28]$$

where

ET_a = actual evapotranspiration (mm/day),
k_c = crop coefficient (-),
k_s = water stress coefficient (-),
ET_0 = reference evapotranspiration (mm/day)

Methods used to estimate the crop coefficient and the water stress coefficient are described in Appendix C. Methods used to estimate the reference evapotranspiration (ET_0) are discussed in the next section.

Calculating reference evapotranspiration (ET_0)

The reference evapotranspiration is defined by Allen el al. (1998) as "the rate of evapotranspiration from a hypothetical crop with an assumed crop height (0.12m) and a fixed canopy resistance (70 s/m) and albedo (0.23) which would closely resemble evapotranspiration from an extensive surface of green grass cover of uniform height, actively growing, completely shading the ground and not short of water" (Trajkovic 2005). Many methods have been developed to estimate the reference evapotranspiration but lately the Food and Agriculture Organization (FAO) of the United Nations and the American Society of Civil Engineers (ASCE) have pushed to develop a standardized method for estimation of ET_0. The International Commission for Irrigation and Drainage and the FAO have proposed using the Penman-Monteith method as the standard method for estimating reference evapotranspiration (Trajkovic, 2005) and for evaluating other methods (Allen et al., 1994a, b). The FAO-56 Penman-Monteith (FAO-56 PM) method uses

$$ET_0 = \frac{0.408\Delta\left(R_h - G\right) + \gamma \frac{C_n}{T+273} U_2 \left(e_a - e_d\right)}{\Delta + \gamma\left(1 + C_d U_2\right)} \qquad [3.29]$$

where

ET_0 = reference evapotranspiration (mm day^{-1})
Δ = saturation vapor pressure function slope (kPa °C^{-1})
T = air temperature (°C)
γ = psychometric constant (kPa °C^{-1})
G = soil heat flux density (MJ m^{-2} day^{-1})
U_2 = the average 24 hour wind speed at 2 m height (m s^{-1})
R_h = net solar radiation (MJ m^{-2} day^{-1})
$e_a - e_d$ = vapor pressure deficit (kPa)
C_n = numerator constant
C_d =denominator constant

The constants depend on reference type and time scale of estimate and are listed in Table 3.1. 'Short reference (ET_{os})' in Table 3.1 refers to clipped grass and 'tall reference (ET_{ot})' refers to alfalfa. For calculations in this paper, we will estimate reference evapotranspiration (ET_0) as short reference grass.

Table 3.1 Value for C_n and C_d

	Short reference (ET_{os})		Tall reference (ET_{ot})		
Calculation time step	C_n	C_d	C_n	C_d	Units for ET
Daily	900	0.34	1600	0.38	mm/day
Hourly or shorter during daytime[a]	37	0.24	66	0.25	mm/hr
Hourly or shorter during nighttime[e]	37	0.96	66	1.7	mm/hr

[a]For application , daytime is defined as time when net radiation,$R_n > 0$, nightime when $R_n=0$
Taken from Itenfisu et al. (2003)

The extensive weather data required by the FAO-56 PM method may not be available at all sites. Therefore less climate data intensive methods are used to estimate a reference ET_0. These methods include a temperature based modified Penman-Monteith equation, the Hargreaves equation, and two equations developed by Irmak et al. (2003). The temperature based modified Penman-Monteith equation uses the FAO-56 PM equation and estimates the required climate data using temperature based equations. These equations are given in Appendix C.3.

The Hargreaves equation is one of the simplest equations to estimate ET_0 and is expressed as (Hargreaves et al. 1985):

$$ET_0 = 0.0023 R_a \left(\frac{T_{\max} + T_{\min}}{2} + 17.8 \right) \sqrt{T_{\max} - T_{\min}} \qquad [3.30]$$

where

R_a = extraterrestrial radiation (MJ $m^{-2} day^{-1}$)
T_{max} = maximum air temperature (°C)
T_{min} = minimum air temperature (°C)

Hargreaves developed the equation from data collected at Davis, California. Hargreaves originally published his equation in 1977 but modified and republished it in 1985. "The 1985 Hargreaves method is often used to provide ET_0 predictions for weekly or longer periods for use in regional planning, reservoir operation studies, canal design capacities, regional requirements for irrigation, potential for rain-fed agricultural production, and, under some situations, for irrigation scheduling" (Hargreaves and Allen, 2003). The Hargreaves method requires minimal climate data, and is relatively reliable. Jenson et al. (1990) showed that the Hargreaves equation ranked highest of 20 ET_0 methods that only require air-temperature when compared to lysimeter measurements at 11 locations.

Trajkovic (2005) compared the Hargreaves equation and the temperature-based modified FAO-56 PM (PMt) to the FAO-56 PM method. Trajkovic found that both the PMt method and Hargreaves method tend to overestimate mean annual ET. Trajkovic (2005) derived the following calibration equations for the two methods:

$$ET_{0,cpmt} = 0.949 ET_{0,pmt} + 0.013 \quad [3.31]$$

$$ET_{0,ch\arg} = 0.817 ET_{0,h\arg} + 0.320 \quad [3.32]$$

where $ET_{0,pmt}$ and $ET_{0,harg}$ are the ET_0 estimated by the PMt- method and the Hargreaves-method, respectively, and $ET_{0,cpmt}$ and $ET_{0,charg}$ are the calibrated ET_0 for each method

Another two methods where developed by Irmak et al. (2003) to estimate reference evapotranspiration (ET_0) based on solar or net radiation and mean temperature. The equations were tested for humid climates. Evapotranspiration estimates were good compared to the FAO-56 PM method. Irmak et al.'s equations are

$$ET_0 = -0.611 + 0.149 R_s + 0.079 T_m \quad [3.33]$$

$$ET_0 = 0.489 + 0.289 R_n + 0.023 T_m \quad [3.34]$$

where

ET_0 = grass reference evapotranspiration [mm day^{-1}]
R_s = solar radiation (MJ m^{-2} day^{-1})
R_n = net solar radiation (MJ m^{-2} day^{-1})
T_m = mean daily air temperature (°C).

Any of the methods described above can be used to estimate ET_0. The most widely accepted method is the FAO-56 PM method but it requires data that may not be available at every weather station. All the other methods have shown good results when compared to the FAO-56 PM and all will give good estimates of ET_0.

Methods used to estimate the various parameters needed for the FAO-56 PM equation can are given in Appendix C, along with the methods used to estimate the crop and water stress coefficients.

4.0 Physics-based models of groundwater recharge

The physics-based models use equations for physical processes that occur in a soil column to estimate groundwater recharge. Equation (1.5) indicates that percolation is a function of infiltration, evapotranspiration and soil moisture. The easiest way to describe this relationship is with a water budget in a soil column. The soil column is treated as a hypothetical container that has a depth equal to the root depth of the vegetation that grows on the surface of the container. This depth is also known as the root zone. Estimates for the root depth of different plants are given in Appendix D. The water that percolates below the root zone is assumed to be beyond the reach of the roots; it becomes the groundwater recharge. A schematic picture of the processes in the soil container that influence groundwater recharge is given in Figure 4.1.

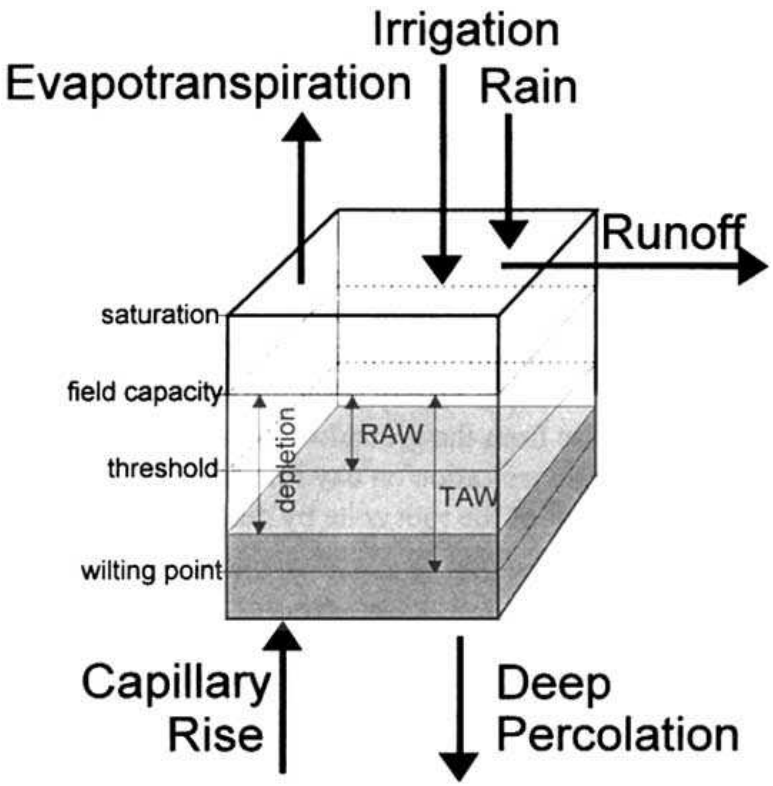

Figure 4.1 Soil water budget (Allen et al. 1998)

A water budget for estimating groundwater recharge (called deep percolation in Figure 4.1) was developed by Allen et al. (1998). A modified version of Allen's groundwater budget is given as

$$R_i = \left(P_i - RO_i\right) + Irr_i + CR_i - ET_{a,i} \pm \Delta S_i / t \qquad [4.1]$$

where

R_i = groundwater recharge for day i (mm),
P_i = precipitation for day i (mm),
RO_i = runoff for day i (mm),
Irr_i = net irrigation depth on day, i, that infiltrates the soil (mm),
CR_i = capillary rise depth from groundwater table on day, i (mm),
$ET_{a,i}$ = crop evapotranspiration depth on day, i (mm),
$\Delta S_i/t$ = change in storage in the soil for day i (mm).

Precipitation minus runoff (P - RO) is infiltration (I) and can be estimated using any of the methods discussed in Section 3.2. If irrigation is present, its contribution depends on land-use, the irrigation schedule and the vegetation type.

The amount of water transported upwards by capillary rise (CR) from the water table to the root zone depends on the soil type, the depth of the water table and the wetness of the root zone. CR can be assumed to be zero when the water table is more than about 1 m below the bottom of the root zone. The change in storage is a function of infiltration, evapotranspiration, soil type, and soil moisture content. Re-writing (4.1), ignoring irrigation and capillary rise, and inserting infiltration gives the relationship

$$R_i = I_i - ET_{a,i} \pm \Delta S_i / t \qquad [4.2]$$

Equation (4.2) gives the water budget assuming a homogeneous soil and vegetative cover (plant type). Larger areas, such as a land development or an entire watershed, that consist of a variety of soil types and vegetative covers, can be divided into workable sub-areas with homogeneous vegetative cover and soil type. To model a land development or watershed, the area should be divided into sections with similar soil type and vegetative cover, and recharge should be estimated for each soil type/vegetative cover combination. After the recharge for each combination is estimated, a weighted average of the combinations can be taken to estimate a representative groundwater recharge rate for the entire development or watershed.

Each physics-based groundwater recharge model tracks the soil water in the container, i.e. the change in storage, and estimates recharge using different equations but each uses the basic relationship (4.2). We will present and use three models: (1) the FAO model, (2) the Green-Ampt model, and (3) an analytical model developed by Kim et al. (1996). Each of the three models is discussed in detail below. In Section 6 an application will be presented.

4.1 FAO model

The FAO model was originally developed by Allen et al. (1998) as part of the FAO Irrigation and Drainage Paper 56 for estimating crop evapotranspiration. The FAO model uses a water budget for a soil container to estimate groundwater recharge (Figure 4.1) by tracking the root zone depletion (i.e. change in storage). Deep percolation (recharge) is the excess soil water depth following heavy rain, when the soil water content in the root zone exceeds field capacity. Below field capacity, the soil moisture is assumed to be held in the soil and the gravitational effect on the water is assumed to be negligible. If the soil moisture content exceeds the field capacity, it is assumed that the soil water content returns to field capacity (θ_{fc}) within the (same) day of the wetting (rainfall) event so that the depletion $D_{w,i}$ in equation (4.4) becomes zero, and all soil water that is above the field capacity will percolate past the root zone under gravity during the same day, Therefore, following heavy rain, deep percolation (groundwater recharge) due to precipitation is given as

$$DP_i = I_i - ET_{a,i} - D_{w,i-1} \geq 0 \qquad [4.3]$$

where

I_i = daily infiltration depth for day i (mm)

$ET_{a,i}$ = daily evapotranspiration depth for day i (mm)
$D_{w,i-1}$ = daily soil water depletion for day i (mm)

The daily soil water depletion is defined as the depth (amount) of soil water depleted by plants that is needed in the soil column to reach field capacity (see Appendix C). As long as the soil water content in the root zone is below field capacity (i.e., $D_{w,i} > 0$), the soil will not drain and $DP_i = 0$. The root zone depletion, D_w, can be estimated by rearranging (4.3) and using the previous day's estimates:

$$D_{w,i} = D_{w,i-1} - I_i + ET_{c,i} + DP_i \quad [4.4]$$

where

$D_{w,i}$ = root zone depletion depth for end of day, i (mm)
$D_{w,i-1}$ = root zone depletion depth at the end of pervious day, i-1 (mm)
I_i = infiltration depth for end of day, i (mm)
$ET_{c,i}$ = crop evapotranspiration depth on day, i (mm)
DP_i = water loss from root zone by deep percolation or on day, i (mm)

This model can be used to estimate annual groundwater recharge on a daily timescale. Infiltration and evapotranspiration can be estimated using any of the previously discussed methods (Section 3.0). Availability of soil and land-use data can influence the choice of method used to estimate infiltration. If little is known about the soil, the SCS method for estimating infiltration is recommended, because only soil type has to be specified. If more is known about the soil's characteristics, the Green-Ampt method can be used. Since the Green-Ampt method (3.12, 3.13) requires the change in soil water content available for infiltration ($\Delta\theta$), a transformation of the root zone depletion can be made to find $\Delta\theta$ using equation (4.5).

$$\Delta\theta = \left(\eta - \theta_{fc}\right) + \frac{D_w}{d_r} \quad [4.5]$$

Any of the methods for estimating reference evapotranspiration (ET_0) can be used, but the FAO-56 PM is recommended, and actual evapotranspiration (ET_a) can be estimated using the methods described in Appendix C. Using climate data from a climate station, each component of the soil water balance can be calculated, and equation (4.3) can be solved for each day of the year. Annual groundwater recharge will be the sum of the daily deep percolation (recharge) from equation (4.3). To initiate the soil water balance computations, an initial depletion, $D_{w,int}$, must be assumed. If the soil moisture is known for the initial soil condition, $D_{w,int}$ can be estimated using

$$D_{w,\text{int}} = \left(\theta_{fc} - \theta_{\text{int}}\right) d_r \quad [4.6]$$

where

$D_{w,int}$ = initial root zone depletion depth (mm),
θ_{fc} = soil moisture content at field capacity (-),
θ_{int} = initial soil moisture content (-),
d_r = root zone depth (mm).

If the initial soil moisture is not known and the soil moisture budget starts in the spring or after a heavy rain, the root zone can be assumed to be at field capacity and $D_{w,int}$ can be assumed to be zero. The step-by-step computational process for the FAO model is described in Section 6.1.

4.2 Green-Ampt model

The Green-Ampt model is similar to the FAO model but instead of tracking the root zone depletion, the Green-Ampt model tracks the soil saturation (s) and relates all the processes of the soil container to the soil saturation. The change in soil saturation can be expressed as

$$\frac{\partial s}{\partial t} = \frac{I - ET - q_p}{d_r \theta_s} \qquad [4.7]$$

and the soil saturation balance can be expressed as:

$$s_i = s_{i-1} + \left(\frac{I_i - ET_{a,i} - q_{p,i}}{d_r \eta} \right) \qquad [4.8]$$

where

s_i = soil saturation for time step i (-),
s_{i-1} = soil saturation for previous time step i (-),
I_i = infiltration depth for time step i (mm),
$ET_{a,i}$ = evapotranspiration depth for time step i (mm),
$q_{p,i}$ = percolation depth for time step i (mm),
d_r = root depth (mm),
η = soil porosity (-).

Each of the components of the soil water balance (4.2) can be related to soil saturation. For infiltration (I), the Green-Ampt method for estimating infiltration depth is used since soil moisture content availability ($\Delta\theta$) is a parameter in the Green-Ampt equations (3.13 & 3.14) and soil saturation can be related to $\Delta\theta$. The availability of soil moisture can be related to effective soil saturation (s_e) using

$$\Delta\theta = (1 - s_e)\theta_e \qquad [4.9]$$

and soil saturation (s) is related to effective soil saturation by

$$\frac{s_e}{s} = \frac{\theta_e}{\eta} \qquad [4.10]$$

where

$\Delta\theta$ = available soil moisture content (-),
s_e = effective soil saturation (-),
s = soil saturation (-),

θ_e = effective porosity (-),
η = porosity (-).

Definitions of the parameters used in (4.9) and (4.10) are given in Section 3.1.

Soil moisture relates to the root zone depletion (D_w) which is used to estimate the water stress coefficient (see Appendix C.3). In the FAO model, D_w is estimated directly using equation (4.4); for the Green-Ampt model, D_w will be estimated using equation (4.11) and the soil saturation.

$$D_{w,i} = (\theta_{fc} - s\eta)d_r \qquad [4.11]$$

where
$D_{w,i}$ = root zone depletion depth for time step i (mm),
θ_{fc} = soil moisture content at field capacity (-),
s = soil saturation (-),
η = soil porosity (-),
d_r = root zone depth (mm).

Percolation (recharge) is estimated directly from the instantaneous percolation rate. If we assume that the vertical driving force of percolation is gravity (i.e. no capillary forces), percolation is equal to the hydraulic conductivity, K, of the soil and is given by equation (3.1).

To initiate the soil water balance, an initial soil saturation level must be estimated. One option is to set the root zone depletion (D_w) equal to zero and to solve for the soil saturation. Since the soil moisture content is at field capacity (θ_{fc}) when D_w is equal to zero

$$s_{\text{int}} = \frac{\theta_{fc}}{\eta} \qquad [4.12]$$

An annual groundwater recharge can be determined by solving the soil water balance on an hourly time scale for one year. The sum of percolation depths for each time step will be the total percolation.

4.3 Analytical method

Kim et al. (1996) developed an approximate analytical solution of Richards' equation to describe a water budget of the unsaturated zone. The model divides time into storm periods (infiltration) and inter-storm periods (evapotranspiration and percolation). The method tracks soil saturation s ($0 \leq s \leq 1$), where $s = \theta/\theta_s$ is the degree of saturation with θ = moisture content, *and* θ_s = saturated value of the moisture content. The model relates infiltration, evapotranspiration and percolation to saturation s.

Kim et al. (1996) assume that infiltration occurs during storm periods and evapotranspiration and percolation occur in inter-storm periods only. In storm periods

Phillip's equation is used to estimate cumulative infiltration. For inter-storm periods, *Kim et al.* (1996) derived a relationship between evapotranspiration and percolation dependent on soil saturation (*s*). The rainfall intensity during storm periods is assumed constant and the potential evapotranspiration intensity is constant during inter-storm periods. The analytical equations are computationally intense and rely on long-term statistical data. The total annual recharge in Kim's model is the sum of recharge from excess infiltration (super saturation) plus the sum of percolation for the year.

Storm periods (Infiltration)

Cumulative infiltration is estimated using an equation derived from Phillip's equation (A.18). The cumulative infiltration equation derived by *Kim et al.* (1996) uses a time compression approximation (TCA) method to estimate infiltration rate and cumulative infiltration. TCA is related to aK_s in Phillip's equation.

Infiltration is given by

$$i(t) = \begin{cases} P & t \le t_p \\ (1/2)S_s(s_0)[t - t_c]^{-1/2} + aK_s & t > t_p \end{cases} \qquad [4.13]$$

and cumulative infiltration is

$$\begin{aligned} F(t) &= Pt & t \le t_p \\ F(t) &= Pt_p + S_r k_s^{1/2}([t - t_c]^{1/2} - t_e^{1/2}) + aK_s(t - t_p) & t > t_p \end{aligned} \qquad [4.14]$$

where

$F(t)$ = cumulative infiltration (mm)
P = rainfall intensity (mm day^{-1})
S_s = sorptivity
S_r = relates to sorptivity S_s
s_0 = initial soil saturation
K_s = saturated conductivity (mm day^{-1})
t_p = actual time to ponding (day)
t = time (day)
t_c = "condensation" time (day)
t_e = a time compression approximation (day)
a = coefficient ($0 \le a \le 1/3$).

A discussion of all parameters is given in Appendix A.

Soil saturation is tracked with the assumption that a uniform moisture profile is maintained by instantaneous redistribution of soil moisture in the root zone. During rainfall, and neglecting percolation, the soil moisture is given by

$$s(t) = s_0 + \frac{F(t)}{d_r \eta} \qquad [4.15]$$

where

s_0 = initial soil saturation (-)
$F(t)$ = cumulative infiltration (mm)
η = total porosity of the soil (-)
d_r = root depth (m).

In the model water cannot leave the soil-water reservoir during a rainfall period. Therefore the root zone may super-saturated ($s \geq 1.0$). When this occurs, the amount of saturation excess will be considered a contribution q_{se}^{cum} to the percolation generated up to time t.

$$q_{se}^{cum}(t) = d_r \eta [s(t) - 1] \qquad [4.16]$$

This amount will be added to the cumulative percolation.

Inter-storm periods (Evapotranspiration and Percolation)

Evapotranspiration and percolation are treated as functions of soil moisture. Percolation, q_p, is the unsaturated flow in a porous medium and is given as the vertical flux out of the soil-water reservoir. It is assumed to be due to gravity only and is related to the hydraulic conductivity, soil saturation and pore size distribution index as given by equation (3.1).

Evapotranspiration (ET) is also dependent on soil moisture s, i.e. higher ET will occur right after rain events and lower ET after the soil has dried out. Evapotranspiration flux out of the soil-water reservoir, ET, is estimated from the relationship

$$ET(s) = \beta(s) ET_p \qquad [4.17]$$

where $\beta(s)$ represents the evapotranspiration efficiency function and ET_p is the potential evapotranspiration rate. For computational ease, Kim *et al.* (1996) specify the evapotranspiration efficiency function as $\beta = s$. Even though this assumption underestimates total evapotranspiration rate under wet conditions and overestimates it under dry conditions it qualitatively describes the decrease of evapotranspiration when the soil dries out. The compensation of both errors depends on the soil hydraulic and vegetation properties, as well as on the climatic conditions. Potential evapotranspiration is calculated using a representative crop coefficient multiplied by the grass reference evapotranspiration estimated by one of the methods described in Appendix B.

The state of saturation in the soil-water reservoir is given by the equation

$$\frac{ds}{dt} = -\frac{q_p + ET}{d_r \eta} = -\frac{s}{d_r \eta}\left(K_s s^c + ET_p\right) \qquad [4.18]$$

where

q_p = the amount of percolation (mm/day),
ET = evapotranspiration (mm/day),

d_r = the root depth (mm),
η = total porosity of the soil (-),
$c = (2 + 2m)/m$,
m = pore size distribution index (Brooks and Corey, 1964).

A solution of equation (4.18) is

$$s(t) = \left(\left[s_0^{-c} + \frac{K_s}{ET_p} \right] \exp\left[\frac{cET_p}{d_r \eta} t \right] - \frac{K_s}{ET_p} \right) \qquad [4.19]$$

An approximate solution for the cumulative evapotranspiration E^{cum} is

$$E^{cum}(t) \approx d_r \eta s_0 \varepsilon^{1/c} \left(1 - \frac{s_{1(t)}}{s_0} \right) = \left(\frac{ET_p}{ET_p + K_s s_0^c} \right)^{1/c} E_1^{cum}(t) \qquad [4.20]$$

where
$$E_1^{cum} = d_r \eta s_0 \left(1 - \frac{s_1(t)}{s_0} \right) \qquad [4.21]$$

and
$$s_1(t) = s_0 \exp\left[-\frac{ET_p}{d_r \eta} t \right] \qquad [4.22]$$

For percolation q_p^{cum} an approximate solution is

$$q_p^{cum}(t) = d_r \eta [s_0 - s(t)] - ET^{cum}(t) \qquad [4.23]$$

where *s(t)* is given by (4.19). Further explanations of these equations are given by Kim et al. (1996). These equations can be used to measure groundwater recharge assuming that rainfall intensity is constant. An application of the above equations to the estimation of long term ground water recharge has been developed as follows.

According to *Kim et al.* (1996), the solutions (equations 4.19 and 4.23) require a constant rainfall rate P and a constant potential evapotranspiration intensity ET_p. By modeling the meteorological forcing, after *Eagleson* (1978), as a Poisson arrival process of rectangular rainfall pulses with rainfall intensity P and duration t_d (both exponentially distributed random variables) both requirements are met. A schematic picture of this process is shown in Figure 4.2.

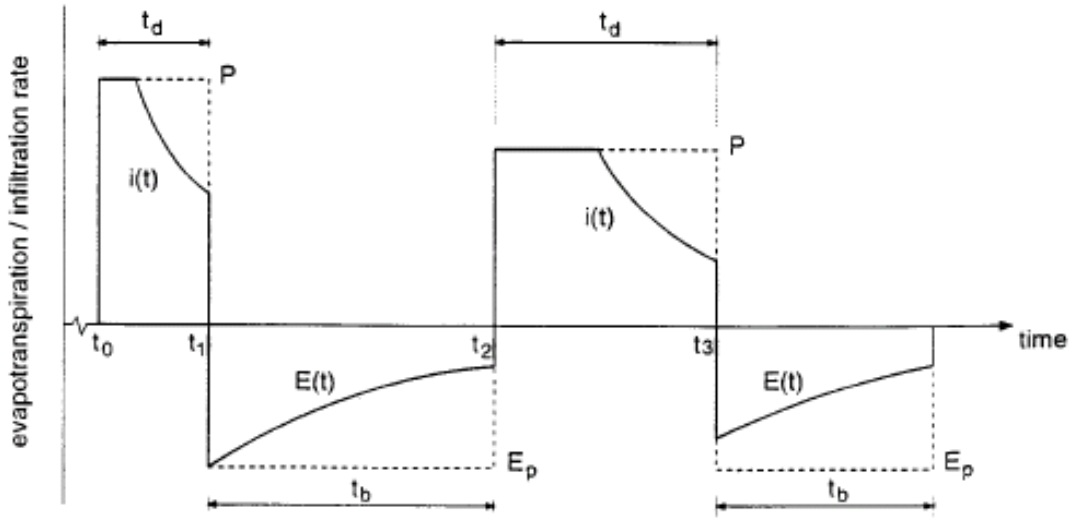

Figure 4.2 Diagram of the Poisson rectangular pulses that constitute the meteorological forcing. Computations are only performed at times t_1, t_2, and t_3, etc. (*Kim et al. 1996*)

It follows from the definition of exponential distributions that a particular climate is completely defined by the mean values $\mu[P]$, $\mu[t_d]$, $\mu[t_b]$, and ET_p. This method is a crude representation of climate but it nevertheless captures the hydrologically important intermittency of rainfall.

Potential evapotranspiration ET_p can be estimated using the following relationship with the long-term average daily potential evapotranspiration $\overline{ET_p}$.

$$\overline{ET_p} = \frac{\mu[t_b]}{\mu[t_d] + \mu[t_b]} ET_p \qquad [4.24]$$

Kim et al.'s analytical solution method was compared to a numerical solution of Richards' equation (Kim *et al.*, 1996) and showed good results for a period of 15 years. Even though the model is computationally intensive, it describes the processes of the groundwater recharge model (equations 1.4 and 1.5) better than the previous methods. It is stipulated that annual mean values $\mu[P]$, $\mu[t_d]$, $\mu[t_b]$, and E_p can be used to estimate annual groundwater recharge. It can be assumed that a in (4.13 & 4.14) can be set to 1/3 if ς is set to 1.0 for real soils. The values used by *Kim et al.* (1996) are given in Appendix B, Tables B.7 & B.8.

5.0 Saturated flow in the soil column (Seepage)

Seepage from a surface water body can recharge a shallow or even a deep aquifer effectively. Surface water bodies are streams, ponds, wetlands, lakes and even ditches. In land use classification they represent a special land surface class. The flow (seepage) from these water bodies is continuous as long as water is stored in them. A water budget for the surface water body can be used to determine the seepage flow into the soil. In most cases the seepage flow will become a groundwater recharge. If a surface water body dries out, the seepage will be interrupted.

Seepage from a water body can be estimated by using flow nets under the water body Examples for seepage from a ditch are shown in Figures 5.1a and b. As the depth to the water table increases, the flow lines approach their vertical asymptotes and the equipotential lines become horizontal. For the example in Fig 5.1a this occurs at an approximate depth y = 3(B + 2H)/2.

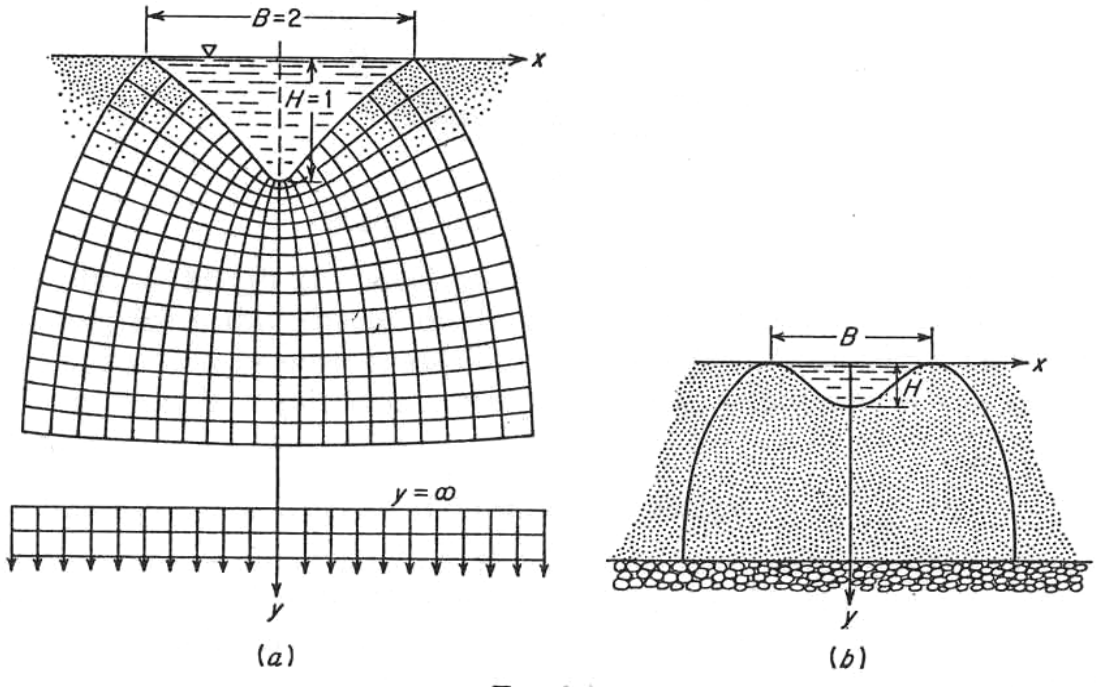

Figure 5.1: Flow net under a ditch (after Harr 1962)

For channels, streams, and ditches with a curvilinear perimeter, the seepage flow can be estimated as

$$q = K(B + 2H) \qquad [5.1]$$

where

q = seepage flow (m^3/s per m length),
K = saturated hydraulic conductivity (m/s) = Darcy permeability coefficient of the homogeneous and isotropic underlying soil,

B = channel width (m),
H = depth of water (m).

For channels, streams, and ditches with a trapezoidal shape, the quantity of seepage is

$$q = K\left(B + A_s H\right) \qquad [5.2]$$

where A_s is a shape coefficient ranging from 2 to 4 (Fig. 5.2)

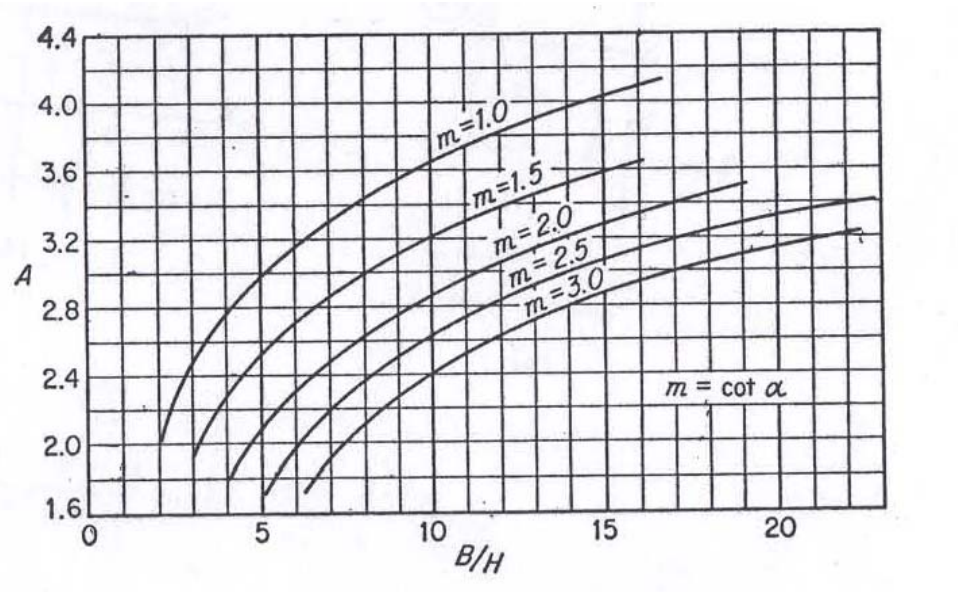

Figure 5.2: Coefficient m in equation 5.2 where m = cot α and α is the side slope angle from the horizontal (from Harr 1962, after Vedernikov 1934)

For channels, streams, or ditches with a triangular cross-section, the seepage flow is also given by equ. (5.2), but the coefficient A_s is given in Figure 5.3.
Considering the uncertainty in the hydraulic permeability K, equation 5.1 is a sufficiently good approximation for most small streams, ditches and channels.

For lakes and ponds with a circular shape, the quantity of recharge is related to the diameter B of the water body and the depth of water H.

$$q = K\left(B + 2H\right)^2 \frac{\pi}{4} \qquad [5.3]$$

where all variable are as previously defined.

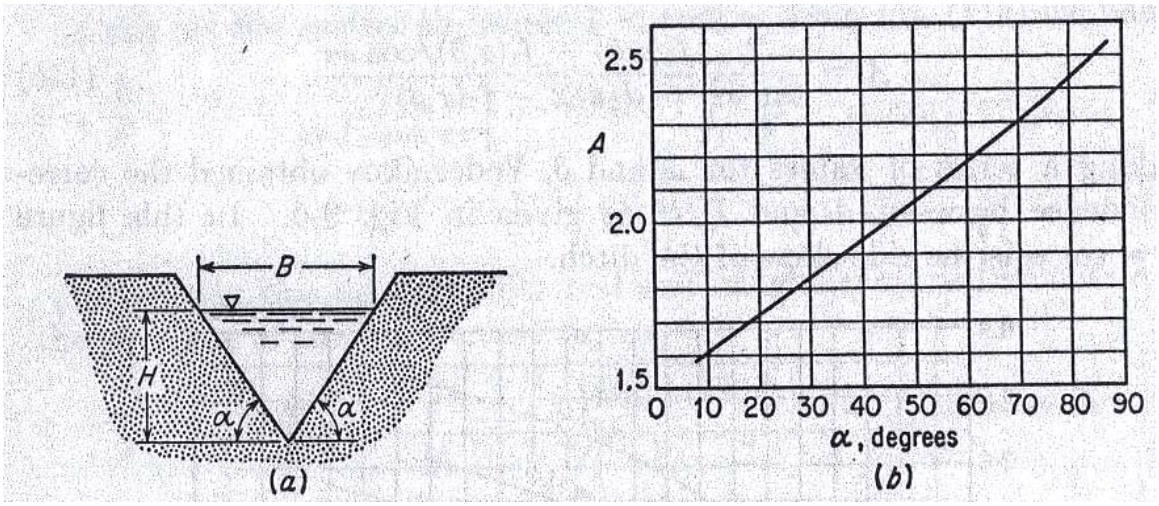

Figure 5.3: Coefficient A_s in equation 5.2 (from Harr 1962 after Vedernikow 1934)

For lakes and ponds of non-circular shape, the quantity of recharge can be estimated from

$$q = K\left(A + HP_r\right) \qquad [5.4]$$

where

A = surface area (m^2)

P_r = circumference (shoreline length) (m)

Seepage is primarily dependent on the shape, depth, and the hydraulic conductivity of the soil underneath the water body. Seepage is important because it can be a constant source of groundwater recharge.

If a surface water body is lined with a highly impermeable material such as clay, or has become filled with fine sediment, seepage through the bottom of the surface water body may be much reduced or even negligeable, but there may still be seepage through the banks near the water surface. Before applying the above equations it is necessary to identify layers of reduced permeability at the bottom of a surface water body.

If an entire pond of surface area A_s and average water depth H is lined with a layer of thickness h and permeability K, the seepage flow is on the order

$$q = KAH/h \qquad [5.5]$$

Refinements can be made by a more detailed seepage flow analysis.

6.0 Application (Example)

A sample problem is presented to compute groundwater recharge estimates by the FAO and Green-Ampt models for a study site which is the watershed of a tributary to the Vermillion River in Dakota County, MN. Four scenarios, i.e. developmental stages, where used to estimate the changes in groundwater recharge with urban development. The scenarios are pre-development (natural), present, and two future development stages (plus 50 years and plus 100 years).

6.1 Study Site

The sub-watershed of an un-named 2nd order tributary of the Vermillion River near Lakeville, Minnesota, was chosen as the study site (Figures 6.1 and 6.2). The Vermillion River is located in Dakota and Scott Counties just south of the Twin Cities in Minnesota, and is a designated DNR trout stream that flows into the Mississippi River. The specific sub-watershed covers about 6.8 km^2 area and was selected because it has both undeveloped (i.e. agricultural and natural) land, and developed (i.e. urban residential and commercial) areas. About 60% of the sub-watershed is undeveloped, and about 40% is developed land. A breakdown of present land-use is given in Table 6.1.The soils in the sub-watershed are mostly glacial deposits of sandy loams, silty loams, silty clay loams, and loams.

6.2 Watershed Properties

Properties of the tributary sub-watershed were extracted from a GIS map of the Vermillion River watershed. Maps was constructed, using ArcMap, with free data from the MNDNR data deli at www.deli.state.mn.us and Metropolitan Council at www.datafinder.org. The multi-layer maps included aerial photography, topography, soil data, the stream networks of Dakota and Scott counties, and land-uses from the 2005 census (Figures 6.2 to 6.5).

The sub-watershed was delineated using the topographic map (Figure 6.3).

The soil types of the sub-watershed are shown in Figure 6.4. The soil types were divided into textural classes and were found to be mostly sandy loams (SL), silty loams (SIL), silty clay loams (SICL), and loams (L). A small section of the watershed consisted of muck and in some areas the soil was unknown. The areas consisting of muck were small and ignored for simplicity of calculations. The areas of unknown soil types were assumed to have the same distribution of the soil types as those in the known areas. In summary the soils in the sub-watershed consist of 5% sandy loam, 38.7% silty loam, 19.2% silty clay loam and 36.8% loam. Soil parameters given in Table 6.2 were estimated using average values from Table B.5 in Appendix B depending on the textural class.

The land-use types in the sub-watershed are shown in Figure 6.5. Data from the 2005 Census gave this land use map. Ten different land-uses were found in the sub-watershed. The associated areas are listed in Table 6.1. For each land-use type, the percent of impervious area was also estimated (Table 6.1) using the values from the SCS curve number table (Table B.2 in Appendix B).

Table 6.1 Land-use types and associated areas in the sub-watershed

Land-use type	Description	Percent of watershed	Area	Percent impervious surfaces
		%	km^2	%
1	Agriculture	25.1	1.695	0
2	Parks/preserves	12.7	0.861	5
3	Industrial	1	0.068	72
4	Institutions	8	0.542	35
5	Multi-family homes	7	0.474	65
6	Retail/office	1.7	0.115	85
7	Single family homes	21	1.423	30
8	Town-homes	1	0.068	65
9	Undeveloped/natural	21.5	1.457	0
10	Roads/impervious	1	0.068	100
Total watershed		100	6.778	

Table 6.2 Estimated soil parameters in the sub-watershed

Soil type (USGS class)	SCS soil class	Porosity	Effective porosity	Field capacity	Wilting point	Saturated hydraulic conductivity	Pore size distribution index	Wetting front soil suction head
		η (θ_s)	θ_e	θ_{FC}	θ_{WP}	K_s	λ	Ψ
		-	-	-	-	cm/hr	-	cm/hr
Sandy loam (SL)	B	0.453	0.412	0.230	0.110	2.18	0.378	11.01
Silty loam (SiL)	B	0.501	0.486	0.290	0.150	0.68	0.234	16.68
Loam (L)	B	0.463	0.434	0.250	0.120	1.32	0.252	11.15
Silty clayey loam (SiCL)	B	0.471	0.432	0.335	0.205	0.2	0.177	27.3

A curve number (CN) was assigned (Table 6.3) to each land-use type for each AMC class (see Appendix B) for use with the SCS infiltration method in the FAO model. The curve numbers were taken from the CN tables (Table B.2 in Appendix B).

A vegetation (plant) type was assigned to each land-use type using the vegetation descriptions in the evapotranspiration tables in Appendix D. Land-uses with similar plant types were grouped together into land cover groups. Three plant (vegetation) types (row crops, turf grass, and trees with grass) were assumed to be associated with the different land-use types in the study area: (1) row crops were associated with corn for agriculture;

(2) turf grass was associated with industrial and institutional developments, multi-family homes, retail/offices, single family homes, and town-homes; (3) trees with grass were associated with parks/preserves and undeveloped/natural land uses. For each vegetation type, three crop coefficients (early, middle, and end of season) were assigned from Table D.1 in Appendix D. A root depth was assigned for each vegetation type and a p value was obtained from table D.3. The crop coefficients, root depths, and p values for the study site can be found in Table 6.4

Table 6.3 SCS curve numbers in the sub-watershed

Land-use type	Description	Curve numbers		
		AMC I	AMC II	AMC III
1	Agriculture	62	78	92
2	Parks/preserve	41	61	80
3	Industrial	77	88	97
4	Institutions	50	69	86
5	Multi-family homes	70	85	97
6	Retail/office	79	92	98
7	Single family homes	51	70	87
8	Town-homes	70	85	97
9	Undeveloped/natural	30	48	69
10	Roads/impervious	100	100	100

Table 6.4 Vegetation types and evapotranspiration parameters in the sub-watershed

Vegetation type	Land-use types	Crop coefficient			Root depth	p
		k_{early}	k_{mid}	k_{end}	d_r	
		-	-	-	mm	-
Row crops	1	0.15	1.15	0.5	1700	0.5
Turf grass	3,4,5,6,7,8	0.9	0.95	0.95	500	0.5
Trees / grass	2,9	0.8	0.85	0.85	1000	0.5

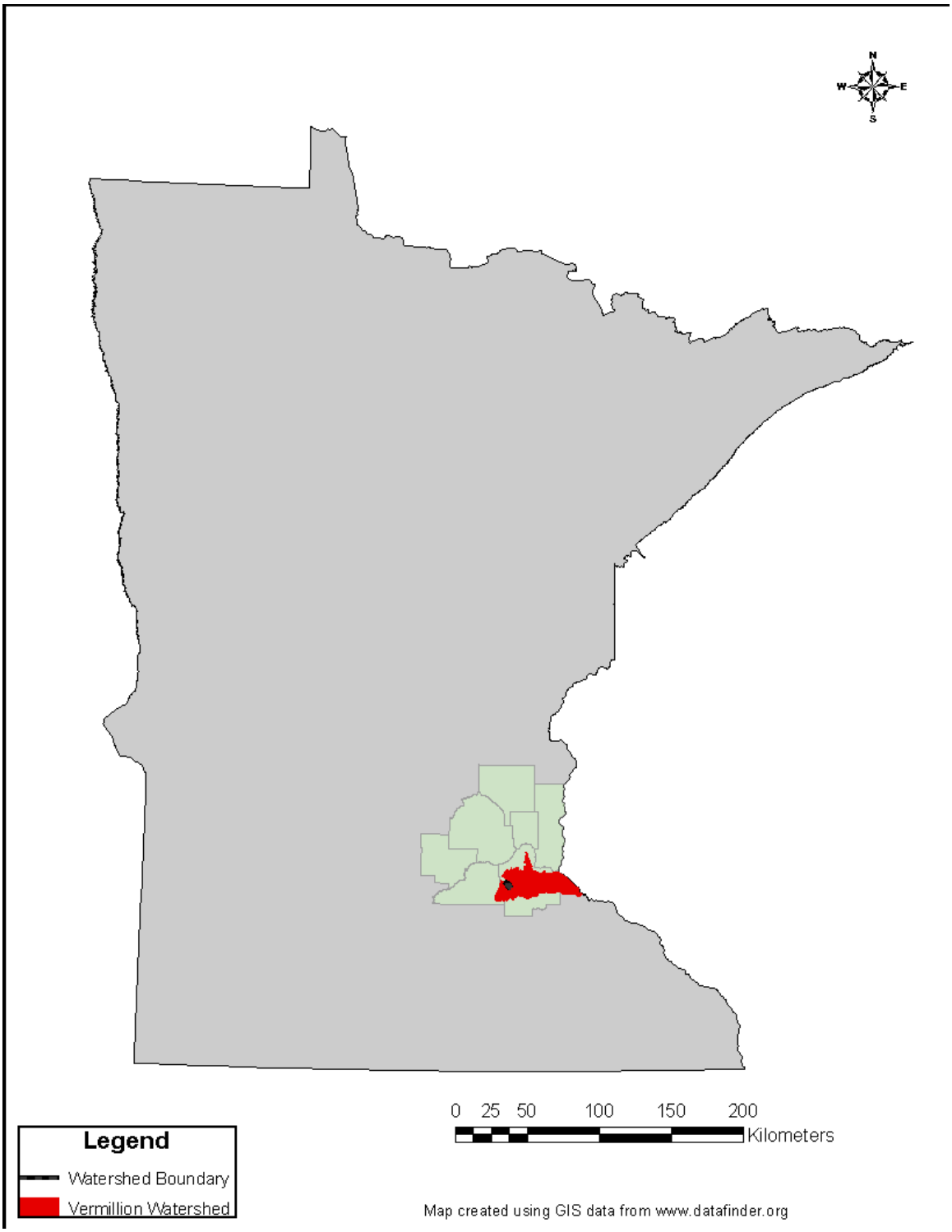

Figure 6.1a: Vermillion River watershed location in the Twin Cities metropolitan area of Minnesota

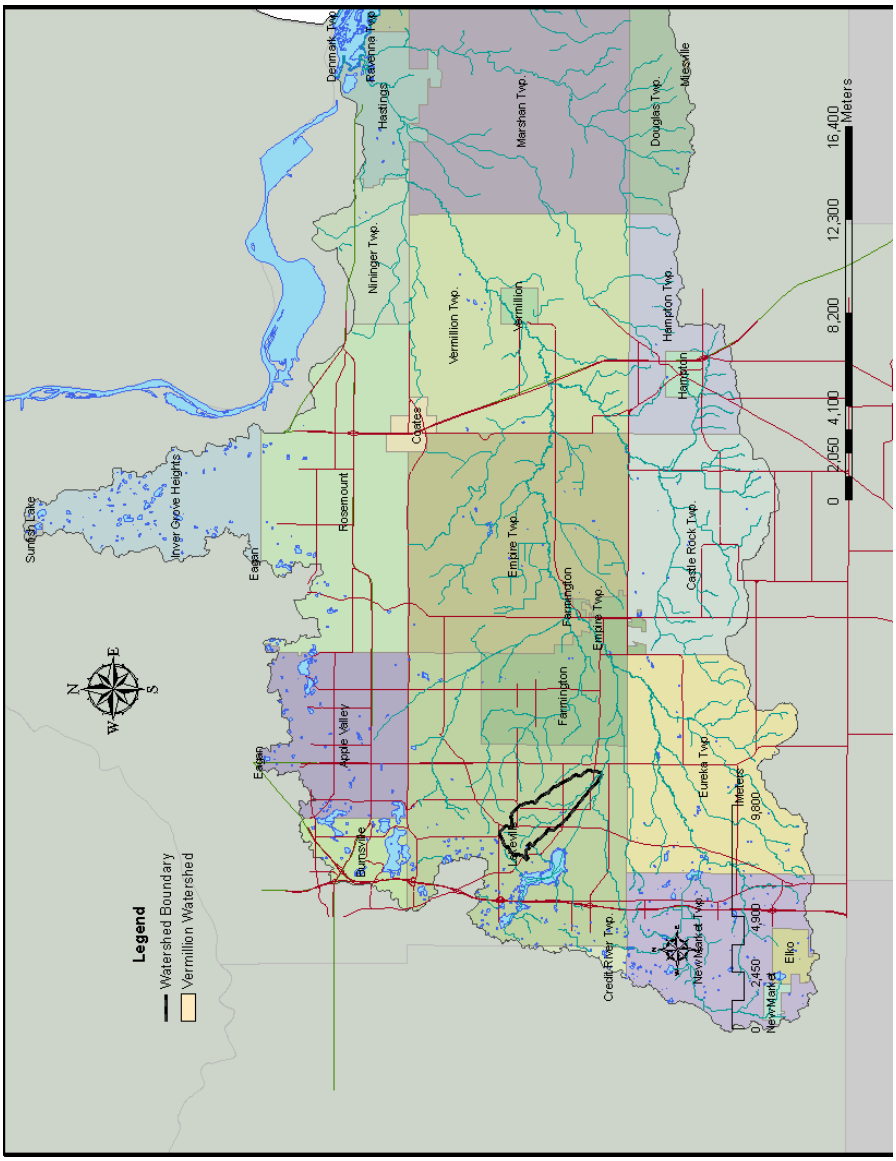

Figure 6.1b Vermillion River watershed – stream network, townships and study site sub-watershed location

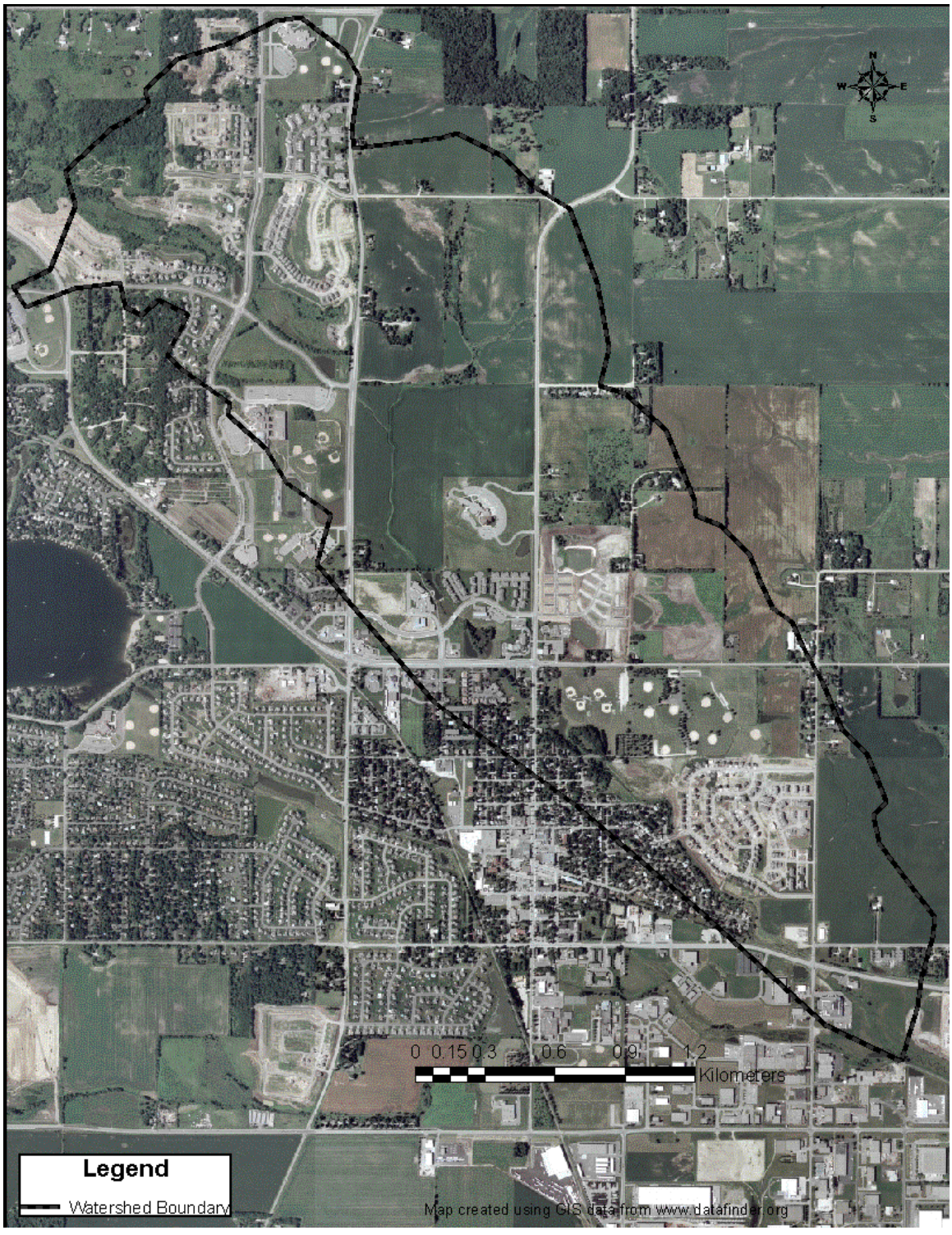

Figure 6.2 Aerial photograph of the sub-watershed

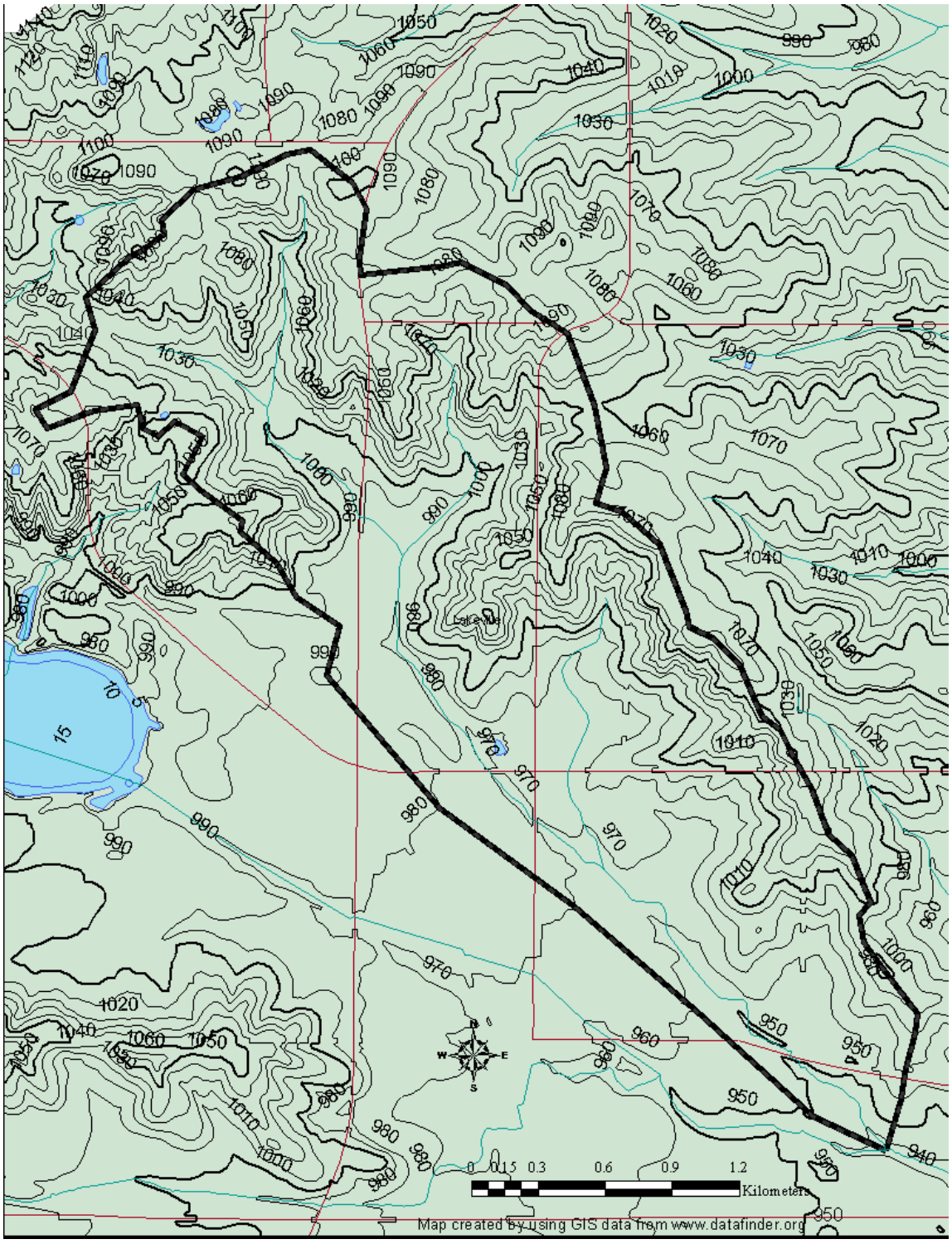

Figure 6.3 Topographic map of the sub-watershed

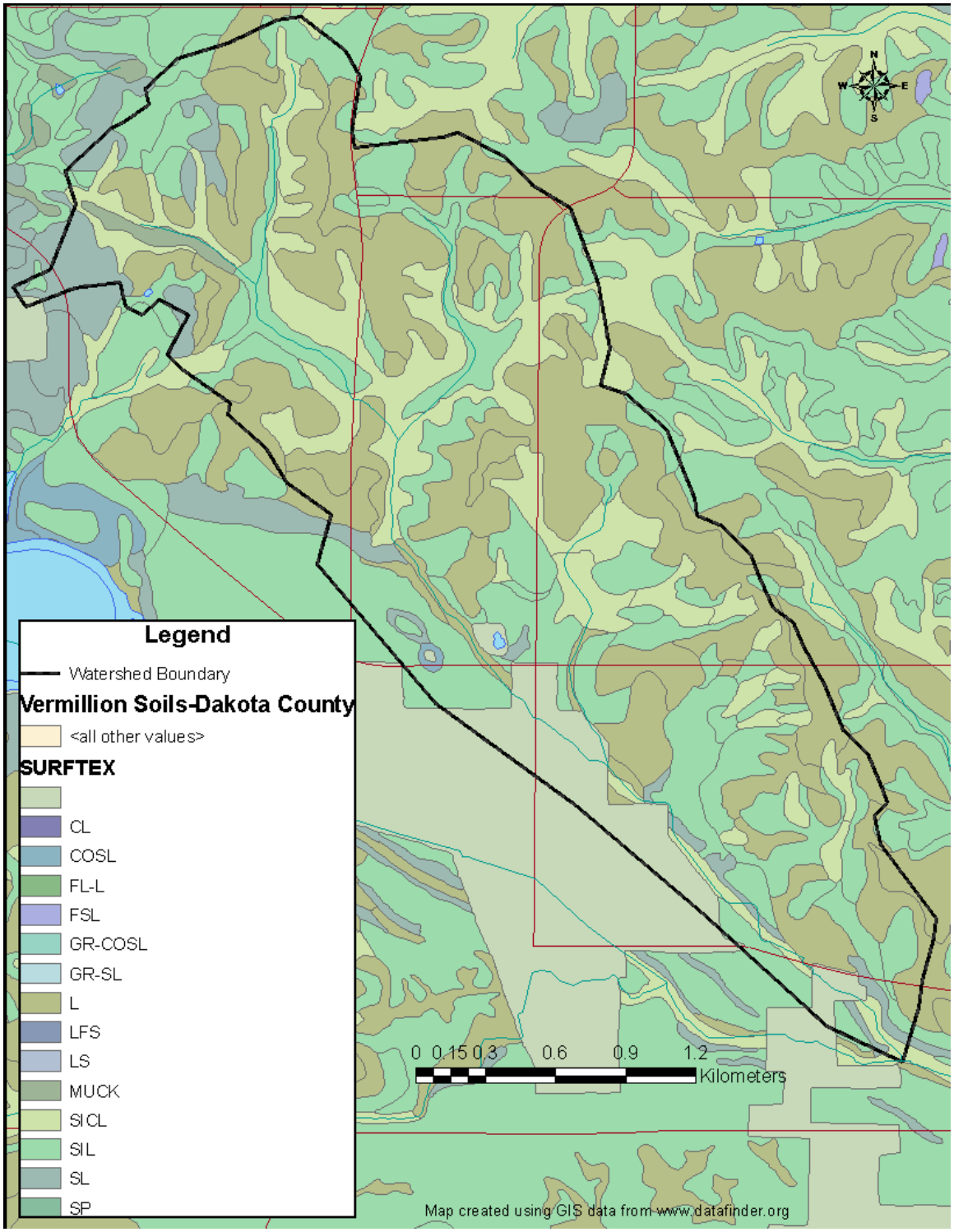

Figure 6.4 Soil map of the sub-watershed

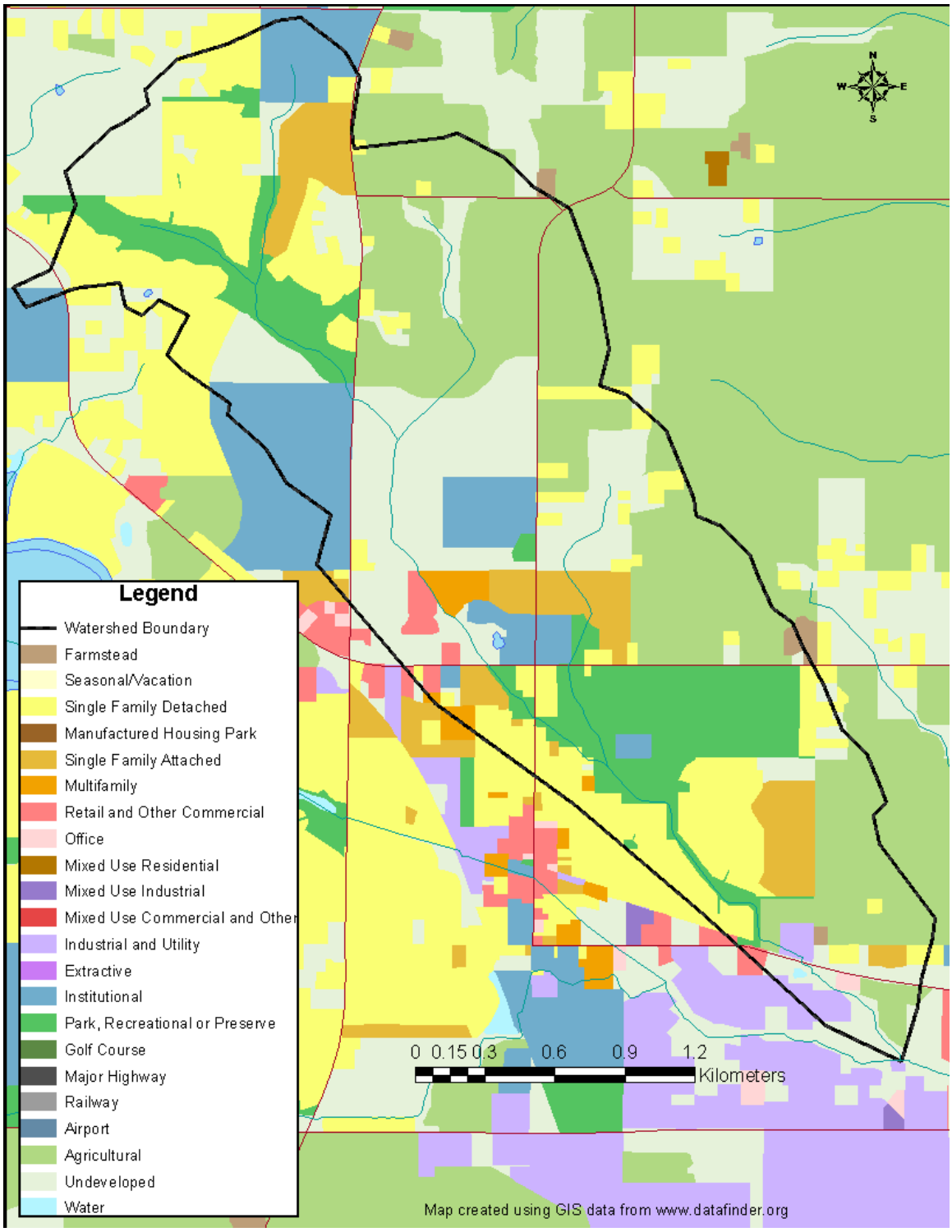

Figure 6.5 Land-use map of the sub-watershed

6.3 Land development scenarios

To estimate the change in groundwater recharge with the progressive urbanization of the sub-watershed over time, four land-use scenarios were developed. The scenarios represent four different levels of urbanization and are (1) a pre-development condition, (2) the present (2005) condition, (3) a plus 50 years future condition, and (4) a plus 100 years future condition. For each scenario, the annual groundwater recharge due to percolation was estimated using climate data for 2004 and 2005. The percentages of the total sub-watershed area occupied by each land-use type are listed in Table 6.5 for each of the four scenarios.

Table 6.5 Past and future land-use percentages

Land-Use Type	Description	Scenario			
		Past	Present	Plus 50yrs	Plus 100yrs
		Percent of sub-watershed area			
		%	%	%	%
1	Agriculture	50	25.1	13.2	0
2	Parks/preserve	0	12.7	14.6	16.5
3	Industrial	0	1	1.1	1.1
4	Institutions	3	8	9.2	10.3
5	Multi-family homes	0	7	8.6	9.9
6	Retail/office	0	1.7	2.2	2.4
7	Single family homes	12	21	23.9	25.7
8	Town-homes	0	1	9.2	20.8
9	Undeveloped/natural	35	21.5	16.8	12
10	Roads/impervious	0	1	1.1	1.2

Scenario Development

The areas covered by present land-uses were measured on the map of the sub-watershed, and the percentages were estimated. These land-use types and percentages are the parameters for the "present" condition scenario. They are listed in Tables 6.1 and 6.5.

For the pre-development condition, the land-use percentages were estimated using subjective judgment to represent what the area might have been during early (pre-urban) settlement. The "past" pre-development scenario consists mostly of natural ground cover and agricultural lands with sparse homes.

For the future conditions, both "plus 50 years" and "plus 100 years", the level of urbanization was interpolated using land-use data from the 1990 census and 2005 census for Lakeville, Minnesota, where the sub-watershed is located. Trends in land-use changes between 1990 and 2005 in Lakeville were extrapolated 50 years and 100 years, to obtain land-use percentages for the future scenarios. Table 6.6 lists the areas covered by each land-use in 1990 and 2005 and the difference between 1990 and 2005. Table 6.6 was

taken from the Metropolitan Council website http://gis.metc.state.mn.us/landuse/tables. For land-use types that were not listed in Table 6.6, i.e. town homes, judgment was used to estimate the change in land-use.

Table 6.6 Land-use comparisons between 1990 and 2005 census for Lakeville, MN

Land Use Categories	1990 Total (in acres)	2005 Total (in acres)	Change 1990-2005	
			Absolute (in acres)	Relative (percentage)
Residential Total	**3,856**	**7,502**	**3,646**	**+95%**
Single Family Residential	3,541	6,741	3,200	+90%
Farmsteads	208	104	-104	-50%
Multi-family Residential	107	657	550	+514%
Mixed Use	**N/A**	**19**	**N/A**	**N/A**
Commercial	**193**	**510**	**317**	**+164%**
Industrial Total	**593**	**999**	**406**	**+68%**
Industrial & Utility	593	655	62	+11%
Extractive	N/A	343	N/A	N/A
Railway	N/A	0	N/A	N/A
Institutional	**272**	**774**	**502**	**+185%**
Parks, Recreation & Preserves	**759**	**2,261**	**1,502**	**+198%**
Major Vehicular Rights-of-Way	**251**	**333**	**82**	**+33%**
Airports	**13**	**44**	**31**	**+237%**
Agriculture & Undeveloped Total	**17,193**	**10,598**	**-6,595**	**-38%**
Agriculture	N/A	5,350	N/A	N/A
Undeveloped Land	N/A	5,249	N/A	N/A
Agricultural & Vacant	16,824	N/A	N/A	N/A
Industrial Parks not Developed	345	N/A	N/A	N/A
Public & Semi-Public Vacant	24	N/A	N/A	N/A
Open Water	**985**	**1,131**	**146**	**+15%**
Total	**24,115**	**24,172**	**57**	**+0%**

Notes: Bold print designates major land use categories.

The differences between the scenarios were assumed to be land-use and vegetative cover; the soils were assumed not to change. In reality the soils might change due to the re-

grading and development of a site but this effect would be impossible to predict and to model.

For each scenario, a representative curve number was estimated for each land-cover group using the weight average method described in Appendix C. These curve numbers were used in the FAO model where infiltration was estimated by the SCS method. The curve numbers (CN) for each AMC class and scenario are given in Table 6.7.

Table 6.7 SCS curve numbers for each urban development scenario of the sub-watershed

Scenario	Cover type	Curve numbers (CN)		
		AMC I	AMC II	AMC III
Past				
	Row crops	62.0	78.0	92.0
	Turf grass	50.8	69.8	86.8
	Trees / grass	30.0	48.0	69.0
Present				
	Row crops	62.0	78.0	92.0
	Turf grass	56.5	74.2	89.5
	Trees / grass	34.1	52.8	73.1
Plus 50 years				
	Row crops	62.0	78.0	92.0
	Turf grass	58.7	76.0	90.8
	Trees / grass	35.1	54.0	74.1
Plus 100 years				
	Row crops	62.0	78.0	92.0
	Turf grass	60.5	77.4	91.8
	Trees / grass	36.4	55.5	75.4

6.4 Climate data

Climate data for 2004 and 2005 were obtained from the MnDOT weather station near Monticello, Minnesota about 60 miles from the study site. This station was chosen because weather data have been recorded at 15-minute intervals. It was assumed to be close enough to the study site to give representative weather data. Hourly data of air temperature (°C), dew point (°C), air pressure (kPa), precipitation (cm), relative humidity (%), solar radiation (MJ m^{-2} day^{-1}), and wind speed (m/s) were used.

The precipitation for the two years is plotted in Figure 6.6. The year 2005 had higher total precipitation as well as higher intensity storms with larger amounts of precipitation than the year 2004.

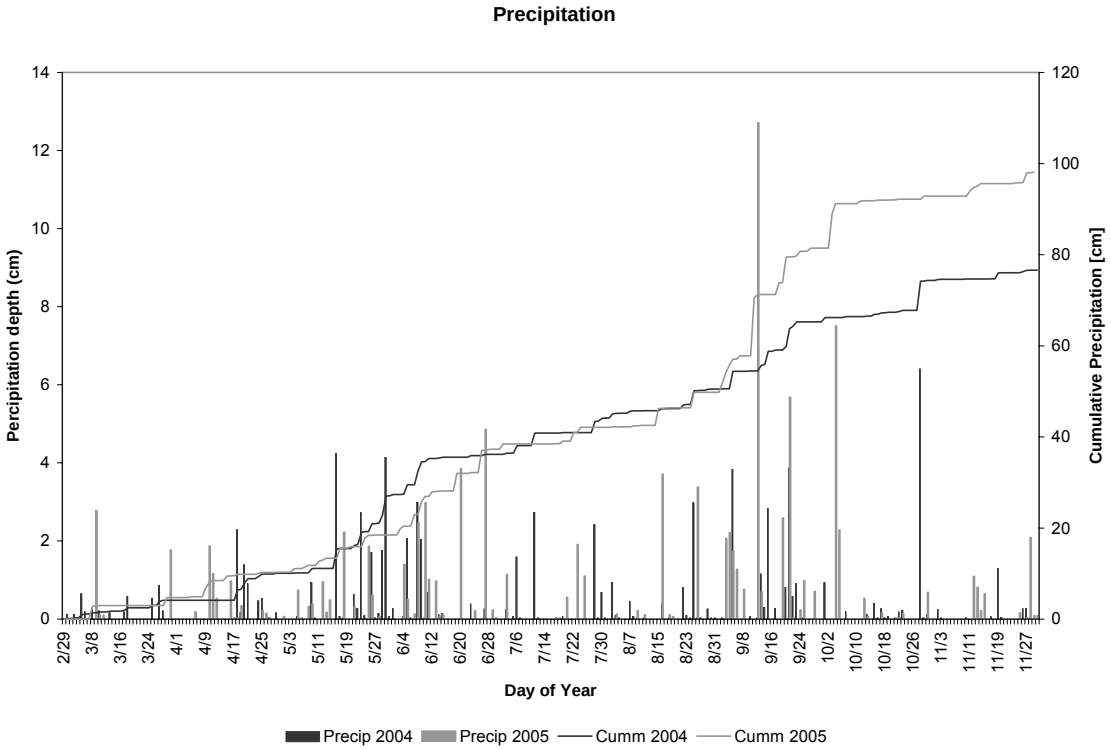

Figure 6.6 Precipitation and cumulative precipitation for 2004 and 2005

6.5 Simulation results

With the data from the previous sections as input, the seasonal groundwater recharge in the sub-watershed of the Vermillion River was estimated using some of the models previously described. Seasonal recharge occurs during the months when the ground is not frozen (April through November) and is essentially the result of rainfall. The three models used to estimate recharge are: (1) the FAO model using the SCS method for infiltration on a daily timescale, (2) the FAO model using the Green-Ampt method for estimating infiltration on an hourly timescale, and (3) the Green-Ampt model on an hourly timescale. For each model the estimated elements of the water budget (equation 1.6) were infiltration, runoff, evapotranspiration, and groundwater recharge. The results are listed in Table 6.8. Run-off was calculated by subtracting the infiltration from the precipitation.

The water budget components in Table 6.8 are estimates for the warm season from April to November. Four months (December to March) were excluded because no significant groundwater recharge occurs when the ground is frozen during those months.

Estimates of the water budget components were made for two years (2004 and 2005) that varied in total precipitation and intensity of rainfall (Figure 6.6). The year 2005 had more total precipitation and higher intensity rainfall events. The estimates in Table 6.8 are

averages for the entire sub-watershed. If volumes are desired, the total area of the sub-watershed (6.8 km^2) can be multiplied by the depths in Table 6.8.

Table 6.8 Estimates of annual water budget components

Scenario	Year	Precipitation P mm/yr	Potential evapo-transpiration ET_0 mm/yr	Infiltration I mm/yr	Actual evapo-transpiration ET_a mm/yr	Groundwater recharge R mm/yr	Change in storage ΔS mm/yr
Past							
FAO-SCS	2004	724.9	584.1	602.7	441.6	204.9	4.7
FAO-GA	2004	724.9	691.1	604.4	458.9	156.5	-11.0
GA model	2004	724.9	691.1	601.3	491.8	111.6	-2.1
FAO-SCS	2005	933.2	611.0	623.1	444.8	225.1	-46.8
FAO-GA	2005	933.2	722.5	665.1	490.3	176.6	-1.8
GA model	2005	933.2	722.5	661.4	508.6	127.4	25.4
Present							
FAO-SCS	2004	724.9	584.1	602.3	453.1	172.7	-23.5
FAO-GA	2004	724.9	691.1	520.0	405.7	120.9	-6.6
GA model	2004	724.9	691.1	517.8	423.6	94.3	-0.1
FAO-SCS	2005	933.2	611.0	626.6	458.9	191.2	-23.5
FAO-GA	2005	933.2	722.5	571.5	431.5	141.0	-1.0
GA model	2005	933.2	722.5	568.2	438.2	110.6	19.4
Plus 50 Year							
FAO-SCS	2004	724.9	584.1	564.4	455.4	127.6	-18.6
FAO-GA	2004	724.9	691.1	466.9	369.5	101.7	-4.3
GA model	2004	724.9	691.1	465.0	379.6	84.6	0.8
FAO-SCS	2005	933.2	611.0	592.2	440.6	163.9	-12.3
FAO-GA	2005	933.2	722.5	512.6	392.3	120.9	-0.6
GA model	2005	933.2	722.5	509.6	393.3	100.3	16.0
Plus 100 Years							
FAO-SCS	2004	724.9	584.1	557.4	462.1	104.6	-9.3
FAO-GA	2004	724.9	691.1	406.6	327.9	79.9	-1.2
GA model	2004	724.9	691.1	404.6	329.5	73.3	1.8
FAO-SCS	2005	933.2	611.0	564.8	429.5	135.3	0.0
FAO-GA	2005	933.2	722.5	445.3	347.2	98.2	-0.1
GA model	2005	933.2	722.5	442.5	341.9	88.3	12.3

Table 6.8 shows some expected results: Infiltration decreases as development increases; evapotranspiration, which depends on infiltrated water, also decreases. Estimates of recharge for the "present" scenario range from 94 to 173 mm/yr for 2004, and from 110 to 191 mm/yr for 2005. All three models produced acceptable results and were able to show a change in recharge due to progressive urban development in the sub-watershed.

For the "plus 100-years" scenario groundwater recharge estimates range from 73 to 105mm/yr in 2004, and from 88 to 135mm/yr to 2005. Expressed a s a fraction of annual precipitation, groundwater recharges are projected to decrease from a present 13% - 24% to a future 10% - 14%, under the "plus 100 year" scenario.

There are significant differences in the infiltration, evapotranspiration and groundwater recharge estimates by the three models (Table 6.8).

Differences in infiltration estimates

Differences in infiltration estimates by the SCS method and the Green-Ampt method are smallest for the "past" scenario (less than 7%) and largest for the "plus 110 years" scenario (up to 38%). Impervious areas play a significant role in the estimation of infiltration rates.

The SCS method views the rainfall event as a whole; it does not consider the intensity of the storm, a high intensity storm may have less infiltration than a low intensity storm with the same total precipitation. In the SCS method soil's attributes are not specified. The SCS method also lacks the ability to describe different infiltration rates due to soil moisture. On the other hand, the Green-Ampt method describes the physical processes of infiltration with much higher resolution (e.g. hourly timescale) than the SCS method (daily timescale) and takes into account the soil's attributes. Although the Green-Ampt method is good for estimating point source infiltration, it may be less suitable for estimation of infiltration over a large area, because soil parameters are spatially variable and may have a high degree of uncertainty.

For all these reasons, the Green-Ampt method for estimation of infiltration is considered better suited to our application than the SCS method. The SCS method appears to over predict infiltration in our case study.

Differences in evapotranspiration (ET) estimates

Differences between the SCS method and the Green-Ampt method are slightly smaller for ET estimates than for infiltration estimates. Differences in ET estimates by the SCS method and the Green-Ampt method are smallest for the "past" scenario (less than 14%) and largest for the "plus 110 years" scenario (up to 29%). This result is analogous to the infiltration estimates, since ET depends on infiltrated water.

6.6 Normalization of water budget components to "present" conditions

The large difference in total annual precipitation (725mm/yr in 2004 vs. 933mm/yr in 2005) probably accounts for most of the variation in the infiltration, evapotranspiration and groundwater recharge between the two years (Table 6.8). If the components of the water budget are normalized by present conditions for each year separately, the estimates

of the water budget components for the two climate years are much closer for each model and all four development scenarios (Table 6.9).

Table 6.9 Estimates of annual water budget components normalized to present conditions for each year

Scenario	Year	Infiltration I	Actual evapo-transpiration ET_a	Groundwater recharge R
		Ratio to "present" scenario values		
Past				
FAO-SCS	2004	1.001	0.975	1.186
FAO-GA	2004	1.162	1.131	1.294
GA model	2004	1.161	1.161	1.183
FAO-SCS	2005	0.994	0.969	1.177
FAO-GA	2005	1.164	1.136	1.252
GA model	2005	1.164	1.161	1.152
Present				
FAO-SCS	2004	1	1	1
FAO-GA	2004	1	1	1
GA model	2004	1	1	1
FAO-SCS	2005	1	1	1
FAO-GA	2005	1	1	1
GA model	2005	1	1	1
Plus 50 Years				
FAO-SCS	2004	0.937	1.005	0.739
FAO-GA	2004	0.898	0.911	0.841
GA model	2004	0.898	0.896	0.897
FAO-SCS	2005	0.945	0.960	0.857
FAO-GA	2005	0.897	0.909	0.857
GA model	2005	0.897	0.898	0.907
Plus 100 Years				
FAO-SCS	2004	0.925	1.020	0.606
FAO-GA	2004	0.782	0.808	0.661
GA model	2004	0.781	0.778	0.777
FAO-SCS	2005	0.901	0.936	0.708
FAO-GA	2005	0.779	0.805	0.696
GA model	2005	0.779	0.780	0.798

6.7 Change with progressive urban development

Since the main goals of this study is to investigate the effect of urban development on groundwater recharge, the normalized results in Table 6.9 can also be used to illustrate relative changes. Table 6.9 gives estimates of mean annual infiltration, evapotranspiration, and groundwater recharge relative to the present conditions.

Infiltration is predicted to decrease with urban development, i.e. as imperviousness of the watershed goes up. All methods predict, as they should, zero infiltration for a surface area that is 100% impervious. Infiltration has been plotted against imperviousness (%) in Figures 6.7 and 6.8. It can be seen that infiltration decreases with imperviousness, as expected. The extrapolation to 100% imperviousness is non-linear for the SCS method, but linear fore the GA method. In the Green-Ampt method impervious sub-areas make zero contribution to the total infiltration, which is given as a spatial average over the sub-watershed area. That is why the relationship is linear. The Green-Ampt method for estimating infiltration gave similar results for both the FAO-GA and GA models (Figure 6.8).The SCS method, on the other hand, is a method for estimating surface water runoff (RO), and infiltration is determined from precipitation (P) as (P – RO). In the SCS method a curve number CN = 100 is used for a fully impervious area. Curve numbers diminish as impervious area decreases, but not linearly.

Annual **evapotranspiration (ET)** also appears to go down as the level of urban development increases (Table 6.9), except for one condition in Table 6.9 (The ratio is 1.02). There is a plausible explanation why ET could go up: more area is covered with turf grass that has a high water demand. The FAO-GA model projects that the actual ET goes down by 29% as the level of urban development increases. The plausible explanation for the decrease is that impervious area with zero contribution to ET is increasing with development.

Another result shown in Table 6.9 is that **groundwater recharge** goes down with urban development. This is expected and related to the reduction in infiltration. Reasons - not included in our models - why groundwater recharge could go up with urban development, are increased lawn sprinkler irrigation and leaky storm sewers.

In conclusion, all three methods show that as a watershed experiences more urban development, groundwater recharge decreases. To make the change easier to see, Table 6.10 was developed. It gives the percent **change** relative to estimates for the "present" conditions. Values are rounded to the closest full percentage point. As the watershed becomes fully developed, the annual groundwater recharge drops by an average of about 30% to 40%. This would likely cause a substantial decrease in groundwater availability or seepage from an aquifer, and the effect on groundwater-fed trout streams might be serious.

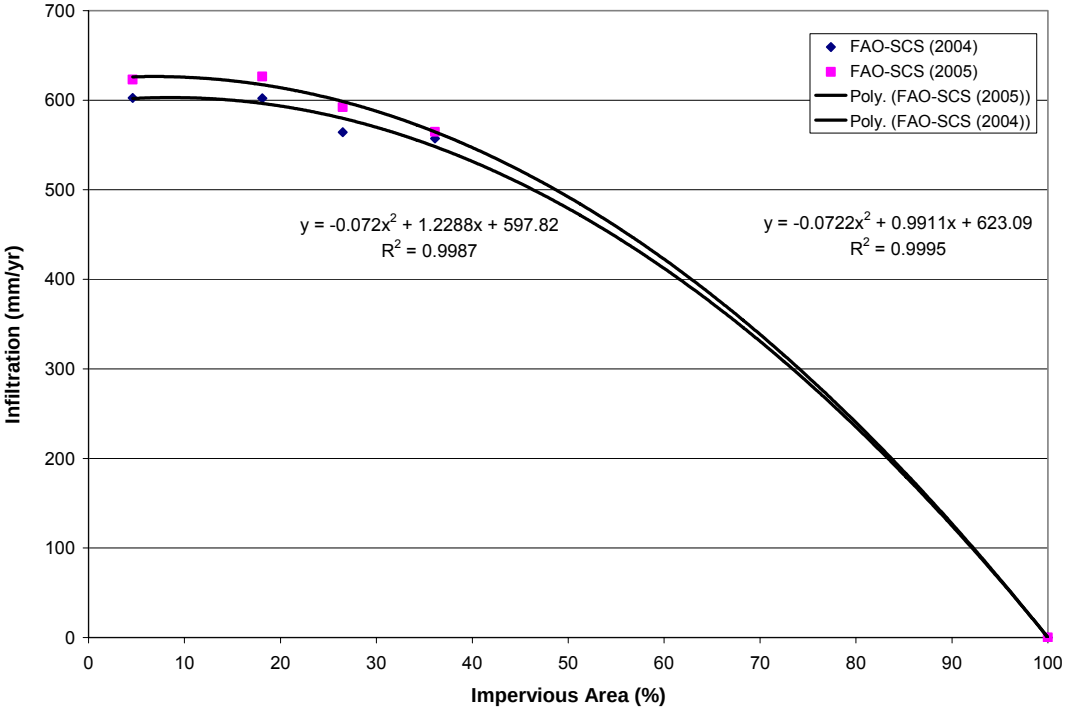

Figure 6.7 Dependence of infiltration on impervious area (FAO-SCS model results)

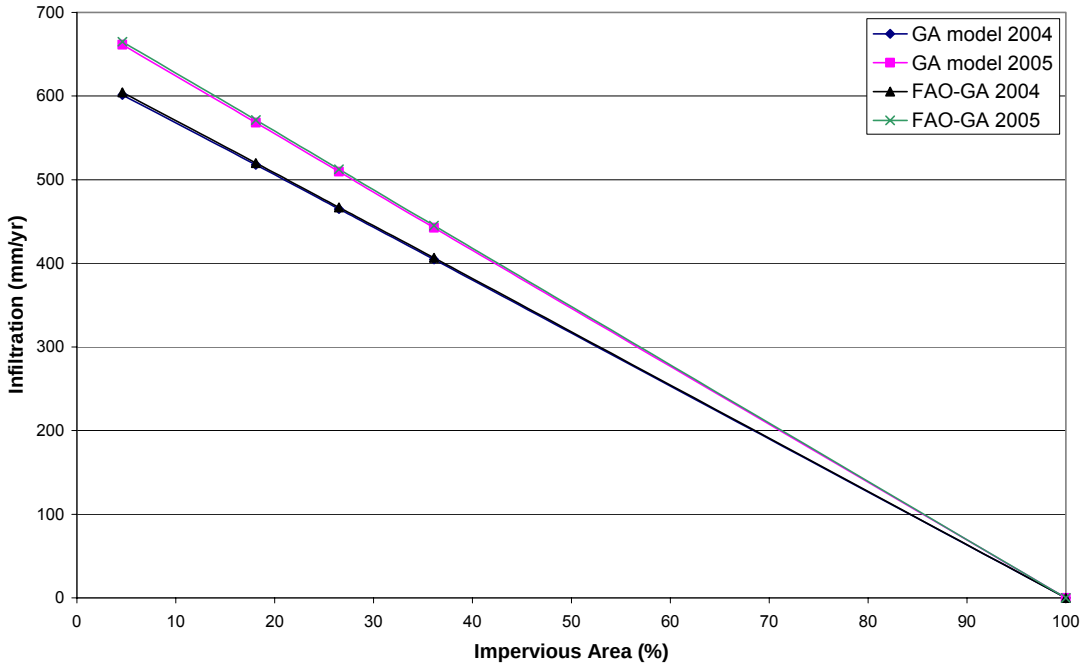

Figure 6.8 Dependence of infiltration (mm/yr) on impervious area (Green-Ampt model results)

Table 6.10 Change in water budget components from present conditions (in %)

Scenario	Year	Infiltration I	Actual evapo-transpiration ET_a	Groundwater recharge R
		Percent change from "present" values		
Past				
FAO-SCS	2004	0	-3	+19
FAO-GA	2004	+16	+13	+29
GA model	2004	+16	+16	+18
FAO-SCS	2005	-1	-3	+18
FAO-GA	2005	+16	+14	+25
GA model	2005	+16	+16	+15
Present				
FAO-SCS	2004	0	0	0
FAO-GA	2004	0	0	0
GA model	2004	0	0	0
FAO-SCS	2005	0	0	0
FAO-GA	2005	0	0	0
GA model	2005	0	0	0
Plus 50 Years				
FAO-SCS	2004	-6	+1	-26
FAO-GA	2004	-10	-9	-16
GA model	2004	-10	-10	-10
FAO-SCS	2005	-6	-4	-14
FAO-GA	2005	-10	-9	-14
GA model	2005	-10	-10	-9
Plus 100 Years				
FAO-SCS	2004	-8	-20	-39
FAO-GA	2004	-22	-19	-34
GA model	2004	-22	-22	-22
FAO-SCS	2005	-10	-6	-29
FAO-GA	2005	-22	-20	-30
GA model	2005	-22	-22	-20

6.8 Normalization of water budget components to annual precipitation

Figure 6.9 gives a diagram by the Federal Interagency Stream Restoration Working Group (1998). It shows components of the water budget as typical percentages of precipitation at different levels of urban development in the watershed. The schematics indicate that as the level of development increases, an ever smaller fraction of precipitation is contributed to infiltration, evapotranspiration and deep infiltration (taken to be groundwater recharge).

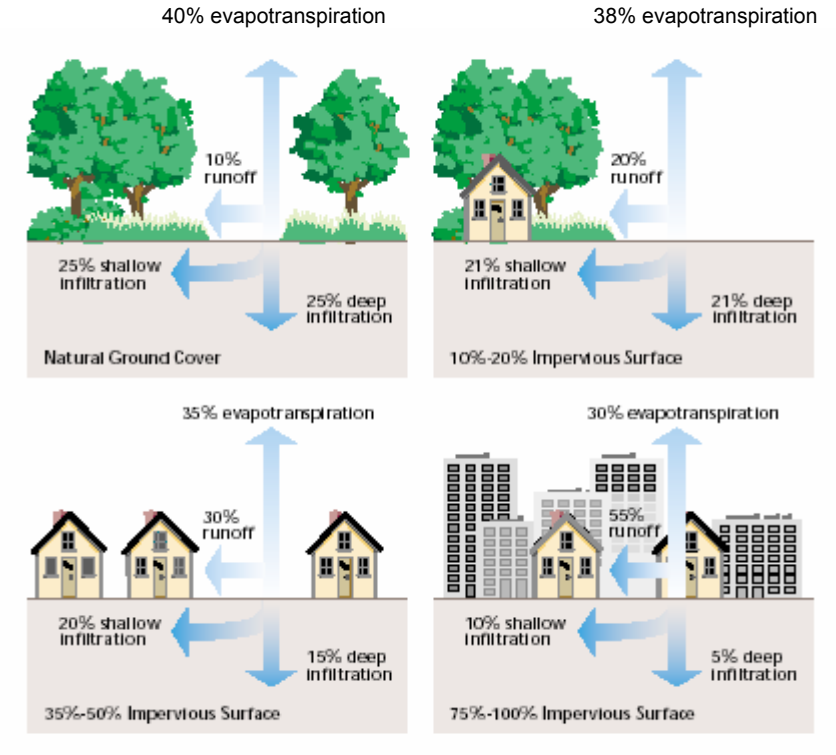

Figure 6.9 Diagram showing water movement (partitioning) at different levels of urban development (USDA, Federal Interagency Stream Restoration Working Group, 1998)

To compare the values given in Figure 6.9 with our simulated estimates of the water budget components, the numerical values in Table 6.8 were normalized to precipitation (They were previously normalized to "present" conditions in Tables 6.9 and 6.10). The values normalized to mean annual precipitation are shown in Table 6.11 and plotted in Figs. 6.10, 6.11 and 6.12 against impervious area along with the values given in Figure 6.9. The mean of the model values has also been calculated, and plotted as solid line in Figure 6.10. In our case study annual infiltration (relative to annual precipitation) islower than in Figure 6.9; evapotranspiration is much more variable in our study than in Figure 6.9, and groundwater recharge (relative to annual precipitation) is within 2% to 5% of the values in figure 6.9. The percentages of impervious areas for the four scenarios (past, present, plus 50 years, and plus 100 years) in our case study are 4.6%, 18.1%, 26.5%, and 36.1%, respectively.

Since our estimates of groundwater recharge are similar to the values in Figure 6.9, we can assume that our model results are representative estimates for the study site.

Table 6.11 Estimates of annual water budget components normalized to precipitation

Scenario	Year	Precipitation	Infiltration	Actual evapo-transpiration	Groundwater recharge
		P	I	ET_a	R
		mm	Fraction of precipitation		
Past Scenario					
FAO-SCS	2004	724.9	0.83	0.61	0.28
FAO-GA	2004	724.9	0.83	0.63	0.22
GA model	2004	724.9	0.83	0.68	0.15
FAO-SCS	2005	933.2	0.67	0.48	0.24
FAO-GA	2005	933.2	0.71	0.53	0.19
GA model	2005	933.2	0.71	0.55	0.14
Present Scenario					
FAO-SCS	2004	724.9	0.83	0.63	0.24
FAO-GA	2004	724.9	0.72	0.56	0.17
GA model	2004	724.9	0.71	0.58	0.13
FAO-SCS	2005	933.2	0.67	0.49	0.20
FAO-GA	2005	933.2	0.61	0.46	0.15
GA model	2005	933.2	0.61	0.47	0.12
Plus 50 Years Scenario					
FAO-SCS	2004	724.9	0.78	0.63	0.18
FAO-GA	2004	724.9	0.64	0.51	0.14
GA model	2004	724.9	0.64	0.52	0.12
FAO-SCS	2005	933.2	0.63	0.47	0.18
FAO-GA	2005	933.2	0.55	0.42	0.13
GA model	2005	933.2	0.55	0.42	0.11
Plus 100 Years Scenario					
FAO-SCS	2004	724.9	0.77	0.64	0.14
FAO-GA	2004	724.9	0.56	0.45	0.11
GA model	2004	724.9	0.56	0.45	0.10
FAO-SCS	2005	933.2	0.61	0.46	0.14
FAO-GA	2005	933.2	0.48	0.37	0.11
GA model	2005	933.2	0.47	0.37	0.09

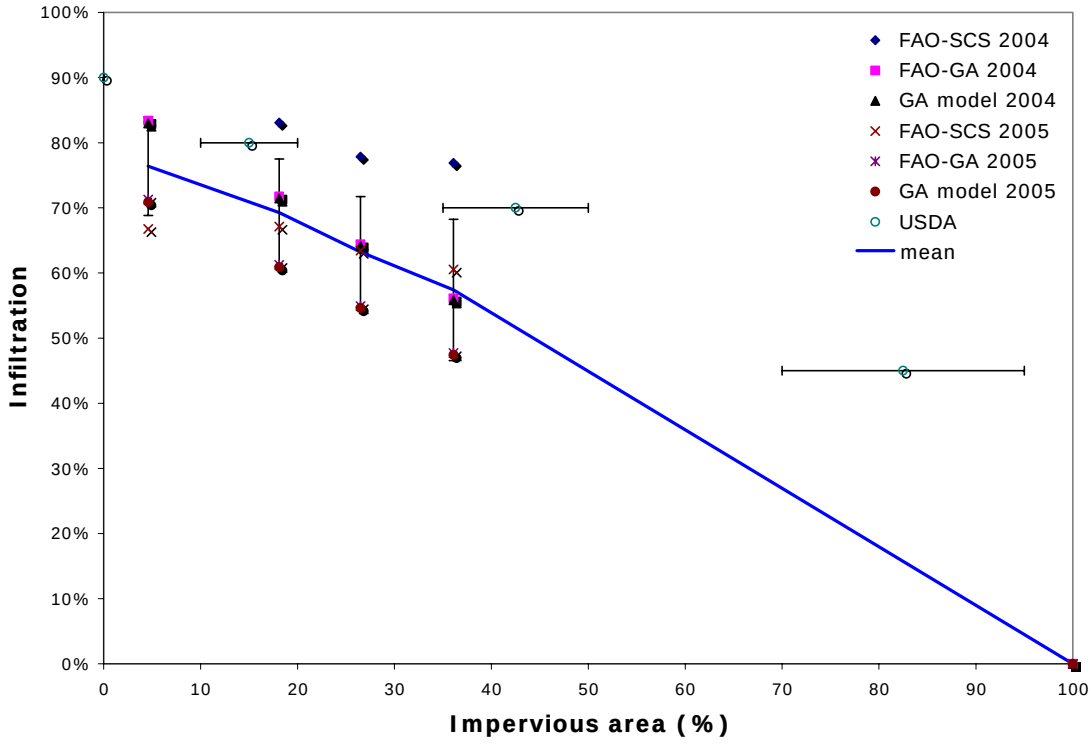

Figure 6.10 Infiltration (percent of precipitation) vs. impervious area (percent of total area) in the Vermillion River sub-watershed and USDA (1998) estimates

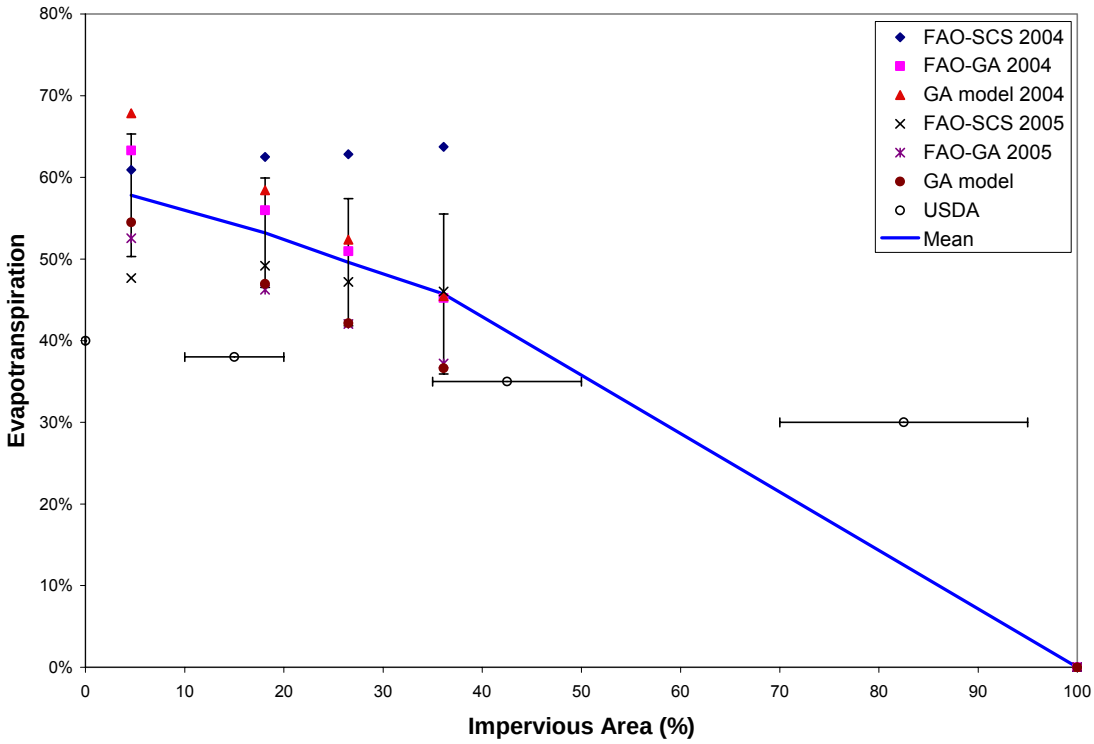

Figure 6.11 Evapotranspiration (percent of precipitation) vs. impervious area (percent of total area) in the Vermillion River sub-watershed

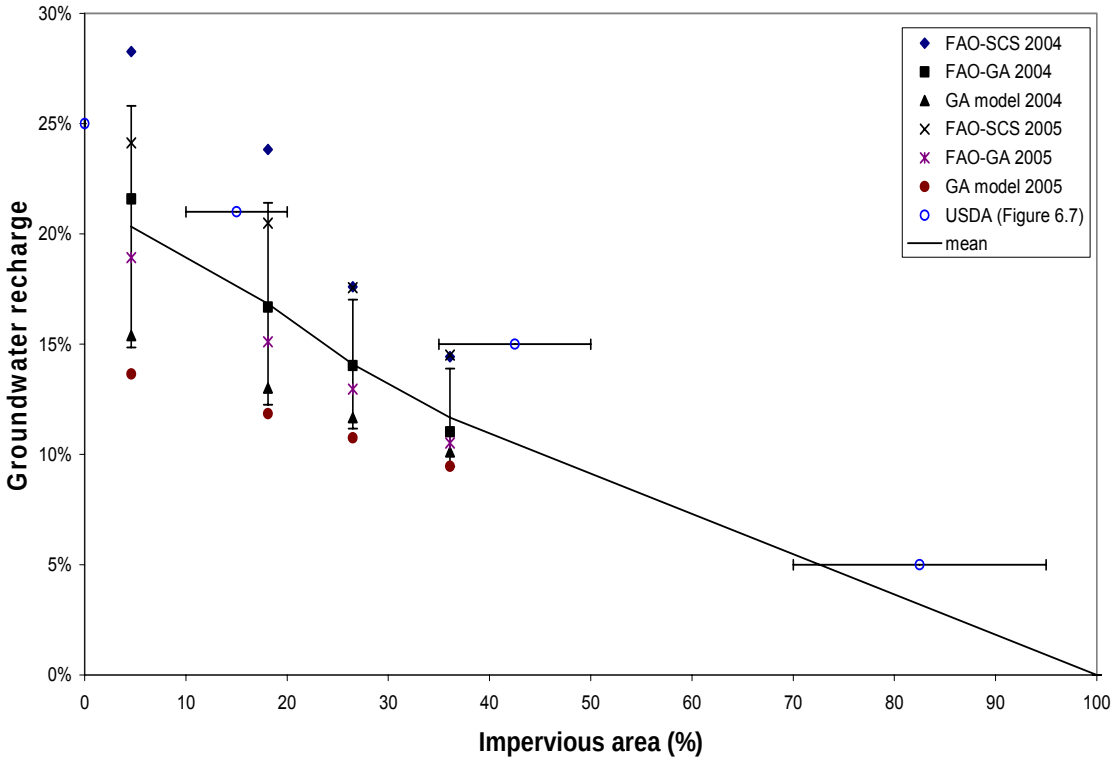

Figure 6.12 Groundwater recharge (percent of precipitation) vs. impervious area (percent of total area) in the Vermillion River sub-watershed and USDA (1998) estimates.

In Figures 6.10, 6.11, 6.12, the mean and standard deviation from Table 6.12 are plotted along with the individual water budget components from Table 6.11. For comparison the USDA (1998) estimates from Figure 6.9 are also given. The mean values were linearly connected and extrapolated to 0% at 100% impervious area. It was assumed that from a 100% impervious area no water would infiltrate, there would be no vegetation for evapotranspiration, and no water would be available for groundwater recharge. Most of the values estimated from the models fall within one standard deviation of the mean, with the exception of the FAO-SCS 2004. This model tended to predict higher values than the rest of the models. The GA model for 2005 predicted the lowest values for the groundwater recharge (Figure 6.12).

When compared to the USDA (1998) values for the water budget components (Figure 6.9), the results for he Vermillion River sub-watershed were close, except for evapotranspiration. The USDA values for evapotranspiration (Figure 6.11) are fairly constant and independent of surface imperviousness; they do not seem to reach zero when the area is 100% impervious which would be expected.

Table 6.12: Mean and standard deviation of normalized estimates for water budget components (see Table 6.11)

Scenario	Infiltration	Actual evapo-transpiration	Groundwater recharge
	I	ET_a	R
	Fraction of precipitation		
Past Scenario			
mean	0.76	0.58	0.20
std. dev.	0.08	0.08	0.05
Present Scenario			
mean	0.69	0.53	0.17
std. dev.	0.08	0.07	0.05
Plus 50 Years Scenario			
mean	0.63	0.50	0.14
std. dev.	0.08	0.08	0.03
Plus 100 Years Scenario			
mean	0.57	0.46	0.12
std. dev.	0.11	0.10	0.02

6.9 Validation

No data on groundwater recharge were available to compare the water budget estimates for the study site with measurements. An indirect validation of the groundwater recharge estimates for the sub-watershed was, however, achieved using four different sources of data: (1) maps of typical groundwater recharge in Minnesota developed by the US Geological Survey and the Minnesota Geological Survey, reproduced in Figures 2.5 and 2.6, (2) typical groundwater recharge rates as a function of land development given by the USGS and reproduced in Figure 6.7, (3) results of studies on two similar individual watersheds in Illinois, and (4) results of a USGS study in the Vermillion River watershed.

The information from these four sources was compared with the simulation results for annual groundwater recharge the study-site in the Vermillion River watershed. It may be recalled that the simulations were made by three methods and for the years 2004 and 2005, giving a total of six numerical values. These values are given in column 7 of Table 6.8. For "present" conditions their average and standard deviation are 138 ±37 mm/yr.

By comparison, the USGS recharge map for Minnesota (Figure 2.5) indicates a groundwater recharge rate between 150 mm/yr to 200 mm/yr for the study site. The minimal recharge for the study site is around 51 mm/yr according to the recharge map by the Minnesota Geological Survey in Figure 2.6. These numbers appear reasonably accurate, and compare favorably with the simulation result of 138mm/yr.

We can also compare our groundwater recharge simulation results for the study site to estimates and measurements of groundwater recharge on other, similar watersheds. Arnold and Allen (1996) estimated the different components of the water budget (equation 1.5) for three watersheds in Illinois using the multi-component water budget model SWAT (Soil and Water Assessment Tool). The three watersheds had characteristics similar to our study site, such as soils consisting mostly of loams, land-uses consisting mostly of agricultural lands, shallow water tables, relatively low surface slopes averaging about 0.0038 (except for one of the watersheds: Hadley Creek's slope ranged from 0.0076 to 0.0273), and similar mean annual precipitation (~850 to 910 mm/year). Impervious areas were not given but can be assumed to be low because the watersheds are mostly undeveloped or agricultural areas. The land cover in the Goose Creek and Panther Creek watersheds compares probably most closely to "pre-development" conditions at the Vermillion River study site..

The measured values of the groundwater recharge for the three watersheds (Goose Creek, Hadley Creek, and Panther Creek) were 264 mm, 99 mm, and 204 mm, respectively, and the annual precipitation values were 944 mm, 1009 mm, and 822 mm, respectively. As a percentage of precipitation, the groundwater recharges for the three watersheds are 27.9%, 9.8%, and 24.8%, respectively. By comparison, the groundwater recharge estimates for the study site (Table 6.11) range from 14% to 28% for the pre-development (past) scenario. These numerical results compare favorably. Since the watersheds have similar characteristics to those of our study site, we can feel comfortable with our estimates of groundwater recharge.

Ruhl et al. (2002) investigated groundwater recharge to unconfined and confined aquifers in the seven-county metro area of Minneapolis and St. Paul. One of the watersheds studied was the Vermillion River watershed, where the study site is located. Ruhl et al. (2002) used six different methods to investigate recharge to the unconfined aquifers. The methods used include percentage of precipitation, stream flow-recession displacement (Section 2.2), ground-water level fluctuations, age-dating of shallow groundwater, the watershed characteristics (Section 2.6), and vertical-hydraulic gradients. Ruhl et al. (2006) found that recharge in the Vermillion River basin using the base-flow separation method, and records from 1974 to 1998 ranged from 66 mm/yr to 340 mm/yr with a mean of 168 mm/yr. The estimates for "present" conditions in Table 6.8 fall within the range found by Ruhl et al. (2002) for the entire Vermillion River watershed.

The comparison of our simulated estimates of annual groundwater recharge in a sub-watershed of the Vermillion River with four different sources of information shows a very reasonable agreement for current watershed conditions. Although the model could not be validated directly because measurement of the groundwater recharge at the study site are not available, the indirect validation provides some assurance that the proposed models might perform well in estimating groundwater recharge under future development conditions. Our preference would be for use of the FAO-GA model.

7.0 Discussion

Urban development of rural and natural areas is believed to reduce groundwater recharge. This is of concern for water resources management and wildlife. Diminishing groundwater supply to streams reduces cold water fish habitat, e.g. for trout. An example is the Vermillion River watershed, which is a world class trout stream on the fringes of the Minneapolis/St. Paul metropolitan area. Substantial changes in groundwater recharge can destroy a cold water habitat.

In this report we have reviewed methods to estimate groundwater recharge and we have used some of them to estimate the changes in recharge to be expected in a developing subwatershed of the Vermillion River, Minnesota.

Changes in land cover, especially an increase in impervious areas, reduce the amount of water available for groundwater recharge. Finch (1998) found that land cover is the most import parameter when groundwater recharge is estimated. For example, a change from an agricultural crop that requires less water during the developmental stage in the spring to a turf grass that has a short development stage can greatly increase the water demand for a given area.

Several methods have been developed to estimate and model groundwater recharge. Scanlon et al. (2002) review the appropriate choice of methods for groundwater recharge estimation. Extensive hydrologic models have been developed to simulate surface water and groundwater interaction. They include: MIKE SHE, HMS, SWATMOD, MODBRANCH, and FHM. The models are described by Said et al. (2005) as follows:
(1) MIKE SHE is used to simulate flow and transport of solutes and sediments in both surface and groundwater (DHI, 1999).
(2) The Hydrologic Model System (HMS) was developed based on the Basin-Scale Hydrologic Model (BSHM) (Yu and Schwartz (1998) and is currently under development at the University of Nevada, Las Vegas.
(3) SWATMOD links the Soil Water Assessment Tool (SWAT) model with the groundwater model, MODFLOW (McDonald and Harbaugh 1988). SWAT is a watershed scale model used to predict water, chemical, and sediment movement in large basins (Sophocleous et al.1999).
(4) MODBRANCH simulates the interaction between stream-flow and subsurface flow in areas with dynamic, hydraulically connected groundwater and surface water systems coupled at the stream/aquifer interface (Swain and Wexler 1993).
(5) FHS (FIPR Hydrological Model) is an integrated model that simulates the full water budget of the surface and ground water systems.

Integrated computer models are good for modeling the hydrologic components of a watershed, but they require substantial knowledge of the watershed to supply a large amount of model input information - more information than an urban development might be able to provide**.** The lumped water budget approach described in this report may be a more viable groundwater recharge model for a sub-watershed scale.

8.0 Summary and Conclusions

Basic methods of analysis to determine or project groundwater recharge are reviewed in this report. Empirical and physics-based methods are discussed.

(1) The empirical models reviewed include the recession-curve-displacement method and the base-flow-separation method (Rutledge 1993, Lee and Chen 2003); both require only stream flow records.

(2) For Minnesota a groundwater recharge map was developed by the U.S. Geological Survey (Lorenz and Delin 2006). For the Minneapolis/St. Paul metropolitan area a minimal recharge map was developed by the Minnesota Geological Survey (Ruhl et al. 2002) using statistical methods.

(3) For Wisconsin a first approximation equation developed by Cherkauer and Ansari (2005) is available for groundwater recharge estimation.

The empirical methods are useful for estimating current groundwater recharge but lack the ability to estimate changes in recharge due to land (urban) development or changes in climate. Methods to estimate changes in groundwater recharge are physics-based models that relate precipitation, infiltration, evapotranspiration and the soil water budget in a quantitative manner. Physics-based descriptions/models of groundwater recharge are:

(1) FAO model developed by Allen et al. (1996) for use with the FAO-56 Penman-Monteith evapotranspiration equation,

(2) Green-Ampt model that estimates groundwater recharge using the Green-Ampt equation for infiltration depth, and

(3) analytical equation for estimating recharge (Kim et al.1996).

Three physics-based models that used different techniques for estimating infiltration and percolation were applied to estimate the effect of urban development on a 6.78 km^2 sub-watershed of the Vermillion River:

(1) the FAO model with the SCS method for infiltration on a daily timescale,

(2) the FAO model with the Green-Ampt method for estimating infiltration on an hourly timescale, and

(3) the Green-Ampt model on an hourly timescale.

The elements of the water budget (runoff, infiltration, evapotranspiration, and groundwater recharge) were estimated from rainfall, with specified soil and land surface characteristics. Each model was applied in a continuous simulation of the months of April to November, 2004 and 2005. In addition to present land use conditions, one pre-

development land use scenario, a future development scenario (plus 50 years) and a full urban development scenario were simulated. The simulation results for the annual groundwater recharge and other water budget components under those four different land-use scenarios are listed in Tables 6.8 to 6.11, and have been plotted in figures 6.7, 6.8, and 6.10 to 6.12.

The study site was a good representation of the Vermillion River watershed at the southern fringe of the Minneapolis/St.Paul metropolitan area. It includes some urban development, some agricultural land, and some natural land. The model estimates for groundwater recharge for the present conditions ranged from 94 mm/year to 173 mm/year and for full development from 73 mm/year to 105 mm/year for a typical year of 720 mm/year precipitation (2004 was used). An increase in impervious area from the present 18% to 36% after full development is projected to decrease the recharge by ~30% to 40% annually according to the study results. The groundwater supply to the cold water reaches of the Vermillion River would be seriously affected by such a decline.

Uncertainty in the estimates of groundwater recharge is introduced by factors not covered in this investigation. One is the spatial variability of soil parameters, especially hydraulic conductivity which can vary over several orders of magnitude (Scanlon et al. 2002). Another source of uncertainty is that errors in the water budget components accumulate; we have attempted to reduce these errors by using small time steps. Another uncertainty is flow between shallow and deep aquifers. If natural inter-aquifer flows in the given hydro-geologic setting are great, it can be difficult to model groundwater flow accurately.

Overall, the urbanization of rural lands may have a smaller impact on groundwater recharge than indicated by the case study in this paper. Water supply to urban areas from external sources such as the Mississippi River Lawn watering and leaky sewer pipes in urban residential areas can increase infiltration and groundwater recharge. Leaky storm sewer pipes may recharge the soil after rain events, but may also extract water from an aquifer if the groundwater table is high. Storm water infiltration ponds and rain gardens may compensate partially for the reduction in infiltration from impervious surfaces.

References

Allen, R.G. 1996. Assessing integrity of weather data for reference evapotranspiration estimation. *Journal of Irrigation and Drainage Engineering* 122(2): 97-106

Allen, R.G., Pereira, L.S., Raes, D., and Smith, M. 1998. Crop evapotranspiration: Guidelines for computing crop water requirements. *FAO Irrigation and Drainage Paper No. 56,* Food and Agricultural Organization of the United Nations (FOA), Rome

Allen, R.G. et al. 2000. Issues, requirements, and challenges in selecting and specifying a standardized ET equation. *Proc., 4th National Irrigation Symposium,* ASAE, St. Joseph, Michigan, 210-208

Arnold, J.G. and Allen, P.M. 1996. Estimating hydrologic budgets for three Illinois watersheds. *Journal of Hydrology* 176: 57-77

Arnold, J.G., Muttiah, R.S., Srinivasan, R. and Allen, P.M. 2000. Regional estimation of base flow and groundwater recharge in the Upper Mississippi river basin. *Journal of Hydrology* 227 (1): 21-40

Barnes, B.S. 1939. The structure of discharge recession curves. *Transactions of American Geophysical Union* 20: 721-725.

Bouwer, H. 1969. Infiltration of water into non-uniform soil. *Journal of Irrigation and DrainageDiv.*, Proc. of ASCE, 95, IR4, 451-462

Brunt, D. 1932. Notes on radiation in the atmosphere. *Q. J. R. Meteorol. Soc.,* 58: 389-420

Brooks, R.H. and Corey, A.T. 1964. Hydraulic properties of porous media. *Hydrology Paper no. 3*, Colorado State University, Fort Collins.

Burman, R.D., Cuenca, R.H., and Weiss, A. 1983. Techniques for estimating evapotranspiration. *Advances in Irrigation*, D. Hillel, ed., Vol. 2, Academic Press, New York.

Chen, W.P. and Lee, C.H. 2003. Estimating ground-water recharge from streamflow records. *Environmental Geology* 44: 257-265

Cherkauer, D.S. 2004. Quantifying ground water recharge at multiple scales using PRMS and GIS. *Ground Water* 42(1): 97-110

Cherkauer, D.S. and Ansari, S.A. 2005 Estimating groundwater recharge from topography, hydrogeology, and land cover. *Ground Water* 43(1): 102-112

Childs, E.C. and Bybordi, M., 1969. The vertical movement of water in stratified porous material. 1:Infiltration. *Water Resources Research* 5(2): 446-459

Clifton, Craig and Perry, David. 1999. Using trees to control groundwater recharge: how many are enough?. Landscape notes, State of Victoria, Austrailia. Department of Sustainability and Environment. www.dpi.vic.gov.au

Chu, S.T. 1978. Infiltration during an unsteady rain. *Water Resources Research* 14(3): 461-466

Delleur, Jacques W. 1998. *The Handbook of Groundwater Engineering.* CRC Press LLC, Boca Raton, Florida.

Dumouchelle, D.H. and Schiefer, M.C. 2002. Use of stream-flow records and basin

characteristics to estimate groundwater recharge rates in Ohio. Ohio Department of Natural Resources Bulletin 46. Columbus: Ohio Department of Natural Resources.

Eagleson, P.S., 1978. Climate, soil, vegetation, 2, The distribution of annual precipitation derived from observed storm sequences. *Water Resource Research* 14(5): 713-721

Finch, J.W. 1998. Estimating direct groundwater recharge using a simple water balance Model - sensitivity to land surface parameters. *Journal of Hydrology* 211: 112-125

Flerchinger, G.N., Watts, F.J., and Bloomsburg, G.L. 1988. Explicit solution to Green-Ampt equation for non-uniform soils. *Journal of Irrigation and Drainage.* Div. of ASCE 114(3): 561-565

Glover, R.E. 1964. Groundwater Movement. U.S. Bureau of Reclamation Engineering Monograph Series 31. pp. 31-34.

Green, W.H. and Ampt, C.A. 1911. Studies on soil physics I. The flow of air and water through soils. *Journal of Agriculture Science* IV (Part 1 1911): 1-24

Hargreaves, G.H, and Allen, R.G. 2003. History and evaluation of Hargreaves evapotranspiration equation. *Journal of Irrigation and Drainage Engineering* 129(1): 53-63

Hargreaves, L.G., Hargreaves, G.H., and Riley, J.P. 1985. Irrigation Water Requirements for Senegal River Basin. *Journal of Irrigation and Drainage Engineering* 111(2): 265-275

Harr, M.E. 1962. *Groundwater and Seepage. McGraw-Hill book Co., New York, 315pp.*

Halford, K.J. and Mayer, G.C. 2000. Problems associated with estimating groundwater discharge and recharge from stream-discharge records. *Groundwater* 38(3): 331-342.

Horton, R.E. 1933. The role o infiltration in the hydrologic cycle. *Transactions of American Geophysical Union* 14: 446-460.

Horton, R.E. 1940. An Approach Towards a Physical Interpretation of Infiltration Capacity. *Soil Science Society of America Proceedings* 5: 399-417

Irmak, S., Irmak, A., Allen, R.G., Jones, J.W. 2003. Solar and Net Radiation-Based Equations to Estimate Reference Evapotranspiration in Humid Climates. *Journal of Irrigation and Drainage Engineering* 129(5): 336-347

James, L.G. and Larson, C.L. 1976. Modeling Infiltration and Redistribution of Sol Water during Intermittent Application. *Transactions of ASAE* 19(3): 482-488

Jensen, M.E., Burman, R.D., and Allen, R.G. 1990. Evapotranspiration and Irrigation Water Requirements. *ASCE Manuals and Reports on Engineering Practice No.* 70, ASCE, New York.

Kim, C.P., Stricker, J.N.M. 1996. Influence of spatially variable soil hydraulic properties and rainfall intensity on the water budget. *Water Resources Research* 32(6): 1699-1712

Kim, C.P., Stricker, J.N.M., Torfs, P.J.J.F. 1996 An analytical framework for the water budget of the unsaturated zone. *Water Resources Research* 32(12): 3475-3484

Li, R.M., Stevens, M.A., and Simons, D.B. 1976. Solutions to Green-Ampt Infiltration Equation. *Journal of Irrigation and Drainage.* Division of ASCE 102(IR2): 239-248

Linsley, R.K. Jr., Kohler, M.A., and Paulhus, J.L.H. 1982. Hydrology for Engineers (3rd Ed.). McGraw-Hill, New York. 508 pp.
Linsley, R.K. Jr., Kohler, M.A., and Paulhus, J.L.H. 1958. Hydrology for Engineers. McGraw-Hill, New York.
Lorenz, D.L. and Delin, G.N. 2007. A regression model to estimate regional ground water recharge. *Groundwater* 45(2): 196-208
Mays, Larry W. *Water Resources Engineering, 2005 Edition*. John Wiley and Sons, Inc., Hoboken, New Jersey, 2005.
Mein, R.G. and Larson, C.L. 1973. Modeling Infiltration during a Steady Rain. *Water Resources Research* 9(2): 384-394.
Meyboom, P. 1961. Estimating ground-water recharge from stream hydrographs. *Journal of Geophysical Research* 66(4): 1203-1214.
Morel-Seytoux, H.J. and Khanji,J. 1974. Derivation of an Equation of Infiltration. *Water Resource Research.* 10(4): 795-800.
Parlange, J.Y. 1975. A Note on the Green and Ampt Equation. *Soil Science* 119(6): 466-467
Parlange, J.Y., Lisle, I., Braddock, R.D., and Smith, R.E. 1982. The Three Parameter Infiltration Equation. *Soil Sceince* 133: 337-341
Phillip, J.R. 1957. The Theory of Infiltration: 4. Sorptivity and Algebraic Infiltration Equations. *Soil Science* 84: 257-264
Phillip, J.R. 1992. Falling Head Ponded Infiltration. *Water Resources Research* 28(8): 2147-2148
Phillip, J.R. 1993. Variable-Head Ponded Infiltration Under Constant or Variable Rainfall. *Water Resources Research* 29(7): 2155-2165
Ravi, V. and Williams, J.R., 1998. Estimation of Infiltration Rate in the Vadose zone: Compilation of Simple Mathematical Models. *EPA Report EPA/600/R-97/128a,* Washington D.C.
Rawls, W.J. and Brankensiek, D.L. 1982 Estimating Soil Water Retention from Soil Properties. *Journal of Irrigation and Drainage Engineering*, Division Proceedings of ASCE 108: 166-171.
Rawls, W.J., Brankensiek, D.L., and Miller, N. 1983 Green-Ampt Infiltration Parameters from Soil Data. *J. Hydraulic Division, ASCE,* 109, no 1: 62-70
Rorabaugh, M.I. 1964. Estimating changes in bank storage and ground-water contribution to streamflow. International Association of Scientific Hydrology. Publication 63: 432-441.
Ruhl, J.F, Kanivetsky, R. and Shmagin, B. 2002. Estimates of recharge to unconfined aquifers and leakage to confined aquifers in the seven-county metropolitan area of Minneapolis/St. Paul, Minnesota. USGS Water-Resources Investigation Report 02-4092. Reston, Virginia: USGS.
Rutledge, A.T. 1993 Computer programs for describing the recession of ground-water discharge and for estimating mean ground-water recharge and discharge from streamflow records. US Geological Survey Water-Resources Invesigations Report 98-4148. USGS
Rutledge, A.T. and Daniel, C.C. 1994. Testing an automated method to estimate ground-water recharge from streamflow records. *Groundwater* 32(2): 180-189
Salvucci, G.D., and Entekhabi, D. 1994. Explicit Expressions for Green-Ampt (Delta

Function Diffusivity) Infiltration Rate and Cumulative Storage. *Water Resources Research* 30(9): 2661-2663

Schilling, K.E. 2003. Increased baseflow in Iowa over the second half of the 20th century. *Journal of the American Water Resources Association* 39(4): 851-860.

Sherman, L.K. 1943. Comparison of F-curves Derived by the Method of Sharp and Holtan and of Sherman and Mayer. *Eos. Trans.* AGU, 24: 465-467

Simmons, C.S., Meyer, P.D. 2000. A simplified model for the transient water budget of a shallow unsaturated zone. *Water Resources Research* 36(10): 2835-2844

Smith, R.E. 1972. The Infiltration Envelop: Results from a Theoretical Infltrometer. *Journal of Hydrology* 17: 1-21

Smith, R.E. and Parlange, J.-Y. 1978. A Parameter-Efficient Hydrologic Infiltration Model. *Water Resources Research* 14(3): 533-538

Swartzendruber, D. and Young, E.G. 1974. A Comparison of Physically-Based Infiltration Equations (Note). *Soil Science.* 177(3): 165-167

Swartzendruber, D. 1987. Rigorous Derivation and Interpretation of the Green and Ampt Equation. *Proceedings Intl. Conf. on Infiltration Development and Application,* Y-K Fok, Ed. Water Resources Center, University of Hawaii, Honolulu, 28-37

Thornthwaite, C.W. 1948. An Approach toward a Rational Classification of Climate. *Geography Review* 38(1): 55-94

Trajkovic, Slavisa 2005. Temperature-Based Approaches for Estimating Reference Evapotranspiration. *Journal of Irrigation and Drainage Engineering* 131(4): 316-323.

U.S. Department of Agriculture Soil Conservation Service (SCS) 1973. A Method for Estimating Volume and Rate of Runoff in Small Watersheds. Technical Paper 149, Washington, D.C.

U.S. Department of Agriculture Soil Conservation Service (SCS) 1986. Urban Hydrology for Small Watersheds. Technical Release no. 55. Washington, D.C.

U.S. Department of Agriculture. Federal Interagency Stream Restoration Working Group. 1998. Stream Corridor Restoration. Natural Resource Conservation Service, Washington, D.C. www.usda.gov/technical/stream restoration.

Vedernikov, V.V. 1934. Seepage from channelsGosstroiizdat, see also Versickerungen aus Kanalen, *Wasserkraft und Wasserwirtschaft,* nos. 12,13 and 14.

Walter, I.A. et al. 2000. ASCE's standardized reference evapotranspiration equation. *Proceedings, Watershed Management and Operations Management 2000*, ASAE, St. Joseph, MI, 209-215

Yoder, R.E., Odhiambo, L.O., Wright, W.C., 2005. Effects of Vapor-Pressure Deficit and Net-Irradiance Calculation Methods on Accuracy of Standardized Penman-Monteith Equation in a Humid Climate. *Journal of Irrigation and Drainage Engineering* 131(3): 228-237

Notations and Units

a = coefficient expressed by $(2 - \varsigma)/3$ (Parlange et al. 1982) (-)
a_1 = regression coefficient (-) = 0.34
A = area (km^2)
A_b = abstractions (in)
A_n = coefficients that are functions of the volumetric moisture content (-)
A_1 = surface area of water body (m^2)
A_s = shape coefficient (-)
B = width of surface water body (m)
b_1 = regression coefficient (-) = 0.14
c = (2 + 3m)/m (-)
C = proportionality coefficients (-)
CN = SCS curve number (-)
D = portion of developed land cover (%)
D_s = soil water diffusivity (m^2/s)
D_w = average depth to water table (m)
d_r = root depth (cm)
e_a = daily average actual vapor pressure (kPa)
e_s = daily average saturation vapor pressure (kPa)
$e^0(T)$ = vapor pressure for given air temperature (kPa)
ET_0 = grass reference evapotranspiration (mm/day)
ET = actual evapotranspiration (mm/day)
ET_p = potential evapotranspiration (mm/day)
F_a = water retention after ponding (in)
F_r = surface roughness (m)
$f(t)$ = infiltration rate (cm/hr)
$F(t)$ = cumulative infiltration (cm)
G = soil heat flux density (MJ m^{-2} day^{-1})
GW_{in} = Groundwater flow in (m^3/s)
GW_{out} = Groundwater flow out (m^3/s)
h = total head (m)
H = depth of water in surface water body (m)
i = rainfall intensity (cm/hr)
I = infiltration (cm)
I_a = infiltration before ponding (in)
K = hydraulic conductivity (cm/hr)
K_s = saturated hydraulic conductivity (cm/hr)
K_v = effective vertical hydraulic conductivity (m/day) = K_s
k_{early} = crop coefficient for the beginning of the growing season (March to May) (-)
k_{mid} = crop coefficient for the middle of the growing season (June to August) (-)
k_{end} = crop coefficient for the end of the growing season (September to November) (-)
L = channel length (km)
L_f = length of flow to main channel (km)
m = pore size distribution index (Brooks and Corey 1964) (-)
N = portion of natural land cover (%)

q_h = horizontal flux (discharge per unit area) (m/day)
Q_p = volume of percolation (m^3/s)
q_p = water depth of percolation (cm)
Q_s = discharge to surface water bodies (m^3/s)
q_{se}^{cum} = percolation from supersaturated soil water reservoir during rain event (cm)
q_v = vertical flux (discharge per unit area) (m/day)
Q_w = abstractions from ground water system through wells (m^3/s)
P = precipitation (cm)
P_a = air pressure (kPa)
P_e = excess precipitation (runoff) (in)
P_r = shoreline length of water body (m)
R = groundwater recharge
R/P = normalized annual recharge (recharge R per unit precipitation P in cm/cm)
R_a = extraterrestrial radiation (MJ m^{-2} day^{-1})
R_n = net radiation (MJ m^{-2} day^{-1})
R_{nl} = outgoing net long-wave radiation (MJ $m^{-2}day^{-1}$)
R_{ns} = incoming net short-wave radiation (MJ $m^{-2}day^{-1}$)
R_s = solar radiation (MJ m^{-2} day^{-1})
RH_{max} = maximum relative humidity (%)
RH_{min} = minimum relative humidity (%)
RH_{mean} = mean relative humidity (%)
s = soil saturation [-]
s_0 = initial soil saturation (-)
S = slope (m/m)
S_s = sorptivity
S_{cn} = potential maximum retention (in)
$\Delta S/t$ = Change in volume stored in aquifer (m^3/s)
t = time (s,hr,day)
t_b = time between rain events (hr,day)
t_c = "condensation" time (hr,day)
t_d = storm duration time (hr, day)
t_e = a time compression approximation (hr,day)
t_p = time to ponding (hr,day)
T = air temperature (°C)
T_{dew} = average estimated dew point temperature (°C)
T_{max} = maximum temperature (°C)
T_{mean} = mean air temperature (°C)
T_{min} = minimum temperature (°C)
U_2 = average 24 hour wind speed at 2 m height (m s^{-1})
V = total potential groundwater discharge (m^3)
Z = elevation, depth (m)
$\beta(s)$ = evapotranspiration efficiency function (-)
α = channel side slope (m/m)
α_r = canopy reflection coefficient (albedo) (≈ 0.23 (Allen et al. 2000))
γ = psychometric constant (kPa $°C^{-1}$)
Δ = slope of saturation vapor pressure function (kPa $°C^{-1}$)

ε_{bulk} = net emittance (combined emissivity for both sky and ground surfaces)
η =porosity (-)
θ = moisture content (-)
θ_e = effective porosity (-)
θ_i = initial water content (-)
θ_s = saturated porosity (-)
$\Delta\theta$ = change of water content available for infiltration = (η - θ_i)
ς = coefficient relating to hydraulic conductivity (-)
σ = Stefan-Boltzmann constant (4.903 X 10^{-9} MJ $K^{-4}m^{-2}day^{-1}$)
Ψ_b = air entry suction head (bubbling pressure head) (cm/hr)
Ψ_f = wetting front suction head (cm/hr)

Glossary

Air entry suction head **(Ψ_b)** also called bubbling pressure head, is the part of total head produced by the air exiting the soil. Rawls et al. (1983) expressed the wetting front suction head in terms of the Brooks and Corey (1964) water retention parameters (Ψ_b and m) (see Section 3.1).

Baseflow is the portion of streamflow that is driven by groundwater and not surface runoff from a rainfall event (Section 2).

Brooks and Corey's pore size distribution index **(m)** is defined as an empirical coefficient quantifying the distribution of pore sizes in a soil and can be estimated using the logarithmic relationship between soil saturation, s, and the soil suction head, Ψ_f. The pore size distribution index can be estimates by draining a soil sample in stages, measuring s and Ψ_f at each stage, and fitting equation (3.8) to the resulting data (Mays 2005) (see equation 3.7).

Crop coefficient is a coefficient that transforms reference evapotranspiration into potential evapotranspiration and depends on plant characteristics and local conditions (Section 3.3 and Appendix C).

Curve number **(CN)** is a land-use and soil type coefficient used in the SCS method (see Section 3.2 and Appendix B)

Degree of saturation **(s)** represents the percentage of the total volume of voids that are filled with water or the ratio of soil moisture content (θ) to saturated soil moisture content (θ_s) (see equation 3.5). The degree of saturation will range from 0 to 1.

Effective porosity **(θ_e)** is the maximum available moisture content that can be abstracted for the soil column (see equation 3.4)

Effective soil saturation **(s_e)** is the ratio of the available moisture to the maximum possible available moisture content (see equation 3.6).

Empirical methods describe the hydrologic processes using empirically derived relationships and coefficients from measured data (Section 2).

Evapotranspiration (ET) is defined as the amount of water extracted from the soil to meet a specific plant needs. It is a combination of the processes of evaporation and transpiration. (Section 3.3).

Field capacity **(θ_{fc})** is defined as the amount of water held in soil after excess water has drained away and the rate of downward movement has materially decreased, which usually takes place within 2 - 3 days after a rain or irrigation in pervious soils of uniform structure and texture. Field capacity can also be defined as the soil moisture content that

is held in the soil against gravitational forces or is the point that gravity forces are no longer the dominating force for drainage (Section 3.1).

Groundwater recharge is the portion of infiltrated water that flows beyond the root zone and ultimately reaches the aquifer.

Hydraulic conductivity **(K)** can be defined as "The volume of liquid flowing perpendicular to a unit area of porous medium per unit time under the influence of a hydraulic gradient of unity" (Delluer 1998).

Hydrograph is a plot of streamflow versus time (Section 2).

Infiltration is the process on which water on the ground surface enters the soil (Section 3.2).

Percolation is the vertical unsaturated flow through a porous medium, usually driven by gravity (Section 4.0).

Physics-based methods describe the physical hydrologic processes that occur in the soil column and usually rely on a soil water balance (Section 4).

Time of ponding is the time during a rainfall event when the infiltration rate of the soil is less than the rainfall rate and water starts to pond on the ground surface (Section 3.2).

Porosity **(η)** of a soil is defined as the percentage of air voids in a soil column and is given as the ratio of the volume of voids over total volume (V) (see equation 3.2).

Potential evapotranspiration is the maximum possible evapotranspiration of a specific plant type given there is plenty of available water in the soil (section 3.3 and Appendix C).

Quickflow is the portion of streamflow associated with surface runoff (Figure 2.1).

Reference evapotranspiration is defined by Allen el al. (1998) as "the rate of evapotranspiration from a hypothetical crop with an assumed crop height (0.12m) and a fixed canopy resistance (70 s/m) and albedo (0.23) which would closely resemble evapotranspiration from an extensive surface of green grass cover of uniform height, actively growing, completely shading the ground and not short of water" (Trajkovic 2005) (Section 3.3).

Readily available water (RAW) is the threshold point at which the plant begins to suffer from water stress. When the soil water reaches this threshold point, the roots can no longer extract water quickly enough to meet the transpiration needs of the plant (Appendix C).

Residual Moisture **(θ_r)** is the soil moisture that can not be drained from the soil, even under strong vacuum pressure, due to strong molecular bonding to the soil particles (Section 3.1).

Root depth/root zone is the zone underneath the ground surface which contains the roots of the vegetative cover (Section 3.0).

Seepage is the saturated flow through a porous medium usually occurring under a surface water body such as a river or lake (Section 5.0).

Seasonal recharge is groundwater recharge that occurs after the spring thaw and before the winter freeze in a given year, approximately April through November for Minnesota (Section 1.).

Soil moisture content **(θ)** represents the amount of moisture in a soil and is defined by the ratio of the volume of water (V_w) over total volume (V) of a soil column (see equation 3.3).

Sorptivity is a measure of the capacity of a porous medium to absorb water (see Phillip's equation, Section 3.2)

Surface runoff is the volume of water that flows over land due to a rainfall event (Section 2).

Total available water (TAW) is the total amount of water retained in a soil for a plant's use. The TAW is the difference between the field capacity and the wilting point of a soil (Appendix C).

Water stress coefficient is a coefficient that accounts for water stress on a plant due to available water in the soil column (see Section 3.3 and Appendix C).

Wetting front suction head **(Ψ_f)** is the energy due to the electrostatic forces between the water molecule polar bonds and the soil particle surfaces that draw the water up around the particle surfaces and leaves air in the center of the voids (see equation 3.8).

Wilting point **(θ_{wp})** is the lowest amount of soil moisture that can be extracted by plants for evapotranspiration. When the soil moisture drops below the wilting point, plants will start to wilt and become permanently damaged (Section 3.1).

Appendix A: Infiltration Estimation Equations

Infiltration is governed by the one-dimensional form of Richards' Equation, for unsteady unsaturated flow in a porous medium (equation 3.11).

Both empirical models and physics-based models were developed as solutions of equation (3.11). Empirical models use coefficients that are obtained by fitting empirical equations to infiltration data. One such model is the SCS method, developed by the U.S. Department of Agriculture. Physics-based models use approximate analytical solutions to Richards' equation. Two widely used solutions are the Green-Ampt method and Phillip's equation. Both assume a homogenous soil with initial uniform moisture content (θ_i). The Green-Ampt equations and Phillip's equation for estimating infiltration have been presented in Section 3. Additional information is given in this appendix.

Green-Ampt Method

The two commonly used Green-Ampt equations used to estimate the infiltration rate (f) and cumulative infiltration (F) are (3.21) and (3.22), respectively. Average Green-Ampt soil parameters can be found in Appendix B.2.

The Green-Ampt model has been the subject of considerable developments in applied soil physics and hydrology owing to its simplicity and satisfactory performance for a great variety of hydrological problems (Ravi and Williams, 1998). The Green-Ampt method was originally developed for ideal conditions, assuming sharp wetting front, constant ponding depth, homogeneous soil, and uniform antecedent water content. Since the formulation of the Green-Ampt (1911) equations (3.21 and 3.22), the conditions of the Green-Ampt concept have been expanded to model many other conditions (Bouwer (1969), Childs and Bybordi (1969), Mein and Larson (1973), Swartzendruber (1974), Morel-Seytoux and Khanji (1974), James and Larson (1976), Li *et al*. (1976), Smith and Parlange (1978), Chu (1978), Flerchinger *et al.* (1988), Philip (1992, 1993), Salvucci and Entekhabi (1994).

Time of Ponding

The Green-Ampt solution assumes constant ponding, but during the early stages of infiltration, all the rainfall percolates into the soil and no ponding on the surface occurs. For a uniform rain event, when the precipitation rate is equal to the infiltration capacity and the pressure head at the surface becomes zero, ponding occurs. The cumulative infiltration at ponding (F_p) can be computed as (Mein and Larson, 1973):

$$F_p = \frac{K\Delta\theta_i\psi_f}{(i-K)} \qquad [A.1]$$

The time of ponding can be computed as

$$t_p = \frac{F_p}{i} \qquad [A.2]$$

where i is the intensity of rainfall.

Nonuniform Rainfall Conditions

For nonuniform rainfall events, ponding occurs when $i > f(t)$. Assuming that ponding occurs in a time interval Δt_j (i.e., $t_{j-1} \le t_p < t_j$), the total cumulative infiltration (F_p) at the time of ponding (t_p) is given by:

$$F_p = \sum_{m=1}^{j-1} \Delta t_m i_m + i_j \left(t_p - t_{j-1}\right) = F_{j-1} + i_j \left(t_p - t_{j-1}\right) \qquad [A.3]$$

Assuming that before ponding the cumulative infiltration equals the cumulative rainfall (i.e., $F_{j-1} = I_{j-1}$), a general expression for time of ponding for nonuniform conditions can be obtained as:

$$t_p = t_{j-1} - \frac{I_{j-1}}{i_j} + \frac{F_p}{i_j} = t_{j-1} - \frac{I_{j-1}}{i_j} + \frac{K\Delta\theta_i\psi_f}{i_j\left(i_j - K\right)} \qquad [A.4]$$

Equation (A.4) can be evaluated for $j = 1,2,3,\ldots$ until $t_j > t_p$. Infiltration capacity $f(t)$, at time t, can be computed using (A.4) with known values of F_t. The computed infiltration capacity (f_t) is then compared to the rainfall intensity (i_j) for the same time interval. If the infiltration capacity is larger than the rainfall intensity, no runoff will occur and the cumulative infiltration capacity ($F_{t+\Delta t}$) is computed as:

$$F_{t+\Delta t} = F_t + i_j \Delta t_j \qquad [A.5]$$

where subscripts t and Δt indicated the quantities computed for the previous and present time steps, respectively. If the infiltration capacity is less than the rainfall, $f_t < i_j$ then ponding occurs throughout the interval and cumulative infiltration can be computed using:

$$F_{t+\Delta t} = F_t + K\Delta t + \Delta\theta_i\psi_f Ln\left[\frac{F_{t+\Delta t} + \Delta\theta_i\psi_f}{F_t + \Delta\theta_i\psi_f}\right] \qquad [A.6]$$

Appendix B

B.1 SCS curve numbers (CN)

A curve number (CN) is a runoff coefficient that is a function of land use, antecedent soil moisture, and other factors that affect runoff and retention (infiltration) in a watershed. The curve number is a dimensionless number that ranges from 0 to 100. $CN = 100$ for impervious areas and water surfaces, and for natural surfaces $CN < 100$. Choosing the correct curve number is important for the accuracy of the model. Curve numbers have been tabulated by the Soil Conservation Service on the basis of soil type and land use in Table B.1 for $I_a = 0.2S$ and antecedent moisture condition II (see Table B.2). The four soil groups in Table B.1 are described as (Mays 2005):

Group A: Deep sand, deep loess, aggregated silts
Group B: Shallow loess, sandy loam
Group C: Clay loams, shallow sandy loam, soils low in organic content, and soils usually high in clay
Group D: Soils that swell significantly when wet, heavy plastic clays, and certain saline soils.

Minimum infiltration rates for each soil group can be found in Table B.2.

The SCS method uses three different antecedent moisture conditions (AMC) to describe soil moisture content and is described in Table B.3. Adjustments for curve numbers for dry (Condition I) and wet (Condition III) antecedent moisture conditions, can be found in Table B.4. For a watershed made up of several different type of land use and soil type, a composite curve number can be calculated using a weighted average, such as:

$$CN_{comp} = aCN_a + bCN_b + cCN_c + ... + nCN_n \qquad [B.1]$$

Where $a,b,c,...,n$ are percentages (in decimal form) of total area for each curve number and $a + b + c + \ldots + n = 1$; CN_a, CN_b, CN_c,…,CN_n are curve numbers for each land use type or soil type.

Table B.1 Runoff curve numbers (average watershed condition, $I_a = 0.2S$)

Land use descriptions	Aveage % impervious[b]	Curve numbers for hydrologic soil groups A	B	C	D
Fully developed urban area[a] (vegetation established)					
Lawns, open spaces, parks, golf courses, cemeteries, etc.					
Good condition: grass cover on 75% or more of the area		39	61	74	80
Fair condition: grass cover on 50% to 75% of the area		49	69	79	84
Poor condition: grass cover on 50% or less of the area		68	79	86	89
Paved parking lots, roofs, driveways, etc.		98	98	98	98
Streets and roads					
Paved with curbs and storm sewers		98	98	98	98
Gravel		76	85	89	91
Dirt		72	82	87	89
Paved with open ditches		83	89	92	93
Commercial and business area	85	89	92	94	95
Industrial districts	72	81	88	91	93
Row houses, town houses, and residential	65	77	85	90	92
With lot sizes 1/8 acre or less					
Residential: average lot size					
1/4 acre	38	61	75	83	87
1/3 acre	30	57	72	81	86
1/2 acre	25	54	70	80	85
1 acre	20	51	68	79	84
2 acre	12	46	65	77	82
Developing urban areas[c] (no vegetation established)					
Newly graded area		77	86	91	94

For non-cultivated agricultural land:
Poor hydrologic condition has less than 25% ground cover density.
Fair hydrologic condition has between 25% and 50% ground cover density.
Good hydrologic condition has more than 50% ground cover density.

For forest-range:
Poor hydrologic condition has less than 30% ground cover density.
Fair hydrologic condition has between 30% and 70% ground cover density.
Good hydrologic condition has more than 70% ground cover density.

Table B.1 Runoff curve numbers (average watershed condition $I_a = 0.2S$) continued.

Land use	Cover: Treatment practice	Cover: Hydrologic condition[d]	Curve numbers for hydrologic soil groups: A	B	C	D
Cultivated agricultural land						
Fallow	Straight row		77	86	91	94
	Conservation tillage	Poor	76	85	90	93
	Conservation tillage	Good	74	83	88	90
Row crops	Straight row	Poor	72	81	88	91
	Straight row	Good	67	78	85	89
	Conservation tillage	Poor	71	80	87	90
	Conservation tillage	Good	64	75	82	85
	Contoured	Poor	70	79	84	88
	Contoured	Good	65	75	82	86
	Contoured and conservation	Poor	69	78	83	87
	tillage	Good	64	74	81	85
	Contoured and terraces	Poor	66	74	80	82
	Contoured and terraces	Good	62	71	78	81
Small grain	Contoured and terraces	Poor	65	73	79	81
	and conservation tillage	Good	61	70	77	80
	Straight row	Poor	65	76	84	88
	Straight row	Good	63	75	83	87
	Conservation tillage	Poor	64	75	83	86
	Conservation tillage	Good	60	72	80	84
	Contoured	Poor	63	74	82	85
	Contoured	Good	61	73	81	84
	Contoured and conservation	Poor	62	73	81	84
	tillage	Good	60	72	80	83
	Contoured and terraces	Poor	61	72	79	82
	Contoured and terraces	Good	59	70	78	81
Close-seeded legumes	Contoured and terraces	Poor	60	71	78	81
or	and conservation tillage	Good	58	69	77	80
rotation	Straight row	Poor	66	77	85	89
meadow[e]	Straight row	Good	58	72	81	85
	Contoured	Poor	64	75	83	85
	Contoured	Good	55	69	78	83
	Contoured and terraces	Poor	63	73	80	83
	Contoured and terraces	Good	51	67	76	80
Non-cultivated agricultural land						
Pasture or						
Range	No mechanical treatment	Poor	68	79	86	89
	No mechanical treatment	Fair	49	69	79	84
	No mechanical treatment	Good	39	61	74	80
	Contoured	Poor	47	67	81	88
	Contoured	Fair	25	59	75	83
	Contoured	Good	6	35	70	79

Table B.1 Runoff curve numbers (average watershed condition $I_a = 0.2S$) continued.

Cover			Curve numbers for hydrologic soil groups			
Land use	Treatment practice	Hydrologic condition[d]	A	B	C	D
Non-cultivated agricultural land (cont.)						
Meadow		--	30	58	71	78
Forestland-grass or		Poor	55	73	82	86
orchard-evergreen or		Fair	44	65	76	82
Deciduous		Good	32	58	72	79
Brush		Poor	48	67	77	83
		Good	20	48	65	73
Woods		Poor	45	66	77	83
		Fair	36	60	73	79
		Good	25	55	70	77
Farmsteads		--	59	74	82	86
Forest-range						
Herbaceous		Poor		79	86	92
		Fair		71	80	89
		Good		61	74	84
Oak-aspen		Poor		65	74	
		Fair		47	57	
		Good		30	41	
Juniper-						
grass		Poor		72	83	
		Fair		58	73	
		Good		41	61	
Sage-grass		Poor		67	80	
		Good		50	63	
		Fair		35	48	

[a]For land use uses with impervious areas, curve numbers are computed assuming that 100% of runoff from
impervious areas directly connected to the drainage system. Pervious areas (lawn) are considered to be equivalent to lawns in good condition and the impervious areas have a *CN* of 98.

[b]Includes paved streets.

[c]Use for the design of temporary measures during grading and construction. Impervious area percent for urban areas under development vary considerably. The user will determine the percent impervious. Then
using the newly graded area CN and Figure 8.7.1a or b, the composite CN can be computed for any degree of
development.

[d]For conservation tillage poor hydrologic condition, 5% to 20% of the surface is covered with residue (less
than 750-lb/acre row crops or 300-lb/acre small grain).
For conservation tillage good hydrologic condition, more than 20% of the surface is covered w/residue (greater than 750-lb/acre row crops or 300-lb/acre small grain).

[e]Close-drilled or broad-cast.

Source: U.S. Department of Agriculture Soil Conservation Service (1986).

Table B.2 Minimum infiltration rates for each soil group

Group	Minimum infiltration rate (in/hr)
A	0.30-0.45
B	0.15-0.30
C	0-0.05

Taken from: Mays, Water Resource Engineering (2005).

Table B.3 Classification of antecedent moisture classes (AMC) for the SCS method of rainfall abstraction

	Total 5-day antecedent rainfall (in)	
AMC group	Dormant season	Growing season
I	Less than 0.5	Less than 1.4
II	0.5 to 1.1	1.4 to 2.1
III	Over 1.1	Over 2.1

Source: U.S. Department of Agriculture, Soil Conservation Service (1972)
Taken from: L.W. Mays, Water Resource Engineering (2005)

Table B.4 Adjustment of curve numbers for dry (Condition I) and wet (Condition III) antecedent moisture conditions

	Corresponding CN for condition	
CN for Condition II	I	III
100	100	100
95	87	99
90	78	98
85	70	97
80	63	94
75	57	91
70	51	87
65	45	83
60	40	79
55	35	75
50	31	70
45	27	65
40	23	60
35	19	55
30	15	50
25	12	45
20	9	39
15	7	33
10	4	26
5	2	17
0	0	0

Source: U.S. Department of Agriculture, Soil Conservation Service (1972)
Taken from: L.W. Mays, Water Resource Engineering (2005)

B.2: Soil parameters

Table B.5 Green-Ampt infiltration parameters for various soil classes

Soil class	Porosity η	Effective porosity θ_e	Wetting front soil suction head Ψ (cm)	Hydraulic conductivity K (cm/h)
Sand	0.437	0.417	4.95	11.78
	(0.374-0.500)	(0.354-0.480)	(0.97-25.36)	
Loamy sand	0.437	0.401	6.13	2.99
	(0.363-0.506	(0.329-0.473)	(1.35-27.94)	
Sandy loam	0.453	0.412	11.01	1.09
	(0.351-0.555)	(0.283-0.541)	(2.67-45.47)	
Loam	0.463	0.434	8.89	0.34
	(0.375-0.551)	(0.334-0.534)	(1.33-59.38)	
Silt loam	0.501	0.486	16.68	0.65
	(0.420-0.582)	(0.394-0.578)	(2.92-95.39)	
Sandy clay loam	0.398	0.33	21.85	0.15
	(0.332-0.464)	(0.235-0.425)	(4.42-108.0)	
Clay loam	0.464	0.309	20.88	0.1
	(0.409-0.519)	(0.279-0.501)	(4.79-91.10)	
Silty clay loam	0.471	0.432	27.3	0.1
	(0.418-0.534)	(0.347-0.517)	(5.67-131.50)	
Sandy clay	0.43	0.321	23.9	0.06
	(0.370-0.490)	(0.297-0.501)	(4.08-140.2)	
Silty clay	0.479	0.423	29.22	0.05
	(0.425-0.533)	(0.334-0.512)	(6.13-139.4)	
Clay	0.475	0.385	31.63	0.03
	(0.427-0.523)	(0.269-0.501)	(6.39-156.5)	

**The numbers in the parentheses below each parameter are one standard deviation around the parameter value given.*

Source: Rawls, Brakensiek, and Miller (1983).

Taken from: L.W. Mays, Water Resource Engineering (2005)

Table B.6 Rawls and Brakensiek's soil parameter estimates

USDA Textural classification	Saturated porosity	Effective porosity	Residual porosity	Wilting point porosity	Bubbing suction head	Pore size distribution index	Saturated hydraulic conductivity	Wetted suction head
	θ_s	θ_e	θ_r	θ_{wp}	Ψ_b	λ	K_s	Ψ_f
					(cm)		(cm/s)	(cm)
Sand	0.437	0.417	0.020	0.033	7.26	0.694	23.56	4.95
Loamy sand	0.437	0.401	0.035	0.055	8.69	0.553	5.98	6.13
Sandy loam	0.453	0.412	0.041	0.095	14.66	0.378	2.18	11.01
Loam	0.463	0.434	0.027	0.117	11.15	0.252	1.32	8.89
Silt loam	0.501	0.486	0.015	0.133	20.79	0.234	0.68	16.68
Sandy clay loam	0.398	0.330	0.068	0.148	28.08	0.319	0.30	21.85
Clay loam	0.464	0.390	0.075	0.197	25.89	0.242	0.20	20.88
Silty clay loam	0.471	0.432	0.040	0.208	32.56	0.177	0.20	27.30
Sandy clay	0.430	0.321	0.109	0.239	29.17	0.223	0.12	23.90
Silty clay	0.479	0.423	0.056	0.250	34.19	0.150	0.10	29.220
Clay	0.475	0.385	0.090	0.272	37.3	0.165	0.06	31.63

Table B.7. Parameters of the Poisson rectangle pulses model for rainfall and potential evapotranspiration for three climates (from Kim et al. 1996)

Parameter	A	SH	H
$\mu[P]$, mm d^{-1}	29.9	50.7	16.1
$\mu[t_d]$, d	0.48	0.25	0.72
$\mu[t_b]$, d	6.46	3.44	3.77
E_p, mm d^{-1}	4.1	3.3	1.9
$\bar{P}$, mm d^{-1}	2.0	3.3	2.6
$\overline{E_p}$, mm d^{-1}	3.8	3.1	1.6

Parameters according to *Hawk and Eagleson* [1992]. A, arid; SH, semihumid; H, humid.

Table B.8. Brooks and Corey parameters for three soils (*from Kim et al. 1996*)

Parameter	C	L	S
k_s, mm d^{-1}	2.94e1	2.94e2	2.94e3
ψ_s, mm	−900	−450	−250
θ_s [−]	0.45	0.35	0.25
m [−]	0.44	1.2	3.3
c [−]	6.5	3.7	2.6

After *Bras* [1990]. C, clay; L, loam; S, sand.

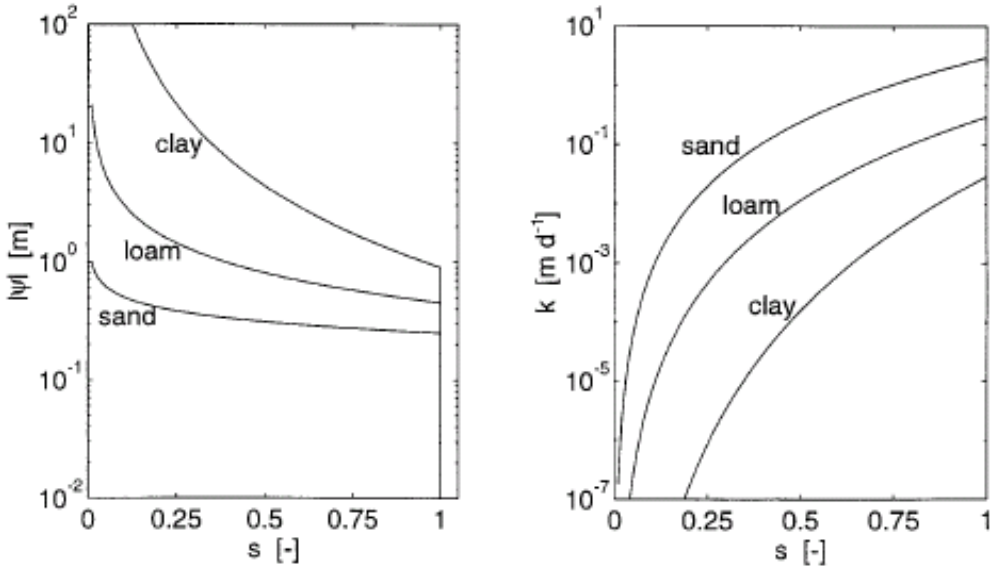

Figure B.1. Absolute soil matrix head |ψ| in (3.7) and hydraulic conductivity K_s in (3.8) as functions of saturation (*s*) corresponding to the parameters of clay, loam, and sand in Table 4.2 (*from Kim et al.1996)*

Appendix C: Evapotranspiration equations

Evapotranspiration is the portion of soil water that is used by vegetation. It combines evaporation of water from the soil and transpiration from the vegetation. Both depend on the energy supply, vapor pressure gradient and wind. When estimating evapotranspiration solar radiation, air temperature, air humidity and wind speed must therefore be considered. There is no easy way to distinguish between evaporation and transpiration because they occur simultaneously. They are estimated together in evapotranspiration.

Evapotranspiration reduces groundwater recharge because rainwater that infiltrates into the soil is returned to the atmosphere by evapotranspiration. Evapotranspiration is especially high during the summer and early fall when the plants' need for soil moisture is at its peak.
A common way to estimate evapotranspiration is to first estimate a reference evapotranspiration (ET_0) for a grass reference crop and then estimate the crop evapotranspiration (ET_c) using a crop coefficient (k_c) for a specific crop. Actual evapotranspiration (ET_a) is then estimated by using a water stress coefficient (k_s) to account for variation in soil moisture content. The relationship for evapotranspiration is given by equation (3.28) in Section 3. This equation is from the Food and Agriculture Organization of the United Nations (FAO) Irrigation and Drainage Paper 56. More information on the FAO Irrigation and Drainage Paper 56 can be found on the FAO website at **http://www.fao.org/docrep/X0490E/x0490e00.htm**.

Additional information for estimating each part of equation 3.28 is given below.

C.1 Reference evapotranspiration (ET_0)

ET_0 is evapotranspiration from a hypothetical crop which would closely resemble a green grass cover of uniform height, actively growing, completely shading the ground and not short of water (Trajkovic 2005). Equation (3.29) can be used for estimation of ET_0 by the FAO-56 PM method (Allen el at. 1998).

C.2 Climate parameter estimation

If the extensive weather data required as input to equation (3.29) are missing or not reliable, ET_o can be estimated using the temperature-based modified Penman-Monteith method. The temperature-based Penman_Monteith method uses equation (3.29) and then estimates each of the variables using the following temperature-based equations. The slope of the saturation vapor function (Δ) and the psychometric constant (γ) are given as, respectively:

$$\Delta = \frac{2504 \exp\left(\frac{17.27 T_{mean}}{T_{mean} + 237.3}\right)}{\left(T_{mean} + 237.3\right)^2} \qquad [C.1]$$

$$\gamma = 0.000665P \quad [C.2]$$

The following equation can be used to estimate air pressure (P)

$$P = 101.3\left(\frac{293 - 0.0065Z}{293}\right)^{5.26} \quad [C.3]$$

where

Δ = the slope of vapor pressure curve [kPa/°C];
T_{mean} = mean air temperature (°C)
γ = the psychometric constant [kPa/°C]
P = atmospheric pressure [kPa]
Z = elevation [m]

The daily soil heat flux G beneath the grass reference surface is relatively small and therefore ignored (G≈0). Where no wind data are available, a suibstitute wind speed of 2 m s^{-1} can be used as an acceptable estimate for most locations (Jensen *et al.*, 1997; Allen *et al.*, 2000). Net radiation and vapor pressure deficit for the FAO-56 PM can be estimated using the following procedures given by Yoder et al. (2005). Where measurements of solar radiation are not available, the difference between the maximum and minimum air temperature can be used (Hargreaves *et al*., 1985; Allen, 1997) to estimate it.

$$R_s = K\left(T_{\max} - T_{\min}\right)^{0.5} R_a \quad [C.4]$$

where

R_s = solar radiation (MJ m^{-2} day^{-1})
R_a = extraterrestrial radiation (MJ m^{-2} day^{-1})
T_{max} = maximum air temperature (°C)
T_{min} = minimum air temperature (°C)
K = an adjustment coefficient (0.16 for "interior" locations and 0.19 for coastal locations).

If solar radiation is known or it is estimated from equation (C.4), net solar radiation can be calculated as the difference between incoming net short-wave irradiance (R_{ns}) and the outgoing net long-wave irradiance (R_{nl}) (Yoder *et al.* 2005). Equations for calculating R_{ns}, R_{nl}, and R_n are given by Allen et al. (1998).

$$R_{ns} = (1 - \alpha)R_s \quad [C.5]$$

$$R_{nl} = \varepsilon_{bulk}\sigma\left[\frac{T_{\max,^\circ}K^4 + T_{\min,^\circ}K^4}{2}\right] \quad [C.6]$$

$$R_n = R_{ns} - R_{nl} \quad [C.7]$$

where

R_{ns} = incoming net short-wave radiation (MJ $m^{-2}day^{-1}$)
R_s = measured or estimated solar radiation (MJ $m^{-2}day^{-1}$)
R_{nl} = outgoing net long-wave radiation (MJ $m^{-2}day^{-1}$)
R_n = net solar radiation (MJ $m^{-2}day^{-1}$)
α = canopy reflection coefficient (albedo) (≈ 0.23 (Allen et al. 2000))
ε_{bulk} = net emittance (combined emissivity for both sky and ground surfaces)
σ = Stefan-Boltzmann constant (4.903 X 10^{-9} MJ $K^{-4}m^{-2}day^{-1}$)
$T_{max,K}$ = maximum absolute temperature during 24-hour period (°K)
$T_{min,K}$ = minimum absolute temperature during 24-hour period (°K)

To estimate net emittance (ε_{bulk}) an empirical relationship has been proposed (Brunt 1932).

$$\varepsilon_{bulk} = a - b\sqrt{e_a} \qquad [C.8]$$

where a and b = regression coefficients
e_a = actual vapor pressure (kPa).

For a hypothetical grass reference crop a and b have been determined to be 0.34 and 0.14, respectively (Allen et al. 1998; Allen 2000). Methods for estimating e_a are described below.

Estimates for the vapor pressure deficit can be given as the difference ($e_s - e_a$) between the saturation vapor pressure (e_s) and the actual vapor pressure (e_a). An estimate for saturation vapor pressure (e_s) can be obtained by averaging the saturated vapor pressure at maximum and minimum air temperatures, $e^0(T_{max})$ and $e^0(T_{min})$, respectively (Jensen *et al.*, 1997; Kimball *et al.*, 1997; Allen *et al.*, 1998; Thornton *et al.*, 2000).

$$e_s = \frac{e^0(T_{\max}) + e^0(T_{\min})}{2} \qquad [C.9]$$

where e_s is saturated vapor pressure (kPa), T_{min} is minimum air temperature (°C), T_{max} is maximum air temperature (°C), and $e^0(T)$ for a given air temperature (T) is given by

$$e^0 = 0.6108 \exp\left[\frac{17.27T}{T + 237.3}\right] \qquad [C.10]$$

Actual vapor pressure (e_a) can be estimated using relative humidity and air temperature. Common relationships used to estimate e_a are (Jensen et al. 1990; Burman and Pochop 1994; Allen et al. 1998)

$$e_a = \frac{e^0(T_{\min})\frac{RH_{\max}}{100} + e^0(T_{\max})\frac{RH_{\min}}{100}}{2} \qquad [C.11]$$

$$e_a = 0.6108 \exp\left[\frac{17.27 T_{\min}}{T_{\min} + 237.3}\right] \quad [C.12]$$

$$e_a = 0.6108 \exp\left[\frac{17.27 T_{dew}}{T_{dew} + 237.3}\right] \quad [C.13]$$

where

e_a = actual vapor pressure (kPa)
RH_{max} = maximum relative humidity (%)
RH_{min} = minimum relative humidity (%)
T_{min}, T_{max} = minimum and maximum air temperature (°C), respectively
T_{dew} = estimated dew point temperature (°C)

To estimate daily ET_0, equation (C.11) has given the best results for estimating actual vapor pressure (Yoder et al. 2005). The above equations can be used to estimate the climate parameters required by the FAO-56 PM method when climate data are sparse.

C.3 Crop evapotranspiration (ET_c)

While reference crop evapotranspiration accounts for variations in weather and offers a measure of the "evaporative demand" of the atmosphere, crop coefficients account for the difference between the vegetative types of crops. A crop coefficient (k_c) is the ratio of evapotranspiration (ET_c) by a particular crop relative to reference evapotranspiration (ET_0) for a reference crop such as grass or alfalfa. The reference evapotranspiration, ET_0, is multiplied by the crop coefficients (k_c) to produce an estimate for the potential evapotranspiration, ET_c, given that sufficient water is available.

$$ET_c = k_c \, ET_0 \quad [C.14]$$

where ET_c is potential evapotranspiration (mm/day), k_c is crop coefficient (-), ET_0 is reference evapotranspiration. According to Allen et al. (1998), the crop coefficients incorporates four primary characteristics that distinguish the crop from the reference crop: the crop height, which influence the aerodynamic resistance and turbulent transfer of vapor from the crop into the atmosphere; the albedo (reflectance) of the crop-soil surface, and is affected by the fraction of ground covered by vegetation and by the soil surface wetness; the canopy resistance of the crop to vapor transfer affected by leaf area (number of stomata), leaf age and condition, and the degree of stomatal control; and evaporation from the soil.

The crop coefficient for a specific crop type depends on the crop's life cycle. Each plant's life cycle is broken into five stages: initial stage, crop development, middle stage, late season, and end stages. Each stage has a different crop coefficient corresponding to different water uses and plant size. A crop coefficient curve (Figure C.1) can be constructed to determine the crop coefficients depending on the life cycle of the crop.

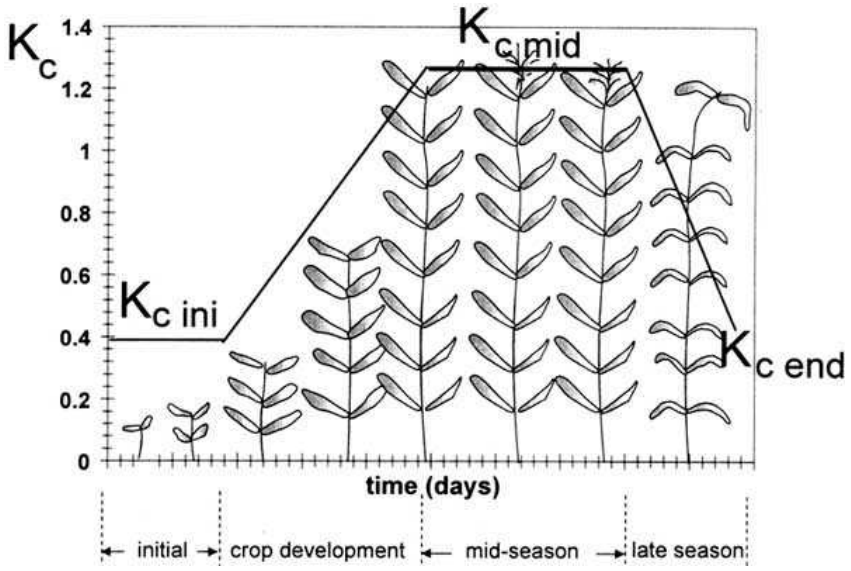

Figure C.1 Crop coefficient (k_c) (from FAO-56)

Figure 3.1 shows three crop coefficients ($k_{c\ int}$, $k_{c\ mid}$, $k_{c\ end}$) which are provided in Appendix D (Table D.1) along with the length of the different stages of development for different crops (Table D.2). The crop coefficient for the crop development and late season stages is a linear interpolation between the initial crop coefficient and the mid-season crop coefficient, and mid-season crop coefficient and end crop coefficient, respectively. According to Allen et al. (1998), the rate at which vegetation cover develops and the time at which it attains effective full cover are affected by weather conditions in general and by mean daily air temperature in particular. Therefore, the length of time between planting and effective full cover will vary with climate, latitude, elevation, and planting date; and will also vary with cultivar (crop variety). Crop development time periods for different areas are given in Table D.2.

C.4 Evapotranspiration under soil-water stress

The potential crop evapotranspiration, ET_c, assumes that the plant will have sufficient water to meet its needs. If the water conditions are not ideal, an adjustment factor, k_s, must be used to estimate actual evapotranspiration.

A crop's evapotranspiration ability is affected by the amount of water present in the soil. When the soil is wet, the water is in abundance, is free to move, and is easily taken up by the plant's roots. When the soil is dry, the water is strongly bound to the soil matrix and harder for the plants to extract. When the soil water drops below a threshold value, the crop becomes water stressed. The effects of soil water stress can be described by multiplying the potential evapotranspiration, ET_c, by a water stress coefficient, k_s:

$$ET_{cadj} = k_s k_c ET_0 \quad [C.15]$$

where

ET_{cadj} = water stress potential evapotranspiration (mm/day)
k_s = water stress coefficient (-) ($0 < k_s > 1$)
k_c = crop coefficient (-)
ET_0 = reference evapotranspiration (mm/day).

The water stress coefficient, k_s, is dependent on the total available water (TAW) and the readily available water (RAW) in the soil matrix (Figure C.2).

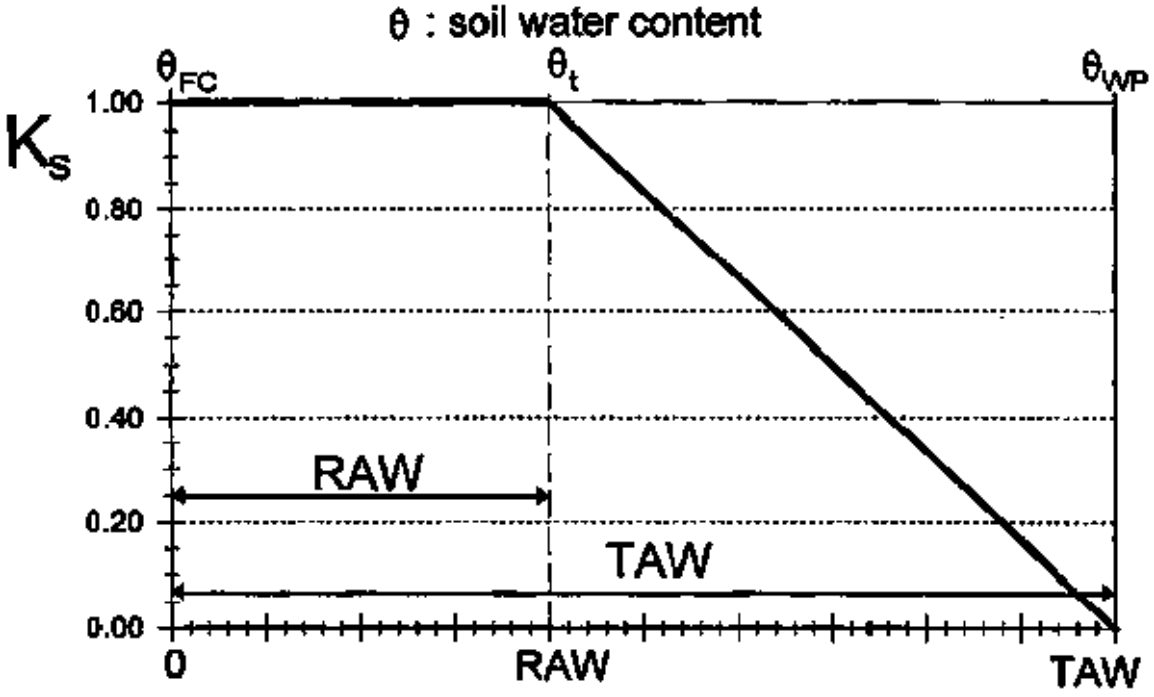

Figure C.2: Water stress coefficient (k_s) (from FAO-56)

Total available water (TAW)

The soil's total available water (TAW) is the total amount of water retained in a soil for a plant's use. The TAW is the difference between the field capacity and the wilting point of a soil. The field capacity is the amount of water a well-drained soil can hold against gravitational forces. The wilting point is the water level when the plant can no longer extract water from the soil matrix; it is the water content at which plants will wilt. Since the water content above field capacity will drain, and plants can not extract the water content below the wilting point, the total available water (TAW) is:

$$TAW = (\theta_{FC} - \theta_{WP}) d_r \quad [C.16]$$

where

TAW = total available water (mm)

θ_{FC} = water content at field capacity (-)
θ_{WP} = water content at wilting point (-)
d_r = root zone depth (mm)

Typical values for field capacity and wilting point for various soil types are shown in Table C.2.

Table C.2 Typical soil water characteristics for different soil types (after Allen et al. 1998).

Soil type (USGS soil texture classification)	Soil water characteristics		
	Field capacity θ_{FC}	Wilting point θ_{WP}	Available water content (θ_{FC} - θ_{WP})
	m^3/m^3	m^3/m^3	m^3/m^3
Sand	0.07 - 0.17	0.02 - 0.07	0.05 - 0.11
Loamy sand	0.11 - 0.19	0.03 - 0.10	0.06 - 0.12
Sandy loam	0.18 - 0.28	0.06 - 0.16	0.11 - 0.15
Loam	0.20 - 0.30	0.07 - 0.17	0.13 - 0.18
Silt loam	0.22 - 0.36	0.09 - 0.21	0.13 - 0.19
Silt	0.28 - 0.36	0.12 - 0.22	0.16 - 0.20
Silt clay loam	0.30 - 0.37	0.17 - 0.24	0.13 - 0.18
Silty clay	0-30 - 0.42	0.17 - 0.29	0.13 - 0.19
Clay	0.32 - 0.40	0.20 - 0.24	0.12 - 0.20

Readily available water (RAW)

Readily available water (RAW) is the threshold point at which the plant begins to suffer from water stress. When the soil water reaches this threshold point, the roots can no longer extract water quickly enough to meet the transpiration needs of the plant. The fraction of TAW at which the plant suffers no water stresses is known as the readily available water (RAW):

$$RAW = pTAW \qquad [C.17]$$

where
RAW = readily available water in the root zone (mm)
p = faction of total available water that can be depleted without water stress (-)
TAW = total available water in the root zone (mm)

The faction p varies from one crop to another and is a function of crop type and evaporation power of the atmosphere. The fraction p normally varies from 0.30 for shallow rooted plants at high rates of ET (> 8 mm/day) to 0.70 for deep rooted plants at low rates of ET (< 3 mm/day). A p value of 0.50 is commonly used for many crops and typical values for p can be found in Table D.3 in Appendix D. Since p is a function of the atmosphere's evaporative power, p varies depending on the daily amount of ET. The values in Table D.3 need to be adjusted, depending on how much daily ET_c varies from 5 mm/day, this adjustment is give by:

$$p = p_{table} + 0.04(5 - ET_c) \qquad [C.18]$$

where

p = adjusted fraction of total available water (-) limited to $0.1 \leq p \leq 0.8$
p_{table} = Table D.3 value of p (-)
ET_c = daily potential evapotranspiration (mm/day)

Expressing the tolerance of crops to water stress as a function of the fraction (p) of TAW is not wholly correct (Allen et al. 1998). The rate of root water uptake is in fact influenced more directly by the potential energy level of the soil water (soil matrix potential and the associated hydraulic conductivity) than by water content. As a certain soil matrix potential corresponds in different soil types to different soil water contents, the value for p is also a function of the soil type. Generally, it can be stated that for fine textured soils (clay) the p values listed in Table D.3 can be reduced by 5-10%, while for more coarse textured soils (sand), they can be increased by 5-10%.

Water stress coefficient (k_s)

As illustrated by Figure C.2, the water stress coefficient, k_s, is dependent on the amount of water in the soil column. The water stress coefficient, k_s, is a function of TAW and RAW. The soil water content can also be expressed as root zone depletion, D_w, i.e. water shortage relative to TAW. At field capacity the root zone depletion is equal to zero (D_w = 0) and at the wilting point, the root zone depletion is equal to TAW (D_r = TAW). Knowing that a plant's ET is hindered by water stresses after the root zone depletion is greater than the RAW, the water stress coefficient (k_s) can be estimated from the relationship

$$k_s = \frac{TAW - D_w}{TAW - RAW} = \frac{TAW - D_w}{(1-p)TAW} \qquad [C.19]$$

where

ks = the water stress coefficient (-)
TAW = total available water in root zone (-)
D_w = root zone depletion (mm) ($0 \leq D_w \leq$ TAW)
RAW = readily available water in root zone (-)
p = fraction of TAW readily available for plants (-)

The root zone depletion (D_w) can be estimated using a soil water balance such as

$$D_{w,i} = D_{w,i-1} - I_i - Irr_i - CR_i + ET_{c,i} + DP_i \quad [C.26]$$

where

$D_{w,i}$ = root zone depletion depth for end of day, i (mm)
$D_{w,i-1}$ = root zone depletion depth at the end of pervious day, i-1 (mm)
I_i = infiltration depth on day, i (mm)
Irr_i = net irrigation depth on day, i, that infiltrates the soil (mm)
CR_i = capillary rise depth from groundwater table on day, i (mm)
$ET_{c,i}$ = crop evapotranspiration depth on day, i (mm)
DP_i = water loss from root zone by deep percolation or on day, i (mm)

The follow parameter definitions for (C.26) are taken from Allen et al (1998):

Infiltration (I) and irrigation (Irr)

I_i is equivalent to daily infiltration due to daily precipitation (I = P – RO, where p is precipitation and RO is runoff). Daily precipitation in amounts less than about 0.2 ET_0 is normally entirely evaporated and can usually be ignored in the water balance calculations especially when the single crop coefficient approach is being used. Infiltration into the soil during precipitation can be predicted using standard procedures from hydrological texts. Irr_i is equivalent to the mean infiltrated irrigation depth expressed for the entire field surface.

Capillary rise (CR)

The amount of water transported upwards by capillary rise from the water table to the root zone depends on the soil type, the depth of the water table and the wetness of the root zone. CR can normally be assumed to be zero when the water table is more than about 1 m below the bottom of the root zone. Some information on CR was presented in FAO Irrigation and Drainage Paper No. 24. CR will be a topic in a future FAO publication.

Evapotranspiration (ETc)

Where the soil water depletion is smaller than RAW, the crop evapotranspiration equals $ET_c = k_c\ ET_0$. As soon as $D_{w,i}$ exceeds RAW, the crop evapotranspiration is reduced and ET_c can be computed from (C.15).

Deep percolation (DP)

Following heavy rain or irrigation, the soil water content in the root zone might exceed field capacity. In this simple procedure it is assumed that the soil water content is at θ_{FC} within the same day of the wetting event, so that the depletion $D_{w,i}$ in (C.26) becomes zero. Therefore, following heavy rain or irrigation

$$DP_i = I_i + Irr_i - ET_{c,i} - D_{w,i-1} \geq 0 \quad [C.27]$$

As long as the soil water content in the root zone is below field capacity (i.e., $D_{w,i} > 0$), the soil will not drain and $DP_i = 0$.

Initial depletion

To initiate the soil water balance, an initial depletion, $D_{w,int}$, must be assumed. If the soil moisture is known for the initial soil condition, $D_{w,int}$ can be estimated using

$$D_{w,\text{int}} = (\theta_{FC} - \theta_{\text{int}})d_r \qquad [C.28]$$

where

$D_{w,int}$ = initial root zone depletion depth (mm)
θ_{FC} = soil moisture content at field capacity (-)
θ_{int} = initial soil moisture content (-)
d_r = root zone depth (mm)

If the initial soil moisture is not known and the soil moisture budget starts in the spring or after a heavy rain, the root zone can be assumed to be at field capacity and $D_{w,int}$ can be assumed to be zero.

Appendix D: FAO-56 Evapotranspiration Tables

Table D.1: Single (time-averaged) crop coefficients, k_c, and mean maximum plant heights for non stressed, well-managed crops in sub-humid climates (RH_{min} » 45%, u_2 » 2 m/s) for use with the FAO Penman-Monteith ET_o (After Allen et al. 1998).

Crop		$k_{c\ int}$	$k_{c\ mid}$	$k_{c\ end}$	Maximum crop height (h) (m)
d. Roots and Tubers		**0.50**	**1.10**	**0.95**	
Potato			1.15	0.75	0.6
Sugar beets		0.35	1.20	0.71	0.5
e. Legumes *(Leguminosae)*		**0.40**	**1.15**	**0.55**	
Beans, green		0.5	1.05[2]	0.90	0.4
Beans, dry, and pulses		0.4	1.15[2]	0.35	0.4
Green gram and cowpeas			1.05	0.60-0.35[6]	0.4
Peas	- fresh	0.5	1.15[2]	1.10	0.5
	- dry/seed		1.15	0.30	0.5
Soybeans			1.15	0.50	0.5-1.0
i. Cereals		**0.3**	**1.15**	**0.4**	
Barley			1.15	0.25	1
Oats			1.15	0.25	1
Spring wheat			1.15	0.25-0.4[10]	1
Winter wheat	- with frozen soils	0.4	1.15	0.25-0.4[10]	1
	- with non-frozen soils	0.7	1.15	0.25-0.4[10]	
Maize, field (grain) *(field corn)*			1.20	0.60-0.35[11]	2
Maize, sweet *(sweet corn)*			1.15	1.05[12]	1.5
j. Forages					
Alfalfa hay	- averaged cutting effects	0.40	0.95[13]	0.90	0.7
	- individual cutting periods	0.40[14]	1.20[14]	1.15[14]	0.7
	- for seed	0.40	0.50	0.50	0.7
Bermuda hay	- averaged cutting effects	0.55	1.00[13]	0.85	0.35
	- Spring crop for seed	0.35	0.90	0.65	0.4
Clover hay, Berseem	- averaged cutting effects	0.40	0.90[13]	0.85	0.6
	- individual cutting periods	0.40[14]	1.15[14]	1.10[14]	0.6
Rye grass hay	- averaged cutting effects	0.95	1.05	1.00	0.3
Grazing pasture	- Rotated grazing	0.40	0.85-1.05	0.85	0.15-0.30
	- Extensive grazing	0.30	0.75	0.75	0.10
Turf grass	- cool season [15]	0.90	0.95	0.95	0.10
	- warm season [15]	0.80	0.85	0.85	0.10

n. Fruit Trees					
Apples, cherries, pears [19]	- no ground cover, killing frost	0.45	0.95	0.70[18]	4
	- no ground cover, no frosts	0.60	0.95	0.75[18]	4
	- active ground cover, killing frost	0.50	1.20	0.95[18]	4
	- active ground cover, no frosts	0.80	1.20	0.85[18]	4
Conifer trees [23]		1.00	1.00	1.00	10
o. Wetlands - temperate climate					
Cattails, bulrushes, killing frost		0.3	1.20	0.30	2
Cattails, bulrushes, no frost		0.6	1.20	0.60	2
Short vegetation, no frost		1.05	1.10	1.10	0.3
Reed swamp, standing water		1	1.20	1.00	1-3
Reed swamp, moist soil		0.9	1.20	0.70	1-3
p. Special					
Open water, < 2 m depth or in sub-humid climates or tropics			1.05	1.05	
Open water, > 5 m depth, clear of turbidity, temperate climate			0.6525	1.2525	

[1] These are general values for $K_{c\ ini}$ under typical irrigation management and soil wetting. For frequent wettings such as with high frequency sprinkle irrigation or daily rainfall, these values may increase substantially and may approach 1.0 to 1.2. $K_{c\ ini}$ is a function of wetting interval and potential evaporation rate during the initial and development periods and is more accurately estimated using Figures 29 and 30, or Equation 7-3 in Annex 7, or using the dual $K_{cb\ ini} + K_e$.

[2] Beans, Peas, Legumes, Tomatoes, Peppers and Cucumbers are sometimes grown on stalks reaching 1.5 to 2 meters in height. In such cases, increased K_c values need to be taken. For green beans, peppers and cucumbers, 1.15 can be taken, and for tomatoes, dry beans and peas, 1.20. Under these conditions h should be increased also.

[6] The first $K_{c\ end}$ is for harvested fresh. The second value is for harvested dry.

[10] The higher value is for hand-harvested crops.

[13] This $K_{c\ mid}$ coefficient for hay crops is an overall average $K_{c\ mid}$ coefficient that averages K_c for both before and following cuttings. It is applied to the period following the first development period until the beginning of the last late season period of the growing season.

[14] These K_c coefficients for hay crops represent immediately following cutting; at full cover; and immediately before cutting, respectively. The growing season is described as a series of individual cutting periods (Figure 35).

[15] Cool season grass varieties include dense stands of bluegrass, ryegrass, and fescue. Warm season varieties include bermuda grass and St. Augustine grass. The 0.95 values for cool season grass represent a 0.06 to 0.08 m mowing height under general turf conditions. Where careful water management is practiced and rapid growth is not required, K_c's for

turf can be reduced by 0.10.

[18] These $K_{c\ end}$ values represent K_c prior to leaf drop. After leaf drop, $K_{c\ end}$ » 0.20 for bare, dry soil or dead ground cover and $K_{c\ end}$ » 0.50 to 0.80 for actively growing ground cover (consult Chapter 11).

[23] Confers exhibit substantial stomatal control due to reduced aerodynamic resistance. The K_c, can easily reduce below the values presented, which represent well-watered conditions for large forests.

[24] These coefficients represent about 40 to 60% ground cover. Refer to Eq. 98 and footnotes 21 and 22 for estimating K_c for immature stands. In Spain, Pastor and Orgaz (1994) have found the following monthly K_c's for olive orchards having 60% ground cover: 0.50, 0.50, 0.65, 0.60, 0.55, 0.50, 0.45, 0.45, 0.55, 0.60, 0.65, 0.50 for months January through December. These coefficients can be invoked by using $K_{c\ ini}$ = 0.65, $K_{c\ mid}$ = 0.45, and $K_{c\ end}$ = 0.65, with stage lengths = 30, 90, 60 and 90 days, respectively for initial, development, midseason and late season periods, and using K_c during the winter ("off season") in December to February = 0.50.

Table D.2 Lengths (days) of crop development stages* for various planting periods and climatic regions (after Allen et al. 1998).

Crop	Init. (L_{ini})	Dev. (L_{dev})	Mid (L_{mid})	Late (L_{late})	Total	Plant Date	Region
d. Roots and Tubers							
Potato	25	30	30/45	30	115/130	Jan/Nov	(Semi) Arid Climate
	25	30	45	30	130	May	Continental Climate
	45	30	70	20	165	Apr/May	Idaho, USA
Sugar beets	30	45	90	15	180	March	Calif., USA
	50	40	50	40	180	April	Idaho, USA
e. Legumes *(Leguminosae)*							
Beans (green)	20	30	30	10	90	Feb/Mar	Calif., Mediterranean
Beans (dry)	20	30	40	20	110	May/June	Continental Climates
	25	25	30	20	100	June	Idaho, USA
Green gram, cowpeas	20	30	30	20	110	March	Mediterranean
Peas	15	25	35	15	90	May	Europe
	35	25	30	20	110	April	Idaho, USA
Soybeans	15	15	40	15	85	Dec	Tropics
	20	30/35	60	25	140	May	Central USA
i. Cereals							
Barley/oats/wheat	20	25	60	30	135	March/Apr	35-45 °L
	40	30	40	20	130	Apr	

Grains (small)	20	30	60	40	150	April	Mediterranean
	25	35	65	40	165	Oct/Nov	Pakistan; arid reg.
Maize (grain)	30	50	60	40	180	April	East Africa (alt.)
	30	40	50	50	170	April	Idaho, USA
Maize (sweet)	20	20	30	10	80	March	Philippines
	30	30	30	103	110	April	Idaho, USA
j. Forages							
Alfalfa, total season [4]	10	30	var.	var.	var.		last -4°C in spring until first -4°C in fall
Alfalfa [4] 1st cutting cycle	10	20	20	10	60	Jan Apr (last -4°C)	Calif., USA.
	10	30	25	10	75		Idaho, USA.
Alfalfa [4], other cutting cycles	5	10	10	5	30	Mar	Calif., USA.
	5	20	10	10	45	Jun	Idaho, USA.
Bermuda for seed	10	25	35	35	105	March	Calif. desert, USA
Bermuda for hay (several cuttings)	10	15	75	35	135	---	Calif. desert, USA
Grass pasture [4]	10	20	--	--	--		7 days before last -4°C in spring until 7 days after first -4°C in fall
n. Fruit Trees							
Deciduous orchard	20	70	90	30	210	March	High latitudes
	20	70	120	60	270	March	Low latitudes
o. Wetlands - Temperate Climate							
Wetlands (cattails, bulrush)	10	30	80	20	140	May	Utah, USA; killing frost
	180	60	90	35	365	November	Florida, USA
Wetlands (short vegetation)	180	60	90	35	365	November	frost-free climate

* Lengths of crop development stages provided in this table are indicative of general conditions, but may vary substantially from region to region, with climate and cropping conditions, and with crop variety. The user is strongly encouraged to obtain appropriate local information.

[3] The late season for sweet maize will be about 35 days if the grain is allowed to mature and dry.

[4] In climates having killing frosts, growing seasons can be estimated for alfalfa and grass as:
alfalfa: last -4° C in spring until first -4° C in fall (Everson, D. O., M. Faubion and D. E. Amos 1978. "Freezing temperatures and growing seasons in Idaho." Univ. Idaho Agric. Exp. station bulletin 494. 18 p.)
grass: 7 days before last -4° C in spring and 7 days after last -4° C in fall (Kruse E. G. and Haise, H. R. 1974. "Water use by native grasses in high altitude Colorado meadows." USDA Agric. Res. Service, Western Region report ARS-W-6-1974. 60 pages)

Table D.3: Ranges of maximum effective root depth (Z_r), and soil water depletion fraction for no stress (p), for common crops (Allen et al. 1998)

Crop		Maximum root depth [1] (m)	Depletion fraction [2] (for ET » 5 mm/day) p
d. Roots and Tubers			
Potato		0.4-0.6	0.35
Sugar beets		0.7-1.2	0.55[3]
e. Legumes *(Leguminosae)*			
Beans, green		0.5-0.7	0.45
Beans, dry and pulses		0.6-0.9	0.45
Green gram and cowpeas		0.6-1.0	0.45
Peas	- fresh	0.6-1.0	0.35
	- dry/seed	0.6-1.0	0.40
Soybeans		0.6-1.3	0.50
i. Cereals			
Barley		1.0-1.5	0.55
Oats		1.0-1.5	0.55
Spring wheat		1.0-1.5	0.55
Winter wheat		1.5-1.8	0.55
Maize, field (grain) *(field corn)*		1.0-1.7	0.55
Maize, sweet *(sweet corn)*		0.8-1.2	0.50
j. Forages			
Alfalfa	- for hay	1.0-2.0	0.55
	- for seed	1.0-3.0	0.60
Bermuda	- for hay	1.0-1.5	0.55
	- Spring crop for seed	1.0-1.5	0.60
Clover hay, Berseem		0.6-0.9	0.50
Rye Grass hay		0.6-1.0	0.60
Grazing Pasture	- Rotated grazing	0.5-1.5	0.60
	- Extensive grazing	0.5-1.5	0.60
Turf grass	- cool season [5]	0.5-1.0	0.40
	- warm season [5]	0.5-1.0	0.50
n. Fruit Trees			
Apples, cherries, pears		1.0-2.0	0.50
Conifer trees		1.0-1.5	0.70

[1] The larger values for Z_r are for soils having no significant layering or other characteristics that can restrict rooting depth. The smaller values for Z_r may be used for irrigation scheduling and the larger values for modeling soil water stress or for rain fed conditions.

[2] The values for p apply for ET_c » 5 mm/day. The value for p can be adjusted for different ET_c according to

$$p = p_{\text{table 22}} + 0.04\ (5 - ET_c)$$

where p is expressed as a fraction and ET_c as mm/day.

[3] Sugar beets often experience late afternoon wilting in arid climates even at p < 0.55, with usually only minor impact on sugar yield.

[5] Cool season grass varieties include bluegrass, ryegrass and fescue. Warm season varieties include bermuda grass, buffalo grass and St. Augustine grass. Grasses are variable in rooting depth. Some root below 1.2 m while others have shallow rooting depths. The deeper rooting depths for grasses represent conditions where careful water management is practiced with higher depletion between irrigations to encourage the deeper root exploration.